Summer 2019

Role of Epigenome and Microbiome in Cannabinoid and Aryl Hydrocarbon Receptor-Mediated Regulation of Inflammatory and Autoimmune Diseases

Zinah Zamil Al-Ghezi

ROLE OF EPIGENOME AND MICROBIOME IN CANNABINOID AND ARYL HYDROCARBON RECEPTOR-MEDIATED REGULATION OF INFLAMMATORY AND AUTOIMMUNE DISEASES

By

Zinah Zamil Al-Ghezi

Bachelor of Biotechnology
Al-Nahrain University Iraq, 1998

Master of Science
Thi-Qar University Iraq, 2009

Submitted in Partial Fulfillment of the Requirements

For the Degree of Doctor of Philosophy in

Biomedical Science

School of Medicine

University of South Carolina

2019

Accepted by:

Mitzi Nagarkatti, Major Professor

Prakash Nagarkatti, Chairman, Examining Committee

Swapan Ray, Committee Member

Kenneth Walsh, Committee Member

Jun Zhu, Committee Member

Cheryl L. Addy, Vice Provost and Dean of the Graduate School

DEDICATION

Words are the way we express our emotions during events like this, and I want everyone who has helped me on this journey understand that without you, I would not be here today. As this life's chapter comes to a close, I want to ensure two most important people from my life, know the extent of my thankfulness.

I first extend a deep heartfelt thank you to my father, Zamil Al-Chezi, who always encouraged me, from the time I was a little girl, to reach for the stars, and gave me the belief I could be anything I wanted to be, as long as I worked hard towards my goals. Second, to my husband, Saddam Al-Tofan, who is my soul-mate and the leader of our family.

Thank you both for allowing me to become a stronger woman than I ever realized I could be. You never gave up on me and pushed me to attain what seemed like an impossible dream, yet here I stand at the end of my PhD, so grateful to the both of you for all your love and support. I hope you know these are not just words on paper, but feelings flowing from the bottom of my heart. Thank you, Father and Husband, I hope you are proud of what you've allowed me to accomplish.

ACKNOWLEDGEMENTS

I would like to thank my dear country, Iraq, for giving me the opportunity to pursue my Ph.D. in the United States and for sponsor me and my family through my Ph.D. study as well as the Iraqi Embassy and the Iraqi Cultural Attaché office in the United States for their tremendous help and support through all these years.

Also, great thanks to my mentors, Dr. Mitzi Nagarkatti and Dr. Prakash Nagarkatti, for their unique leadership. Thank you for giving me the opportunity to be part of your team.

Thanks to my committee, Dr.Prakash Nagarkatti, Dr. Swapan Ray, Dr.Kenneth Walsh, Dr. Jun Zhu, whose insightful comments and advices which guided me through my study. To my lab faculty, Postdocs, staff and colleagues, thanks for always being friends and family in sadness and happiness times.

Thanks for all my Iraqi friends at the University of South Carolina and in the School of Medicine for their support and encouragements especially Huda Atiya, who's her friendship was exceptional! As well as my dearst friend Dr. Manal Al-Temimi.

Importantly, I would like to thank all my family in Iraq, my mother, my sisters: Afrah and Noor, and my brothers: Moner, Mustafa, Murtadha, Ahmed and my brother in law Zuhair who spiritually supported me throughout my years of study. Thanks for all your prayers and wishes.

I would like to especially thank my daughter, Alzahraa, who's her inspirational stories, her encouragement words and her hugs have an extraordinary impact on me, I love you to the moon and back million-time, Alzahra'a.

Great thanks to the graduate school especially Dr. Dale Moore for his help, encouragement, kindness and for the feeling that there is someone hold my back, and someone I can trust and I can talk to about whatever problem I have and importantly, resolve it. Many thanks for the Biomedical Science Graduate Director, Dr. Edie Goldsmith and the Biomedical Science Graduate staff, Mrs. Debra Poston, Joann Nagy and Kathryn Harris for their tremendous help and support.

I am very grateful to the International Student Services for their incredible help and for whatever they offer me and my family through all these years in the USC especially Mrs. Julia Ferillo.

Many thanks to our department office manager, Mrs. Nicole Holt for all her encouragements, help and treating me like a queen.

Finally, I would like to thank my friends, the security guards in the School of Medicine, Patricia Rembert, Janice Richardson, Roy Anglin and George Hamilton for their great help and support.

Many people have helped me throughout my journey at USC, and even though I could not mention their names due to space, I am grateful for all that you have done!

ABSTRACT

Inflammation is considered to be the underlying cause of a majority of clinical disorders. Thus, studies aimed at understanding the signaling pathways that trigger inflammation could have significant translational impact. In the current study, we investigated the effect of activation of cannabinoid (CB) and Aryl hydrocarbon hydroxylase (AhR) receptors on the inflammatory response. To that end, we used cannabinoids such as Δ (9)-Tetrahydrocannabinol (THC) and cannabidiol (CBD), and a well-established AhR agonist namely 2,3,7,8-Tetrachlorodibenzo-*p*-dioxin (TCDD). These were tested against two inflammatory disease models: 1) Experimental autoimmune encephalomyelitis (EAE), an animal model for human multiple sclerosis (MS), and 2) Exposure to pertussis toxin (PTX), an exotoxin produced by the bacterium, *Bordetella pertussis*, which causes whooping cough. We observed that combination of THC and CBD resulted in attenuation of EAE clinical scores and reduced proinflammatory cytokines secretion like IL-17A, IFN-γ, IL-6, TNF-α and IL-1β in the mononuclear cells of the brain. Treatment of EAE mice with cannabinoids also led to decrease in immune cell infiltration in the CNS, marked amelioration of CNS tissue destruction, and reduced demyelination when compared to control mice. Additionally, treatment with these cannabinoids led to cell cycle arrest and cell death in activated T cells. MicroRNA (miRNA) microarray analysis, revealed altered miRNA profile in brain infiltrating mononuclear cells following treatment with combination of THC and CBD that promoted anti-inflammatory pathways. Interestingly, THC+CBD treatment of EAE

mice caused alterations in gut microbiota with a decrease in the population of *Akkermansia muicinphila*, the bacteria that are increased in MS patients and involved in the pathogenicity of MS. In addition, THC+CBD treatment increased the production of a wide range of short-chain fatty acids (SCFAs) that are anti-inflammatory. In mice treated with PTX, there was significant induction of inflammation with an increase TH17 and TH1 proliferation. AhR activation in PTX-treated mice with TCDD, led to increased induction of FoxP3+ Treg cells and myeloid-derived suppressor cells (MDSC) that are highly immunosuppressive. In addition, TCDD altered the expression of microRNAs that promoted anti-inflammatory T cell phenotype. Together, the current study demonstrates that activation of CB and AhR on immune cells leads to epigenetic modulations as well as alterations in microbiota that promote anti-inflammatory signaling pathways. The current study suggests that targeting CB and AhR constitutes a unique therapeutic modality to treat inflammatory diseases.

.

TABLE OF CONTENTS

Dedication iii

Acknowledgements iv

Abstract vi

List of Tables ix

List of Figures x

Chapter 1: Inroduction 1

Chapter 2: Combination of Cannabinoids, Δ9 -Tetrahydrocannabinol and Cannabidiol, Ameliorates Experimental Multiple Sclerosis by Suppressing Neuroinflammation Through Regulation of miRNA-Mediated Signaling Pathways 10

Chapter 3: Combination of Cannabinoids, Δ9-Tetrahydrocannabinol (THC) and Cannabidiol (CBD), Mitigates Experimental Autoimmune Encephalomyelitis (EAE) By Diminishing The Gut Mucins Degrader Bacteria 47

Chapter 4: Ahr Activation By TCDD (2,3,7,8-Tetrachlorodibenzo-P-Dioxin) Attenuates Pertussis Toxin-Induced Inflammatory Responses by Differential Regulation of Tregs and Th17 Cells Through Specific Targeting Of Microrna..... 76

Chapter 5: Summary And Conclusion 107

References 109

LIST OF TABLES

Table 2.1 3'UTR alignments and scores of miRNAs and their target genes 40

Table 2.2 miRNAs with their seed sequences and fold changes 45

Table 2.3 mRNA quantitative RT-PCR primer sequences 46

Table 3.1 Source and concentration of SCFAs Standards 75

Table 4.1 Up-regulated and down-regulated miRNAs upon TCDD exposure 102

Table 4.2 mRNA related oligonucleotides that used in this study 103

Table 4.3 3'UTR alignments and scores of miRNAs and their target genes 104

LIST OF FIGURES

Figure 2.1 Combination of THC+CBD attenuates EAE by suppressing neuroinflammation 33

Figure 2.2 T cell population and phenotypic changes of WT and $CB1^{-/-}CB2^{-/-}$ EAE mice treated with vehicle or THC+CBD 34

Figure 2.3 Differentially expressed miRNAs in brain-infiltrating CD4+ T cells upon THC+CBD treatment in EAE mice 35

Figure 2.4 Expression of miRNA target genes involved in Th cell polarization..... 37

Figure 2.5 THC+CBD treatment induces cell cycle arrest / apoptosis in brain MNCs 38

Figure 2.6 Role of miR-21a-5p downregulation on THC+CBD-mediated amelioration of EAE 39

Figure 3.1 Combination THC+CBD treatment attenuates EAE disease severity and promotes anti-inflammatory immune response 66

Figure 3.2 Combination THC+CBD treatment alters the gut microbiome during EAE disease 67

Figure 3.3 LefSE analysis identifies *A.Muc* as a potential biomarker of EAE disease which is reduced after THC+CBD treatment 68

Figure 3.4 Combination THC+CBD treatment alters the gut microbiome metabolome during EAE disease 69

Figure 3.5 FMT of THC+CBD altered microbiome attenuates EAE severity 70

Figure 3.6 16S rRNA analysis of EAE treated with THC+CBD at the class level 71

Figure 3.7 16S rRNA analysis of EAE treated with THC+CBD at the order level..... 72

Figure 3.8 16S rRNA analysis of EAE treated with THC+CBD at the family level 73

Figure 3.9 16S rRNA analysis of EAE treated with THC+CBD at the genus level..... 74

Figure 4.1 TCDD suppresses PTX-induced inflammation in mice 95

Figure 4.2 TCDD suppresses PTX-induced Th1 cells and promotes Th2 cells 96

Figure 4.3 TCDD promotes Treg while inhibiting Th17 induction 97

Figure 4.4 TCDD promotes MDSCs production 98

Figure 4.5 MicroRNAs Analysis 99

Figure 4.6 qRT-PCR validation of gene expression 100

Figure 4.7 Role of miR-3082-5p and miR-1224-5p in regulating expression of IL-17A and FoxP3 respectively 101

CHAPTER 1

INTRODUCTION

1.1 MULTIPLE SCLEROSIS

Multiple Sclerosis (MS) is the most autoimmune inflammatory disease of autoimmune originate that affects the central nervous system (1-5). The demyelination effect this disease causes to the sheath which covers the nerves, damages the signals between the central nervous system (CNS) and the rest of the body, starting a massive list of symptoms that patients with MS suffer from. The precise cause of MS is still mysterious, yet its prevalence and incidence rates are increasing worldwide (6). It believes that environmental, genetic factors, and exogenous are the primary agents responsible for MS development (4). MS affects about 400,000 people in the US and close to 2.1 million people worldwide (7). MS is three times prevalent in women than men; it affects young people during their 20s and impairs their quality of life (7-9). Symptoms that disturb the quality of life may include fatigue, depression, reduced mobility, balance, numbness, pain, spasticity, cognitive impairment, dementia, vision , and bladder dysfunction(7). Several studies in Europe connect the mortality rate in multiple sclerosis patients with suicide after they noticed that it increased compared to other general populations (10). MS treatments that are available nowadays don't show any significant relief to the patients besides having immunotoxicity side effects (11). Additionally, this disease is still a diagnostic challenge, and the lack of quick and accurate diagnosis like the limited access to brain tissue could increase the cure challenge

(12). Currently, existing biomarkers for MS diagnosis and management have inherent limitations; that is why additional new biomarkers are required (13). Although the etiology of MS has not been uncovered yet, scientists found that CD4 T cells involved in its pathogenicity (11). CD4+T cells infiltrate across the blood–brain barrier (BBB) and promote inflammation, gliosis, neuroaxonal degeneration and demyelination leading to disruption of neuronal signaling. CD4+T cells infiltrate across the blood-brain barrier (BBB) and promote inflammation, gliosis, neuroaxonal degeneration, and demyelination leading to disruption of neuronal signaling. Differentiated CD4+ T helper 1 (TH1) and TH17 cells can infiltrate the CNS, leading to inflammation and tissue damage. In multiple sclerosis murine model, experimental autoimmune encephalomyelitis (EAE): emulsified central nervous system antigen is administered along with immune stimulants, leading to the generation of pathogenic CD4 T helper 1 (TH1) cells and TH17 cells in the lymph nodes. These cells then enter the circulation and eventually exert their effector functions in the CNS. CD4+ TH1 and TH17 cells then trigger the production of pro-inflammatory cytokines and chemokines that initiate the inflammatory response in the CNS.

1.2 MARIJUANA/CANNABINOIDS

Marijuana Cannabinoids are active components of *Cannabis sativa*, an annual herbaceous plant they have been used by many cultures for centuries in medicine (14-17). Many studies have been done to investigate the active role of these components and others extracted from this plant. Studies showed the anti-inflammatory and neuroprotective effects of Cannabinoids, which are effective in the treatment of several autoimmune diseases, such as MS (16, 18-20). It has been reported that more than 400

chemical components have been extracted from Cannabis Sativa, 80 of them find only in this plant, and they don't in any other plant. Also, over 60 components are cannabinoids (21). Δ(9)-Tetrahydrocannabinol (THC) is one of the major psychoactive constituents of cannabinoids derived from the Cannabis sativa plant and is known for its anti-inflammatory properties(22, 23). THC is well known for its immunoregulatory properties. Precisely, regarding T cell activation, THC treatment has been shown to reduce proinflammatory cytokines, including TNF-α and IFN-γ, and suppress proliferation of T cells through apoptosis and induction of regulatory immune cells (24-26). Also, THC is highly effective as a treatment in many models of T cell-driven inflammatory diseases, including autoimmune hepatitis, allogeneic hematopoietic cell transplantation, and inflammatory lung injury.(22, 26, 27).

CBD is another important cannabinoids component, a non-psychoactive cannabinoid that might be used to moderate effects of THC in the therapeutic setting by providing protection from the acute and permanent cognitive effects of THC (28). CBD has been shown to exhibit anti-inflammatory properties (29). After many clinical trials, the combined of THC and CBD oral/mucosal spray Sativex was approved in Canada for spasticity that associated with multiple sclerosis (23, 30-32). Using marijuana, particularly THC and CBD for therapeutic purposes continues to expand where there is a growing scientific evidence for specific applications in autoimmune diseases like multiple sclerosis (23). Studies showed that THC exerts its effects through CB1and CB2 receptors (15). Unlike THC, CBD does not bind and activate CB1 and CB2 receptors because CBD itself has no affinity for these receptors, but it can act as a negative allosteric modulator of CB receptors (20). Also, CBD has been shown to activate other

receptors such as 5-HT(1A), TRPV1 or GPR55. Both CB1 and CB2 are coupled to G-proteins where CB1 receptor presents in the central nervous system as well in the immune cells, while CB2 receptor represents in specific peripheral tissues, mainly the immune cells. THC shows its immunomodulated effect through CB1 and CB2 receptors, but CBD works indirectly through CB2 receptor (20).

1.3 THE ENDOCANNABINOID SYSTEM

Endocannabinoids are a collection of bioactive lipids that might help as secondary modulators, which when mobilized coincident with first-line immune modulators, either increase or decrease many immune functions. Endocannabinoids lipid mediators are N-arachidonoylethanolamine (anandamide, AEA) primarily isolated from porcine brain and 2-arachidonoylglycerol (2-AG) primarily isolated from canine intestines, which are the first to be discovered and extensively studied (33-35). Additionally, they considered as endogenous ligands for the cannabinoid receptors, CB1, and CB2 (36). AEA is responsible for preserving basal endocannabinoid signaling, binding to both the CB1 and CB2 receptors. In contrast to AEA, 2-AG functions as a full agonist for both CB1 and CB2. Furthermore, Anandamide and 2-arachidonyl glycerol (2-AG) bind to G protein-coupled cannabinoid receptors CB1 and CB2, respectively. These mediators show the immunosuppressive effect of cannabinoids.

1.4 MICRORNAS

MicroRNAs (miRNAs) are short non-coding, single-stranded regulatory RNAs (on average, 22 nucleotides in length) that regulate gene expression at the post-transcriptional level (33, 34). miRNA bind primarily to the 3′-UTR of their respective target mRNA, causing in translational repression or mRNA degradation, leading to a reduction in

encoded protein (35, 36). miRNAs have developed much attention because they control the expression of up to 30% genes and may play an essential role in the development of many complex diseases (9). Recent studies showed that miRNAs play important roles in a variety of physiologic and pathologic processes, most notably autoimmune diseases and cancer (37, 38). Several studies have demonstrated a role for miRNA in modulating immune responses under various inflammatory diseases (26, 39). miRNA dysregulation may contribute to the pathogenesis of multiple sclerosis (40). Identification of novel biomarkers and targets, for example, microRNAs, is beneficial to understand the pathogenetic mechanisms in a disease such as multiple sclerosis (41). Keller *et al.* found that the miRNA expression profiles in blood cells may serve as a biomarker for MS, and deregulation of miRNA expression may play a role in the pathogenesis of this disease (42). Moreover, mice deficient in miR-155 are resistant to developing experimental autoimmune encephalomyelitis (EAE), a mouse model of multiple sclerosis while the overexpression of miR-155 exacerbates the symptoms associated with the disease (19) (13). Collectively, these studies strongly suggest that miRNAs play a principal role in controlling immune cell activation, mostly T cells, in addition to promoting proinflammatory responses (26).

1.5 MICROBIOME AND MULTIPLE SCLEROSIS

Several environmental factors can affect immune function. Human healthy flora consists of bacteria, fungi, yeast, archaea, viruses, helminths, protozoa and parasites, that are mostly circulated in the internal cavity of our body, such as body surface, respiratory tract, digestive tract, urogenital tract, more than 95% of them situated in the large intestine (43, 44). The microbiota has an essential role in the initiation, training, and

function of the host immunity (45). Furthermore, the commensal flora has significant effects on the control of systemic inflammation and the development of autoimmune disorders in animal models (43). Specifically, Gut microbiome dysbiosis has been demonstrated to significantly influence a range of disorders in humans, including rheumatoid arthritis, diabetes, obesity, and multiple sclerosis (MS)(46). MS is a complex neural disease and still not fully understood etiology (6, 47). Whereas certain genetic and environmental factors are involved (48). Changed gut microbiota might be one of the main missing ecological factors contributing to MS since evidence recommends that certain gut microbiota might be connected to either disease susceptibility or defense (49-53). Furthermore, Studies found that metabolic deviation and alterations in the intracellular levels of specific metabolites are linked to the inflammatory phenotype of immune cells involved in autoimmune disorders such as rheumatoid arthritis, systemic lupus erythematosus, diabetes and multiple sclerosis (MS) (54). Short-chain fatty acids (SCFAs), the primary metabolites produced by bacterial fermentation of dietary fiber in the gastrointestinal tract, are estimated to have a critical role in microbiota-gut-brain linking(55). In recent years, the gut microbiota and fermentative metabolites like short-chain fatty acids (SCFAs) have received increased attention in relation to the development and disease course of MS (56, 57). Additional investigations are required to clarify the involvement of the gut microbiota and its metabolites, including potential useful effects of SCFAs, in the development and course of MS.

1.6 PERTUSSIS TOXIN AND INFLAMMATION

Pertussis toxin (PTX) is a multisubunit protein toxin excretes exclusively by *Bordetella pertussis* and it is one of the most potent virulence factors of this pathogen

besides the adenylate cyclase toxin. *Bordetella pertussis* is the bacterial agent of the pertussis disease or whooping cough (59). PTX is conveyed across the bacterial outer membrane via a type IV secretion system encoded by the *ptl* genes (58, 59). PTX has a broad range of effects on host cell activities because of its inhibitory effect on G-protein-coupled receptor pathways (60). During the peak of pertussis disease, and due to the PTX activity, the gene expression of IL-17, TNF-α and IFN-γ was up-regulated, demonstrating a mixed Th1 and Th17 cells response (61). Additionally, PTX has a role in autoimmunity where it involves in exacerbating certain experimental autoimmune diseases in rodent models, like Experimental Autoimmune Encephalomyelitis (EAE), the animal model of multiple sclerosis in humans (62). PTX increases in the permeability of the blood-brain barrier to allow the autoreactive T cells access to the central nervous system, initiating EAE pathology (63). Furthermore, PTX induces IL-6 and IFN-γ production and enhance the generation of Th17 cells to boost EAE effects (64-66).

1.7 AHR AND ROLE IN IMMUNE MODULATION

The aryl hydrocarbon receptor (AhR) is a transcription factor best known as the ligand for the toxin 2,3,7,8-tetrachlorodibenzo-p-dioxin (TCDD). However, it also binds to other toxins and to endogenous ligands. Using gene expression profile analysis, murine Th17 cells were shown to express the AhR which is also an essential component in the development of both regulatory T cells (Treg) and Th17 responses resulting in increased expression of IL-17 and IL-22 by Th17 cells (67). In another study, the AhR was shown to directly regulate Foxp3 expression via a mechanism involving modulation of TGF-β signaling (68)

1.8 TCDD (2,3,7,8-TETRACHLORODIBENZO-P-DIOXIN)

It is an extremely toxic environmental pollutant with a specific epigenetic carcinogen and a potential tumor promoter effects (69).TCDD belongs to the halogenated aromatic hydrocarbons compounds(70). TCDD is the most potent AhR agonist because of its strong binding affinity (K_d 10^{-10}–10^{-9} M) and resistance to metabolism (71). The aryl hydrocarbon receptor (AhR) was the first TCDD receptor to be studied (5). The aryl hydrocarbon receptor (AhR) is a significant cytosolic, ligand-activated receptor represented by different cells in many mammals.(72, 73). The AhR belongs to basic helix-loop-helix/Per-ARNT-Sim (bHLH-PAS) transcription factor families(5). AhR gene encodes a ligand-activated transcription factor over binding to halogenated aromatic hydrocarbons (HAHs) such as TCDD, as well as polynuclear aromatic hydrocarbons (PAHs) cause transformed gene expression and toxicity(74, 75). The AhR is necessary for T cells to generate $Foxp3^+$ Treg cells(76). Also, AhR is critical for the formation of Tr1 cells in mice and humans, which inhibits autoimmune responses by interaction with the transcriptional factor macrophage-activating factor to improve the expression of IL-10, IL-21, and IL-27(77). Additionally, AhR stimulation is involved in the promotion of Th17 to Tr1 transdifferentiation (78).

1.9 HYPOTHESES

In the current study, we tested the central hypothesis that inflammation can be regulated through activation of CB receptors and AhR. To that end, we used two models of inflammation: EAE and PTX and used specific ligands for CB receptors (cannabinoids) and AhR (TCDD) to study epigenetic pathways involving miRNA, and microbiota that may help regulate inflammation. The specific hypotheses tested include:

1.9.1. Combination of cannabinoids, Δ9- tetrahydrocannabinol (THC) and cannabidiol (CBD) can ameliorate experimental autoimmune encephalomyelitis:

1.9.1.1. Through modulation of the systemic or local pro/anti-inflammatory cytokine balance.

1.9.1.2. By promoting cell cycle arrest and apoptosis in activated T cells through miRNA signaling pathways.

1.9.1.3. By altering the gut microbiome.

1.9.2. AhR activation can attenuate PTX-mediated systemic inflammation and regulation of the immune response occurs:

1.9.2.1. Through modulation of the systemic pro and anti-inflammatory cytokine balance.

1.9.2.2. By suppressing Th17 cell proliferation and induction of Treg production through miRNA signaling pathways.

The subsequent chapters are dedicated to test these hypotheses

CHAPTER 2

COMBINATION OF CANNABINOIDS, Δ9 - TETRAHYDROCANNABINOL AND CANNABIDIOL, AMELIORATES EXPERIMENTAL MULTIPLE SCLEROSIS BY SUPPRESSING NEUROINFLAMMATION THROUGH REGULATION OF MIRNA-MEDIATED SIGNALING PATHWAYS

2.1 ABSTRACT

Multiple sclerosis (MS) is a chronic and disabling disorder of the central nervous system (CNS) characterized by neuroinflammation leading to demyelination. Recently a combination of Δ9-tetrahydrocannabinol (THC) and Cannabidiol (CBD) extracted from Cannabis has been approved in many parts of the world to treat MS-related spasticity. THC+CBD combination was also shown to suppress neuroinflammation, although the mechanisms remain to be further elucidated. In the current study, we demonstrate that THC+CBD combination therapy (10mg/kg each) but not THC or CBD alone, attenuates murine experimental autoimmune encephalomyelitis (EAE) by reducing neuroinflammation and suppression of Th17 and Th1 cells. These effects were mediated through CB1 and CB2 receptors inasmuch as, THC+CBD failed to ameliorate EAE in mice deficient in CB1 and CB2. THC+CBD treatment also caused a decrease in the levels of brain infiltrating CD4+ T cells and pro-inflammatory molecules (IL-17, INF-γ, TNF-α, IL-1β, IL-6, and TBX21), while increasing anti-inflammatory phenotype such as FoxP3, STAT5b, IL-4, IL-10 and TGF-β. Also, the brain-derived cells showed increased apoptosis along with decreased percentage in G0/G1 phase with increased percentage in

G2/M phase of cell cycle. miRNA microarray analysis of brain-derived CD4+ T cells revealed that THC+CBD treatment significantly down-regulated miR-21a-5p, miR-31-5p, miR-122-5p, miR-146a-5p, miR-150-5p, miR-155-5p, and miR-27b-5p while upregulating miR-706-5p and miR-7116. Pathway analysis showed that majority of the down-regulated miRs targeted molecules involved in cycle arrest and apoptosis such as CDKN2A, BCL2L11, and CCNG1, as well as anti-inflammatory molecules such as SOCS1 and FoxP3. Additionally, transfection studies involving miR-21 and use of *Mir21*$^{-/-}$ mice suggested that while this miR plays a critical role in EAE, additional miRs may also be involved in THC+CBD-mediated attenuation of EAE. Collectively, this study suggests that combination of THC+CBD suppresses neuroinflammation and attenuates clinical EAE development and that this effect is associated with changes in miRNA profile in brain-infiltrating cells.

2.2 INTRODUCTION

Multiple Sclerosis (MS) is chronic autoimmune disease that affects the central nervous system (CNS)(79-81). The incidence of MS is higher in women who are affected twice as often as men (82). Although the exact etiology of MS remains obscure, observational research has suggested that genetic and environmental factors may cause the onset and progression of the disease (83). Typically, MS is regarded as a T cell mediated autoimmune disorder, primarily driven by inflammatory Th1 and Th17 cells (83), (84). When autoreactive T-lymphocytes cross the blood brain barrier (BBB) and enter the central nervous system, they initiate local inflammation that results in demyelination, gliotic scarring, and axonal damage (85)

Cannabinoids extracted from marijuana (*Cannabis sativa*), as well as synthetic forms have been well characterized for their anti-inflammatory properties (15). Cannabinoids have also been shown to ameliorate spasticity and neuropathic pain in MS patients (86), (87). It is for this reason, a combination of Δ9 - tetrahydrocannabinol (THC) and Cannabidiol (CBD) has been approved as a drug (Sativex) in several countries including Europe, Australia and Canada (88). THC and CBD combination was tested recently in animal models of MS and was found to suppress neuroinflammation (89), (90). However, the precise mechanisms, such as the role of miRNA, in the efficacy of such combination treatment remain to be elucidated further. (THC) is well known for its psychoactive properties. It acts through CB1 receptors primarily expressed in the CNS and CB2 expressed predominantly on immune cells (91). Our laboratory and others have shown that THC increases anti-inflammatory and decreases pro-inflammatory cytokine production (16, 22, 26, 92) THC also mediates apoptosis in T cell driven inflammation, increases $FoxP3^{+}$ Tregs through miRNA induction and epigenetic modifications(22, 26). On the other hand, CBD is a non-psychoactive phytocannabinoid, has also been shown to exhibit anti-inflammatory properties (29). CBD has recently been approved by US FDA as a drug to treat epilepsy (91). Unlike THC, CBD does not bind and activate CB1 and CB2 receptors but can act as a negative allosteric modulator of CB receptors (93). Also, CBD has been shown to activate other receptors such as GPR55, TRPV1 or 5-HT1a (18, 94, 95). Thus, it is possible that a combination of THC+CBD may be more effective in treating inflammation by targeting both cannabinoid CB1 and CB2 receptors as well as other potential receptors such as GPR55, TRPV1 or 5-HT1a.

MicroRNAs (miRNA, miR) are a class of short non-coding single-stranded RNAs 19-24 nucleotides in length, involved in the post-transcriptional regulation of gene expression (81, 96, 97). miRNAs exert their regulatory role when they bind to the 3′ untranslated region (UTR) of target mRNA, eventually causing translational suppression through degradation or sequestration of mRNA (98) Several studies have detected the involvement of circulating miRNAs in physiological and pathological processes and identified them as potential biomarkers, therapeutic agents, or drug targets (99). Numerous miRNAs were found to be differentially expressed in patients with MS compared with controls and to have the potential to be used as diagnostic biomarkers or predictors of drug-response (100). Additionally, recent studies have shown crucial roles of specific miRNAs in controlling oligodendrocyte (OL) differentiation and myelination (101) Dysregulation of miRNAs contributes to the pathogenesis of demyelinating diseases (102) . Moreover, new patents of miRNAs also provide new strategies for gene therapy and miRNA-drug development for demyelinating diseases, especially MS (103). Our lab has previously shown that cannabinoids can suppress inflammation in the periphery through regulation of miRNA(16) (81, 104). However, whether cannabinoids can alter the expression of miRs in the brain-infiltrating cells during EAE and whether such miRs contribute towards suppression of neuroinflammation has not been investigated. In the current study, we used the combination of cannabinoids, THC and CBD, to address the potential ability of these components in ameliorating the symptoms and the progression of the disease in the EAE model, a murine model of MS. We demonstrate for the first time that the neuroprotective and anti-inflammatory properties of THC+CBD can be attributed to their ability to induce cell cycle arrest and apoptosis in

activated T cells as well as a switch of cytokines from pro-inflammatory to anti-inflammatory, through altered expression of miRNAs.

2.3 MATERIALS AND METHODS

Mice

C57BL/6 female mice aged 6-8-week-old and *Mir21*$^{-/-}$ mice were purchased from the Jackson Laboratory (Bar Harbor, ME). CB1$^{-/-}$CB2$^{-/-}$ mice were bred in-house. Mice were housed in a specific-pathogen-free facility at the University of South Carolina School of Medicine. All animal experiments were ethically performed according to the NIH guidelines and protocols approved by the University of South Carolina Institutional Animal Care and Use Committee.

Reagents

The reagents used in this study were purchased as described: THC and CBD from Cayman Chemical (Michigan. USA), myelin oligodendrocyte glycoprotein (MOG_{35-55}) peptide H-MEVGWYRSPFSRVVHLYRNGK-OH (PolyPeptide Laboratories, San Diego, CA, USA). *Mycobacterium tuberculosis* (strain H37Ra) (BD, Franklin Lakes, NJ, USA), complete Freund's adjuvant (Fisher, Hampton, NH, USA), Pertussis toxin (List Biological Laboratories, Campbell, CA, USA), Percoll, GE Healthcare Life Sciences (Pittsburgh, PA.USA); Neural Tissue Dissociation Kit (P) (Miltenyi Biotech, Auburn, CA.USA), RBC lysis buffer (Sigma-Aldrich, St. Louis, MO, USA), RPMI 1640, l-glutamine, HEPES, phosphate-buffered saline, and fetal bovine serum (VWR, West Chester, PA, USA), ELISA Max Kits IL-10, IL-17A, IFN-γ, IL-6, IL-1β, TNF-α and TGF-β and FITC Annexin V/ PI apoptosis kit (Biolegend, San Diego, CA). EasySep PE selection kit (Stemcell Technologies, Cambridge, MA. USA), Propidium Iodide

(PI)/RNase Staining Solution (Cell Signaling Technology, Danvers, MA, USA), miRNeasy Mini Kit, miScript II RT Kit and miRNAs primers (Qiagen, Valencia, CA), mRNAs primers (Integrated DNA technologies, Coralville, IA. USA) and SsoAdvanced™ Universal SYBR® Green Supermix (Bio-Rad, Hercules, CA, USA).

EAE induction, cannabinoid administration, and clinical assessment

EAE was induced in female C57BL/6 mice (6–8 weeks old) through subcutaneous (s.c.) immunization in the hind flank with 100 µl of 150 µg MOG_{35-55} peptide (PolyPeptide Laboratories San Diego, CA. USA) emulsified in complete Freund's adjuvant (Fisher, Hampton, NH, USA) containing 8 mg/ml killed Mycobacterium tuberculosis (strain H37Ra) (BD, Franklin Lakes, NJ, USA), as described previously(104, 105) Following immunization, 200 ng of pertussis toxin (List Biological Laboratories, Campbell, CA.USA) was given to the mice by intraperitoneal injection on day 0, followed by 400ng on day 2. Control mice received CFA+PTX but not MOG. To study the effect of THC+CBD treatment mice were randomized and treated with 10 mg/kg each THC and CBD or vehicle (2% dimethyl sulfoxide (DMSO) + 20% EtOH) diluted with sterile 1X PBS i.p. starting on day 10 after immunization and this treatment continued every day until the end of the experiment. Monitoring the animals and recording the clinical scores were done on a daily basis during the experiment. The mean of the score was calculated for each group every day. Clinical scores were recorded as follow: 0, healthy; 1, flat tail; 2, partial paralysis of hind limbs; 3, complete paralysis of hind limbs or partial hind and front limb paralysis; 4, tetraparalysis; 5, moribund; 6, death (106). Mice were provided daily with food and water (Boost and Hydrogel) in the cage floor after appearance of symptoms to ensure access to essential nourishment.

Nociception assay

Nociception is considered as one of the clinical markers of EAE(107). In the current study, we used the hot plate test to investigate nociception in unrestricted mice by placing each mouse on a platform surface which was maintained at 50°C. The response latency, which is the time taken to observe a nocifensive behavior that includes forepaw withdrawal or licking, hind paw withdrawal or licking, stamping, leaning posture and jumping, was recorded (108).

Histopathology

Perfused spinal cord tissues were isolated at 15 days post MOG immunization. Tissues were immersed in 4% paraformaldehyde for 24hr. Then paraffin blocks were prepared. Microtome sections (7 μm) were cut, and tissue sections were stained with Luxol Fast Blue (LFB) for detection of demyelination, in addition to haemotoxylin and eosin (H&E) staining for visualization of cellular infiltration. The images were acquired by Cytation 5 imaging reader (BioTek).

Isolation of immune cells

On day 15 post MOG immunization, inguinal lymph nodes (iLN) were excised from, EAE+Vehicle and EAE+(THC+CBD) prior to perfusion and were processed immediately to prepare single-cell suspensions. Then, mice were perfused slowly with 10 mL heparinized PBS to get rid of contaminated blood. Whole brain tissues were isolated then homogenized separately into a single-cell suspension by using the Neural Tissue Dissociation Kit (P) (Miltenyi Biotech, Auburn, CA.USA) and red blood cell lysis buffer (Sigma-Aldrich, St. Louis, MO.USA). Mononuclear cells (MNC) from whole brain homogenates were then isolated by centrifugation in media containing 33% (v/v) isotonic

Percoll in FACS buffer (1X PBS, 2% heat-inactivated fetal bovine serum) (GE Healthcare Life Sciences, Pittsburgh, PA, USA). Cells were immediately counted and processed for further assays.

Cell culture

Brain MNCs and splenocytes cells were cultured for 24h in complete RPMI 1640 media supplemented with 10% heat-inactivated fetal bovine serum, 10 mM l-glutamine, 10 mM HEPES, 50 μM β-mercaptoethanol (Sigma-Aldrich St. Louis, MO.USA), and 100 μg/ml penicillin/streptomycin at 37°C, 5% CO_2, 95% humidity (104). Cell culture supernatants were collected for ELISA and/or cells were processed for flow cytometry, apoptosis and cell cycle assays.

Detection of cytokines

Brain and iLN were isolated from EAE+VEH and EAE+(THC+CBD) mice and processed to obtain single-cell suspensions, and 1 x 10^6 cells were cultured for 24 hours at 37°C, 5% CO_2, 95% humidity as described (104). Cell culture supernatants were processed to detect interferon-γ (IFNγ), interleukin-17A (IL-17A), interleukin-6 (IL-6), Tumor Necrosis Factor-α (TNFα), interleukin 1β (IL-1 β), interleukin-10 (IL-10) and transforming growth factor-β (TGF-β) using ELISA kits following the manufacturer's instructions (BioLegend, San Diego, CA). Absorbance at 450nm was read on a plate reader and concentrations were calculated using standard curves.

Antibodies and flow cytometry

Cells were stained with fluorochrome-conjugated antibodies and analyzed via BD FACS Celesta (San Jose, CA) to determine phenotypes of infiltrating brain mononuclear cells. Antibodies used: fluorescein isothiocyanate (FITC) -conjugated anti-CD3 (clone:

145-2C11), Brilliant Violet (BV785)-conjugated anti-CD4 (clone: GK 1.5), from Biolegend (San Diego, CA).

Detection of (THC+CBD)-induced apoptosis in brain MNCs

To determine if (THC+CBD) induces apoptosis in brain MNCs, cells were purified and cultured as described (104). After 24 hr incubation, cells were collected and washed twice with ice-cold 1X PBS, and then resuspended in Annexin V Binding Buffer at a concentration of 0.25-1.0 x 10^7 cells/ml. Next, 100 µl of cell suspension was transferred to a 5 ml flow tube. Next, 5 µl of FITC Annexin V and 10 µl of Propidium Iodide Solution was added. The cells were gently vortexed and incubate for 15 min at room temperature in the dark. Finally, 400 µl of Annexin V Binding Buffer was added to each tube and analyzed by flow cytometry (BioLegend, San Diego, CA. USA).

Cell cycle analysis

Brain MNCs were cultured as described (104) . Cells were collected and stained with the PI/RNAs staining following the manufacturer's instructions (Cell Signaling Technology, Danvers, MA. USA). The data were acquired by flow cytometry and analyzed with ModFit LT 3.3 (Verity Software House, Topsham, ME) after debris and doublets were gated out.

CD4+ T cell selection

Brain MNCs were labeled with Phycoerythrin (PE)-conjugated anti-CD4 (Clone: GK 1.5) antibody (BioLegend, San Diego, CA) then immunomagnetically selected with EasySep PE-positive selection kit according to the manufacturer instructions (StemCell Technologies, Vancouver, BC). After selection, the purity of selected CD4 was measured

by flow cytometry which was routinely > 90%. $CD4^+$ T cells were lysed in Qiazol and stored at -80°C until RNA isolation (Qiagen).

RNA isolation and cDNA synthesis

Total RNA was purified from brain $CD4^+$ T cells by using miRNeasy micro kit according to the manufacturer instructions and the concentration and purity of RNA were determined using the NanoDrop 2000 spectrophotometer from Thermo Scientific (Wilmington, DE). Next, the expression profiling of miRNAs using the Affymetrix GeneChip miRNA 4.0 array platform was performed as previously described (109)(. To validate miRNAs expression, the miScript cDNA synthesis kit used followed by quantitative real-time polymerase chain reaction (qRT-PCR) using the miScript SYBR Green PCR kit. Fold change of the interested miRNAs was determined using the $2^{-\Delta\Delta Ct}$ method and expressed relatively to Snord96a. (Bio-Rad, Hercules, CA, USA). Validation of target genes expression, primers were purchased (Integrated DNA technologies, Coralville, IA. USA) and quantitative real-time polymerase chain reaction (qRT-PCR) was performed using SsoAdvanced universal SYBR Green supermix (Bio-Rad, Hercules, CA, USA). Fold change of the interested mRNAs was determined using the $2^{-\Delta\Delta Ct}$ method and expressed relative to GAPDH.

Transfection with miR-21a-5p mimic and inhibitor

Splenic CD4+ T cells were purified by using the EasySep PE selection kit. The purity of the isolated cells was confirmed to be 97% CD4+ T cells by flow cytometry. Then cells were maintained for 24 hours in complete RPMI 1640 media supplemented with 10% heat-inactivated fetal bovine serum, 10 mM l-glutamine, 10 mM HEPES, 50 μM β-mercaptoethanol, and 100 μg/ml penicillin/streptomycin at 37°C and 5% CO_2 (22)

Cells were seeded at 2 × 10^5 cells/well in a 24-well plate and transfected for 24 hours with mock control or 40 nM synthetic mimic or inhibitor oligonucleotides using HiPerFect transfection reagent (Qiagen, Germantown, MD) according to the manufacturer's instructions. Total RNA and protein were extracted for analysis.

Statistical analysis

We performed statistical analysis using GraphPad Prism 8 (GraphPad Inc, La Jolla, CA). The data shown in this study represent at least three independent experiments to ensure consistency of findings. The statistical differences between groups were calculated using Student's t-test for paired analyses or one- or two-way ANOVA for multiple group analyses. Mann–Whitney *U* test was performed to evaluate the extended clinical scoring in EAE mice, as described (104, 110). Statistical tests with post hoc tests are indicated in each figure legend. A p value of ≤ 0.05 was considered significant.

2.4 RESULTS

Combination of THC and CBD attenuate the development of EAE

Combination of THC+CBD has been used to treat human MS (111). This treatment is known to decrease not only muscle spasticity but also suppress neuroinflammation (89, 90). To further investigate the mechanisms of suppression of neuroinflammation, we used murine model of EAE. Mice were treated daily with THC alone (10mg/kg), CBD alone (10mg/kg), or a combination of THC+CBD (10mg/kg each) starting at 8-10 days after MOG immunization (Figure 1A). Use of CFA+PTX as a control did not trigger any clinical signs of paralysis and furthermore, treatment of these mice with cannabinoids did not have any effect, thereby showing that the subsequent studies reported on EAE development using MOG was antigen-specific. Thus, in all subsequent experiments, we

used CFA+PTX+MOG to induce EAE and study the effect of cannabinoids. The combination THC+CBD treatment resulted in attenuation of the clinical symptoms of EAE vs mice treated with Vehicle (VEH) (Figures 1C & 1D). Also, treatment with THC or CBD alone, at the doses tested, failed to cause significant suppression of clinical symptoms. On day 14, the clinical scores were significantly reduced only in THC+CBD group but not in THC or CBD alone groups (Figure 1D). These results indicated that the combination of THC+CBD was effective to treat mice with EAE. Based on these data, we focused our subsequent studies to combination treatment only. Thus, an extension of the experiment until day 27 demonstrated that THC+CBD treatment was highly effective long-term at reducing clinical signs of EAE (Figures 1E & 1F).

Next, we performed histological analysis on spinal cord tissues harvested at day 15. The spinal cord tissues from EAE+VEH mice showed elevated cellular infiltration vs Naïve mice when stained with H&E (Figure 1G). Also, extensive demyelination was observed in the white matter area with LFB staining in EAE+VEH vs Naïve mice (Figure 1G). Both cellular infiltration and demyelination were reduced in spinal cord tissue of EAE+(THC+CBD) mice (Figure 1F). To test the role of CB1 and CB2 receptors in our model, we induced EAE in both wild-type (WT) and $CB1^{-/-}CB2^{-/-}$ double-knockout mice, and then treated with THC+CBD. Absence of cannabinoid receptors resulted in the inability of THC+CBD to reduce clinical scores of EAE (Figures 1H & 1I). The hot plate test was also performed to test the pain response and WT EAE+(THC+CBD) mice had increased withdrawal latency period indicating that cannabinoid receptor activation with THC+CBD had analgesic effects as well (Figure 1J).

Treatment with THC+CBD attenuates T-cell mediated inflammation in draining lymph nodes and brain

Cell culture supernatants were isolated from draining iLN cells isolated at the peak of the disease. The cells were cultured at equivalent cellular density for 24hr and supernatants were assessed for the Th17 and Th1 pro-inflammatory cytokines, IL-17A and IFNγ, respectively. THC+CBD treatment reduced production of IL-17A and IFNγ in iLN (Figure 2A). Additionally, flow cytometry analysis of encephalitogenic mononuclear cells (MNC) isolated from brain tissue showed decreases in the populations of total MNCs, CD3+ T cells, and of CD3+CD4+ Th cells in the EAE+(THC+CBD) group when compared to other experimental groups (Figures 2B & 2C). Use of $CB1^{-/-}$ $CB2^{-/-}$ double-knockout mice showed that the effect of THC+CBD in decreasing neuroinflammation was mediated through these cannabinoid receptors (Figures 2B & 2C) because THC+CBD was ineffective in these mice.

miRNA analysis of THC+CBD treated EAE mice

Because miRNAs play an important role in autoimmune diseases and neuroinflammation (112, 113), we investigated the role of miRNA in the THC+CBD-induced attenuation of neuroinflammation in EAE mice. To that end, brain CD4+ T cells were isolated from mice treated with THC+CBD or vehicle as described earlier and used for miR microarray analysis. Of approximately 2000 miRNAs tested, 157 miRNAs were differentially expressed (Fold change > +/- 1.5) (Figure 3A). Proportional Venn diagram was generated to represent the fold change of the miRNAs that were up- or down-regulated following treatment with THC+CBD in EAE mice (Figure 3B). A heat map generated showed different expression profile of miRNAs in the experimental groups (Figure 3C). Pathway analysis of the differentially expressed miRNAs was performed

with Ingenuity Pathway Analysis (IPA, Qiagen) and showed interaction with cell cycle, apoptosis, and T cell polarization molecules (Figure 3D). The microarray data and pathway analysis indicated several miRNAs that have been previously involved in the pathogenicity of MS such as, miR-31, -21a, -146a, -155 and -33(41) Quantitative RT-PCR validated that THC+CBD treatment led to downregulation miR-21a-5p, miR-31-5p, miR-122-5p, miR-146a-5p, miR-150-5p, miR-155-5p, and miR-27b-5p (Figures 3E-3K). These miRNAs were found to directly target IL-10, FoxP3, SOCS1, Bcl2L11 and CCNG1 (Figure 3D and Table 1). THC+CBD treatment increased expression of miR-706-5p and miR-7116 (Figure 3L-3M). The IL-17A gene was one of the hallmark genes that is targeted by miR-706-5p (Figure 3D and Table 1). Genes encoding TNF-α and IL-6 were found to be targeted by miR-7116-5p (Figure 3D and Table 1). These genes play a pivotal role in EAE progression. Putative 3' UTR targeting was analyzed for each miRNA-mRNA pairing using TargetScan alignment tools and microRNA.org (Table 1). Collectively, these data indicated that microRNA may have an integral role in the ameliorative effect of THC+CBD in EAE mice.

Cytokine expression at gene and protein levels in EAE brain MNCs

Pathway analysis identified miRNAs that targeted pro-inflammatory and anti-inflammatory cytokines and Th subset transcription factors (Figure 3D). Expression of these target genes was validated by qRT-PCR (Figures 4A-4K). Treg related genes *Foxp3, Stat5b, and IL10* were upregulated in EAE+(THC+CBD) brain-derived CD4+ T cells (Figures 4A-4C). Th2 related genes *Gata3* and *Il4* were also upregulated in CD4+ T cells following treatment (Figures 4D & 4E). Conversely, Th17 related genes *Stat3* and *Il17a* were downregulated following THC+CBD treatment (Figures 4F & 4G). Likewise,

Th1 related genes *Tbx21* (encoding Tbet) and *Ifng* were downregulated in EAE+(THC+CBD) (Figures 4H & 4I). In addition, pro-inflammatory cytokines *Il6* and *Il1b* were downregulated (Figures 4J & 4K). Cell culture supernatant of mononuclear cells from brain was used to evaluate cytokine production. In accordance with gene expression changes, IL-17A, IFNγ, TNFα, IL-6, and IL-1β production was reduced, while IL-10 and TGFβ production was increased in MNC supernatant from EAE+(THC+CBD) mice (Figure 4L).

Detection of cell cycle arrest / apoptosis in brain MNCs

miRNA array and pathway analysis also revealed that some pro-apoptotic and cell cycle arrest genes were targeted by downregulated miRs in EAE+(THC+CBD) mice including *CDKN2A, SOCS1, Bcl2L11,* and *CCNG1* (Figure 3D). We validated upregulation of these genes by qRT-PCR (Figures 5A-5D). Fold change was expressed relative to GAPDH. The primers used in the study are highlighted in Table 3. In addition, PI staining demonstrated that WT EAE+(THC+CBD) mice, in brain MNCs, had less cells in G0/G1 phase but more cells in G2/M phase of cell cycle when compared to WT EAE+Veh group (Figures 5E &5F). We also used a combination staining of Annexin V-FITC with PI double-staining to identify early apoptotic ($AnnexinV^+/PI^-$) and late apoptotic cells ($AnnexinV^+/PI^+$). Late apoptosis was elevated in WT EAE-(THC+CBD) (Figures 5G & 5H). In some of these experiments, we also used $CB1^{-/-}CB2^{-/-}$ double knockout mice to test if the action of THC+CBD was mediated through cannabinoid receptors and we did find that to be true. However, these mice showed some changes in apoptosis when compared to WT mice which can be explained by the fact that in these

mice, endocannabinoids were not able to act or that these mice had some compensatory mechanisms acting.

Mir21$^{-/-}$ mice are more resistant to EAE than wild-type mice

In our study, we found that THC+CBD treatment downregulated miR-21a-5p expression in brain CD4+ T cells (Figures 3C-3E). To further address the role of this miRNA, we performed an in vitro miRNA transfection assay in $CD4^+$ T cells and used qRT-PCR validation to test for miR-21 and target genes in cells transfected with mock, mimic or inhibitor (Figures 6A-6D). The data showed that use of miR-21 mimic led to a decrease in the expression of target genes while inhibitor caused significant induction of the target genes. In addition, we also used mice deficient in miR-21. Genotyping for the parents and the first generation of *Mir21*$^{-/-}$ mice (miR-21 KO) confirmed inactivation of the miR-21 gene (Figure 6E). To test the role of miR-21 in THC+CBD-mediated amelioration of EAE, we induced EAE in WT and *Mir21*$^{-/-}$ mice then treated with THC+CBD when symptoms appeared. The clinical scores revealed that *Mir21*$^{-/-}$ mice had less disease severity when compared with WT EAE mice (Figures 6F and 6G). Treatment with THC+CBD in *Mir21*$^{-/-}$ mice further reduced clinical symptoms of EAE similar to WT EAE+(THC+CBD) (Figures 6F & 6G). We performed cell cycle analysis in brain MNCs stained with PI to detect cell cycle by flow cytometry. The EAE-induced *Mir21*$^{-/-}$ mice were more similar to EAE+(THC+CBD) group in that these mice showed less cells in G0/G1 phase and more cells G2/M phase and furthermore, THC+CBD treatment in these mice failed to further cause significant changes in cell cycle thereby showing that THC+CBD-mediated effects on cell cycle are mediated through miR-21 (Figures 6H-6I).

Because *Mir21*$^{-/-}$ mice were more resistant to EAE when compared to WT mice, these data suggested that miR-21 does play a critical role in EAE and therefore, THC+CBD mediated down-regulation of miR-21 may play a role in cannabinoid-mediated attenuation of EAE. However, when we treated *Mir21*$^{-/-}$ mice with THC+CBD, we found that these mice exhibited further reduction in EAE thereby suggesting that additional miRNAs may also be involved in the efficacy of cannabinoids to suppress EAE.

2.5 DISCUSSION

MS is an immune-mediated inflammatory disease of the CNS (114, 115). The precise mechanisms of pathogenesis of MS remain unknown, although environmental as well as genetic components are believed to participate in this demyelinating disease(116) Current treatments for MS often consist of immunosuppressive drugs with many side-effects after prolonged use. In the current study, we investigated the role of miRNA in the attenuation of EAE by a combination of cannabinoids, THC and CBD, and found that such a treatment altered the expression of miRNA in brain MNCs that targeted inflammatory pathways leading to decreased expression of inflammatory cytokines as well as promotion of cell cycle arrest and apoptosis in encephalitogenic T cells in brain.

Recently, a combination of THC+CBD, extracted from Cannabis plant, named Sativex, has been approved to treat MS in over 28 countries, including Europe and Canada to help improve muscle spasticity(111, 117). It is noteworthy that in the current study, while we used a combination THC and CBD, these were pure compounds, whereas in Sativex, the THC+CBD extract from *Cannabis* also includes low levels potentially other minor phytocannabinoids and terpenes, which may enhance the effects of

THC+CBD, called the 'entourage' effect. Thus, this finding constitutes a limitation in comparing our studies to Sativex. Nonetheless, our studies also demonstrate that pure forms of THC+CBD can also serve as therapeutic modality in the treatment of MS. We and others have shown that both THC and CBD are potent suppressors of inflammation in a variety of autoimmune and inflammatory disease models (16, 26). Thus, it is likely that THC+CBD combination can also suppress neuroinflammation, in addition to suppressing muscle spasticity. In fact, recent studies demonstrated that THC+CBD combination can attenuate EAE by suppressing neuroinflammation (89, 90)and our study further supports this finding. It should be noted that we and others have shown that THC and CBD when used alone, can suppress EAE (16, 19, 118, 119) In the current study, we observed that CBD or THC when administered alone at 10mg/kg failed to suppress clinical scores in MOG-induced EAE. We found in a previous study that a dose of 20mg/kg of CBD was necessary to attenuate clinical signs in EAE (16) . There are limited studies on THC and the dose and efficacy may depend on the model of EAE, its use as preventive or treatment measure, the strain/species model used and the like (120) Nonetheless, we found in our current study, using cannabinoids after disease onset, that a single dose of CBD or THC at 10 mg/kg was not effective while a combination of these was highly effective in suppressing clinical symptoms and neuroinflammation in EAE. It should be noted that in a previous study, the authors treated EAE mice with THC (20mg/kg), CBD (20mg/kg) or THC+CBD (10mg/kg each), daily from the day symptoms appeared till the first relapse of the disease and found that the three treatments delayed the onset of symptoms. However, only THC+CBD or THC alone were able to attenuate neurological disability while CBD failed. The difference between this study and the

current study is that we used lower doses of THC or CBD alone (10mg/kg) and we treated the mice for much shorter duration. The reason for the design of our study was to identify the miRNA which would be induced early on and characterize them. Thus, it is possible that if we had continued treatment with CBD or THC alone for the entire duration of the study, we could have found these to be effective.

It is well-established that THC acts through CB1 and CB2 receptors while CBD does not bind to these receptors or binds with very low affinity but in vivo, may act through other receptors such as GPR55, TRPV1, 5-HT1a or PPAR-□ (18, 94, 95) (121),(90). Nonetheless, CBD can alter the uptake and breakdown of endocannabinoids thereby indirectly affecting the activation of CB receptors or it can mediate CB1 antagonism (122, 123) In the current study, we used mice deficient in CB1 and CB2 and found that these mice bearing EAE when treated with THC+CBD failed to exhibit EAE amelioration which suggested that THC+CBD treatment was acting through these receptors. However, these mice showed similar levels of clinical disease as the wild-type mice. This may be because they may exhibit some compensatory mechanisms or that the endocannabinoids in the absence of CB1 and CB2 may act on other receptors such as the vanilloid receptors (124) To the best of our knowledge, there are no previous studies on the use of such double-knockout mice in EAE. However, the use of mice deficient in CB1 or CB2 alone has provided evidence for the involvement of these receptors and endocannabnoids in EAE. For example, mice deficient in CB1 receptor showed a more severe clinical course indicating that endogenous cannabinoids activate CB1 that helps control neuroinflammation and EAE (125) Also, CB2 knockout mice were shown to exhibit exacerbated EAE. However, pharmacological agonism or antagonism of CB2

failed to affect EAE in ABH mice (126). Such studies have raised some concerns about the translational value of some transgenic/gene knockout studies which may depend on susceptibility genetic backgrounds (127). Additionally, the knockout mice may have different microbiota which may influence EAE as shown in our studies in mice with CD44 deletion (128) Thus, clearly, additional studies are necessary on use of CB receptor knock out mice in understanding the role of cannabinoids in EAE. In the current study, the anti-inflammatory properties of THC+CBD were evident in their ability to decrease the expression of pro- inflammatory cytokines (IL-17A, IL-6, TNF-α, IFNγ and IL-1β) induced in EAE. Also, Chalah MA *et al*. found that the pro-inflammatory cytokines IL-6, TNF-α, and IFNγ are related to MS fatigue, which is one of the distinct symptoms that the MS patients are suffering from(129) T-bet is a Th1 cell-specific transcription factor that controls the expression of the hallmark Th1 cytokine, IFN-γ (130) In our study we found that its expression was repressed along with other cytokine transcription factors of IL-17A, IL-6 and TNF-α after treatment with the THC+CBD, which demonstrate the inflammatory suppressive role of the cannabinoids. Increased GATA-3 expression plays an important role in enhancing IL-4 production in differentiated Th2 and inhibiting Th1 differentiation (131) On the other hand, we also found that the cannabinoids increased the expression of the anti-inflammatory cytokines (IL-10 and TGF-β). It has been reported that the deficiency or abnormal expression of IL-10 can increase inflammatory response to microbial challenge but also lead to development of inflammatory bowel diseases (IBDs) and several autoimmune diseases (132, 133) Overall, our data are consistent with the previously reported studies demonstrating that cannabinoids suppress cytokine production and promote Th2 while

suppressing Th1 cells (22, 25, 134) Our previous studies have also identified the mechanisms through which cannabinoids such as THC suppress cytokine production. One of the mechanisms include epigenetic modifications in which THC treatment leads to the association of active histone modification signals to Th2 cytokine genes and suppressive modification signals to Th1 cytokine genes, leading to a switch from Th1 to Th2 (135)

We have previously shown that miRNA play a critical role in cannabinoid-mediated suppression of inflammation. In delayed-type hypersensitivity (DTH) model, we noted that THC suppressed Th17 cell differentiation through suppression of miR-21 expression, which induced SMAD7 consequently suppressing Th17 (22) THC also caused downregulation of miR-29b, an IFN-γ inhibitor. THC treatment reversed this miR dysregulation. Additionally, when we transfected primary cells from DTH mice with miR-21 inhibitor or miR-29b mimic, there was an increase in SMAD7 and decrease in IFN-γ expression, respectively. In the current study, we observed downregulation of miR-155 in EAE mice treated with THC+CBD. Recent studies have focused on the participation of miR-155 in EAE. MiR-155 mediates inflammatory response through promoting the development of inflammatory Th1 and Th17 cells. Furthermore, miR-155 has been involved in inhibiting the protein suppressor of cytokine signaling 1 (SOCS1) in activated CD4+ T cells (136) Mice lacking miR-155 (mir-$155^{-/-}$) have reduced EAE disease severity accompanied by less CNS inflammation and decreased Th1 and Th17 responses (136) In addition, in the current study, we also noted that cannabinoid treatment led to down-regulation of miR-31, which targeted FoxP3. This is consistent with previous findings that miR-31 targets Foxp3 and it is under expressed in human

natural Tregs (137) Also, it has been shown that conditional deletion of miR-31 leads to an increase in peripheral Tregs and reduced severity of EAE (138)

Studies from our laboratory have shown that THC and CBD when tested individually can trigger apoptosis in immune cells as well as in some cancer cell lines (94) (17, 139-141) However, roles of miRNA in the regulation of cannabinoid-mediated apoptosis in immune cells are not clearly understood, especially with respect to MNCs isolated from the brain during neuroinflammation. In the current study, we noted that THC+CBD treatment led to significant increase in apoptosis in brain MNCs, which also showed decrease in G0/G1 phase of cell cycle and increase in G2M phase. Our results demonstrated that THC+CBD treatment caused downregulation of some miRNAs like miR-122-5p and miR-21a-5p, which may target genes that regulate cell cycle arrest and apoptosis such as *Bcl2L11*, *CCNG1* and *CDKN2A*, which were found to be upregulated. Moreover, treatment with THC+CBD led to upregulation of miRNAs such as miR-706-5p. It has been reported that miR-706-5p affects the expression of cell division cycle associated 4 gene, *Cdca4*, a gene that is important for cell cycle G1 phase progression specifically through the E2F/retinoblastoma protein pathway (142) Also, miR-706-5p downregulates the activity of *Cacul1,* which is a cell cycle associated protein capable of promoting cell proliferation through the activation of CDK2 at the G1/S phase transition(143) In addition, some of the miRNA may also target FoxP3 expression. For example, our pathway analysis showed that miR-31 may regulate FoxP3 consistent with previously published findings that this miR negatively regulates FoxP3 expression in Tregs (137). Interestingly, we noted that THC+CBD treatment led to significant down-regulation of miR-31 and an increase in *FoxP3* expression in brain MNCs.

While THC+CBD treatment led to alterations in many miRNAs, we further focused our studies on Mir-21. We observed that *Mir21*$^{-/-}$ mice were more resistant to EAE when compared to WT mice; these data suggested that miR-21 does play a critical role in EAE. These data are consistent with previous studies showing that miR-21 deficiency leads to increased resistance to EAE (144) Because our data also demonstrated that THC+CBD treatment caused down-regulation of miR-21, these data together suggested that miR-21 may play a critical role in cannabinoid-mediated attenuation of EAE. However, when we treated *Mir21*$^{-/-}$ mice with THC+CBD, we found that these mice exhibited further reduction in EAE thereby suggesting that additional miRNAs may also be involved in the efficacy of cannabinoids to suppress EAE.

In conclusion, this combination therapy resulted in alleviation of the clinical symptoms of EAE, a mouse model of human MS. Treatment of THC+CBD resulted in reduction of the clinical signs of disease, reduction in pro-inflammatory cytokine production, and decreased inflammatory infiltration of cells into the CNS, which prevents the hallmark of disease progression, which is the demyelination of neuronal cells. Acting in a neuroprotective manner, we observed that THC+CBD induced apoptosis and cell cycle arrest (G2/M) in brain-infiltrating cells. From a mechanistic standpoint, we found that this combination therapy leads to dysregulation of several miRNA, post-transcriptional modifiers of gene expression. We were able to correlate this miRNA dysregulation to several features of cellular pathways, such as apoptosis and cell cycle arrest. Specifically, in the current study we show decreased expression of miR-21 correlates with increased expression of the target *Bcl2L11*, a pro-apoptotic factor belonging to the BCL-2 family of proteins.

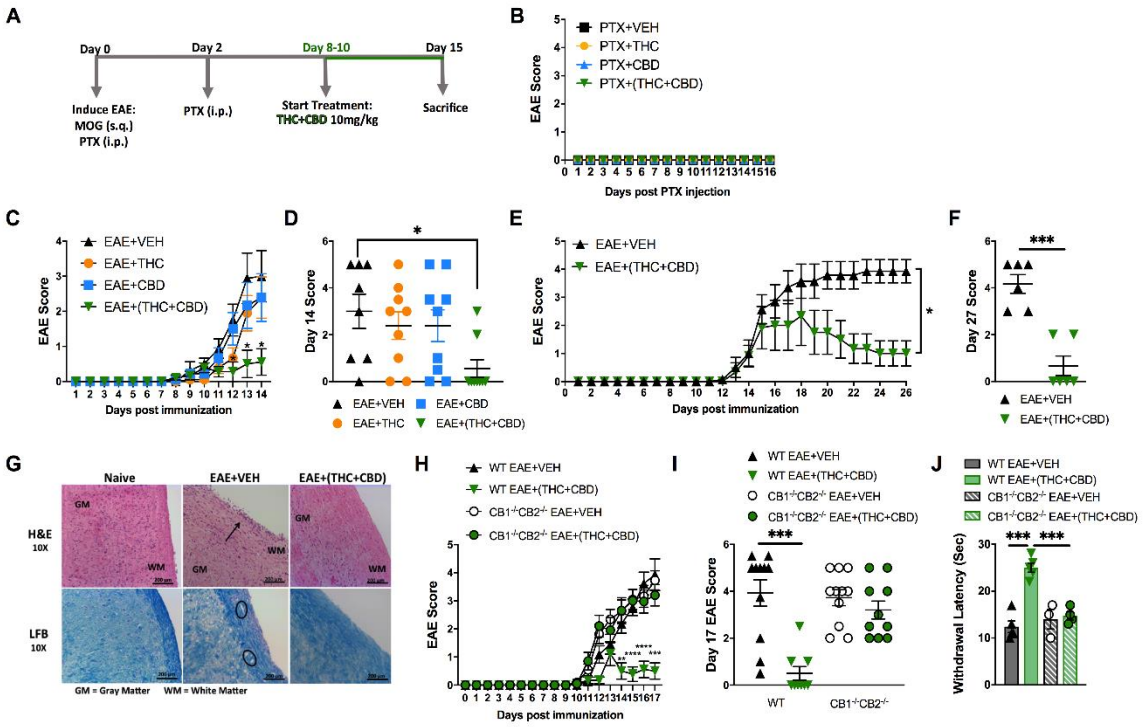

Figure 2.1 Combination of THC+CBD attenuates EAE by suppressing neuroinflammation. EAE was induced in C57BL/6 mice using CFA+PTX+MOG, as described in Methods. These mice were treated with cannabinoids and the mice were studied for clinical signs of paralysis and neuroinflammation. (A) Experimental timeline. EAE mice were treated daily with THC (10mg/kg), CBD (10mg/kg), or a combination of THC+CBD (10mg/kg each) starting at 8-10 days after MOG immunization. (B) Controls consisting of mice that received CFA+PTX only that received cannabinoids. (C&D) Clinical scoring of EAE symptoms in mice treated with Veh, THC, CBD, or THC+CBD. (E&F) EAE scoring in an extended experiment until day 27 in Veh vs THC+CBD treated EAE mice. (G) Representative H&E images and LFB staining in spinal cord tissues to detect cellular infiltration and demyelination, respectively. (H&I) EAE scoring in WT or CB1-/-CB2-/- double knockout mice treated with either Veh or THC+CBD. (J) Withdrawal latency time during the hot plate test to quantify analgesic sensitivity. Data presented are mean +/- SEM. For (B-C & H), significance was determined by two-way ANOVA with a Dunnett post hoc test. For (D & I), one-way ANOVA with a Dunnett post hoc test was used. For (E) Mann-Whitney U test was performed excluding scoring values before initiation of treatment. For (F), an unpaired two-tailed T-test was performed. For (J), one-way ANOVA with a Sidak correction was used. ****p<0.0001, ***p<0.001, *p<0.05.

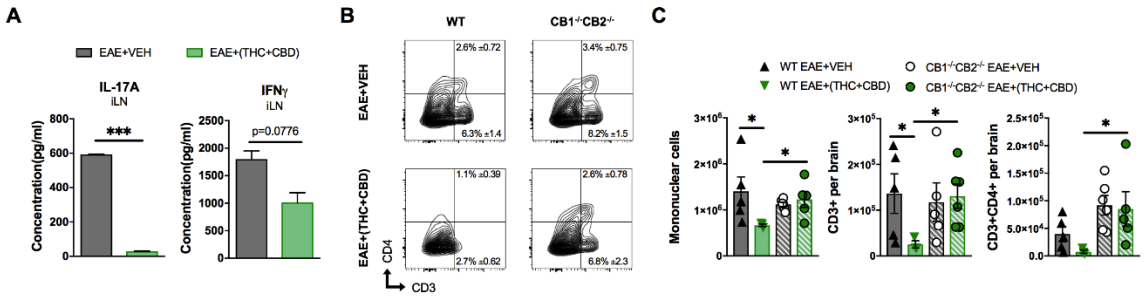

Figure 2.2 T cell population and phenotypic changes of WT and CB1$^{-/-}$CB2 $^{-/-}$ EAE mice treated with vehicle or THC+CBD. As shown in Figure 1, EAE was induced in naïve mice then mice were treated with Veh or THC+CBD when symptoms appeared. Inguinal lymph nodes and brain MNCs were collected at the peak of disease (Day 15 post immunization). (A) IL-17A and IFNγ concentration in inguinal lymph node 24h culture supernatant measured by ELISA. (B) Representative flow cytometry contour plots of encephalitogenic T cells. (C) Quantification of total MNCs, CD3+ T cells, and CD3+CD4+ Th cells per brain. Data presented are mean +/- SEM. ***p<0.001, *p<0.05 by unpaired two-tailed T test (A), or Kruskal-Wallis test (C).

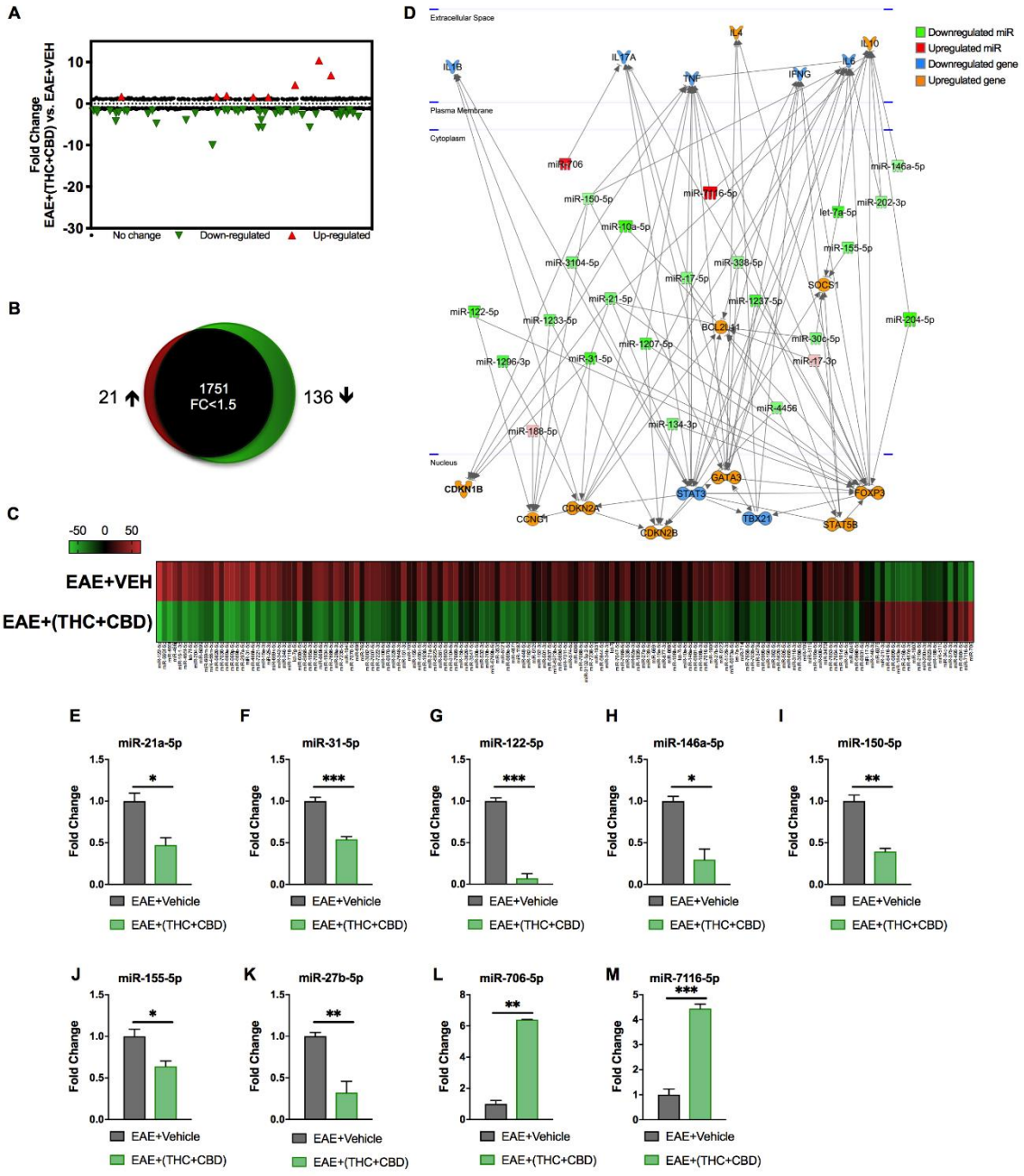

Figure 2.3 Differentially expressed miRNAs in brain-infiltrating CD4+ T cells upon THC+CBD treatment in EAE mice. Total RNA was isolated and pooled from CD4+ T cells obtained from the brains of EAE mice post-treated with vehicle (n = 5) or THC+CBD (n = 5) on day 15. MicroRNA microarray expression levels of differentially expressed miRNAs were generated. (A) The fold change distribution of all 1,908 miRNAs tested. (B) Proportional Venn diagram illustrating fold change of miRNAs that were >1.5- fold dysregulated following treatment with THC+CBD in EAE mice. (C) Heat map of the 157 dysregulated miRNAs. The color scale denotes those miRNAs that

were upregulated (red) and downregulated (green). (D) Pathway analysis of miRs mediating dysregulation in gene expression following THC+CBD treatment. (E-M) Expression levels of selected upregulated and downregulated miRNAs were validated by qRT-PCR using Snord96a as a small RNA endogenous control. Data presented are mean +/- SEM. ***p<0.001, **p<0.01, *p<0.05 by unpaired two-tailed T test.

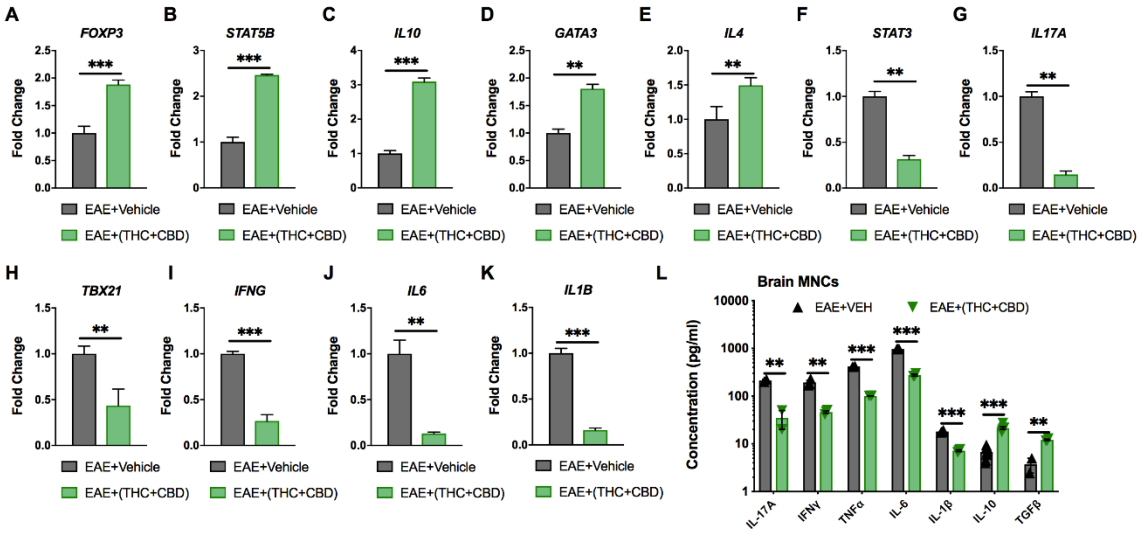

Figure 2.4 Expression of miRNA target genes involved in Th cell polarization. As described in Figures 2 and 3, CD4+ T cells or total MNCs were isolated from brains of EAE mice on day 15 post immunization. For panels A-K, RNA was extracted from CD4+ T cells and used for miR target gene validation. For panel L, total MNCs were cultured for 24h and supernatants were collected for cytokine analysis. (A-K) qRT-PCR validation of the target genes (A) Foxp3, (B) STAT5B, (C) IL-10, (D) GATA3, (E) IL-4 (F) STAT3, (G) IL-17A, (H) TBX21, (I) IFN-γ, (J) IL-6 and (K) IL-1β using GAPDH as endogenous control. (L) IL-17A, IFN-γ, TNF-α, IL-6 IL-1β, IL-10 and TGF-β concentration measured in MNC culture supernatants by ELISA. Data are expressed as the mean ± S.E.M. and statistical significance is indicated as ***p<0.001, **p<0.01 by unpaired two-tailed T test.

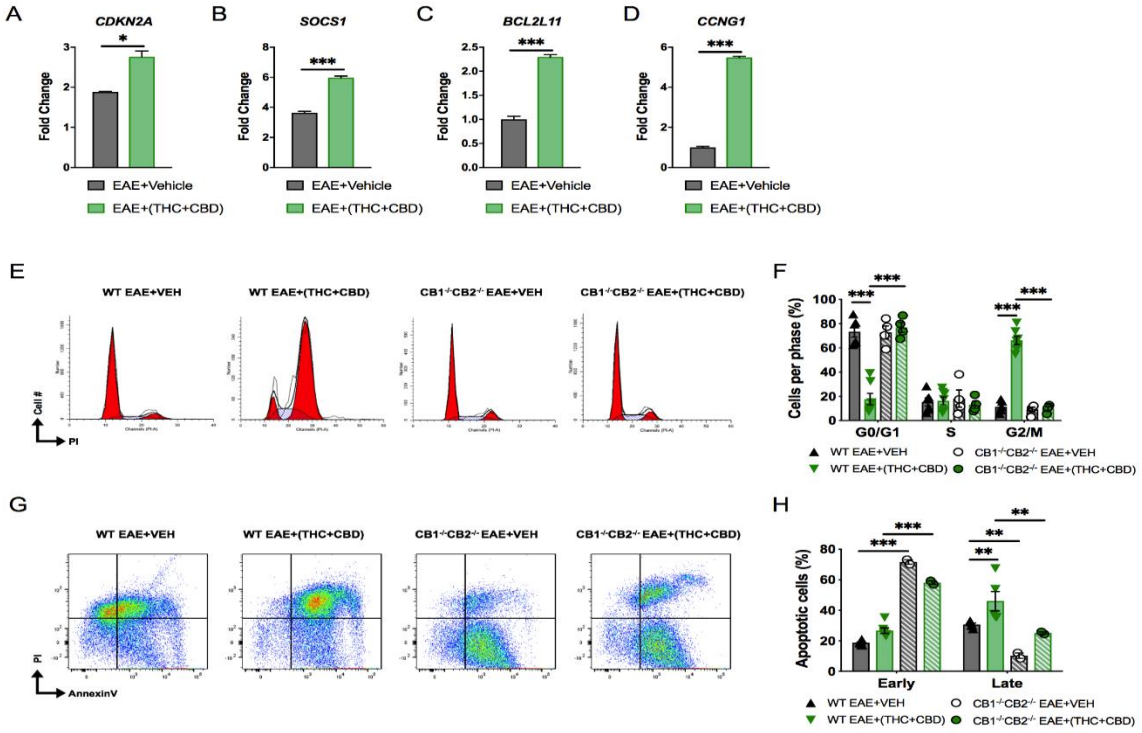

Figure 2.5 THC+CBD treatment induces cell cycle arrest / apoptosis in brain MNCs. As shown in Figure 1, EAE was induced in naïve mice and treatment with Veh or THC+CBD was initiated at the onset of symptoms. CD4+ T cells and total MNCs were isolated from the brains of mice on day 15 post immunization for gene and cell cycle analysis. (A-D) qRT-PCR validation of miR target genes involved in cell cycle/apoptosis. (E) Representative flow cytometry histograms of PI staining in brain MNCs using ModFit software. (F) Cell cycle phase quantification. (G) Representative flow cytometry pseudocolor plots of brain MNCs in early apoptosis ($AnnexinV^+PI^-$) or late apoptosis ($AnnexinV^+PI^+$). (H) Quantification of brain MNCs in early or late apoptosis. Data represented are mean +/- SEM. ***p<0.001, **p<0.01 by unpaired two-tailed T test (A-D), or two-way ANOVA with a Tukey post hoc test (F & H).

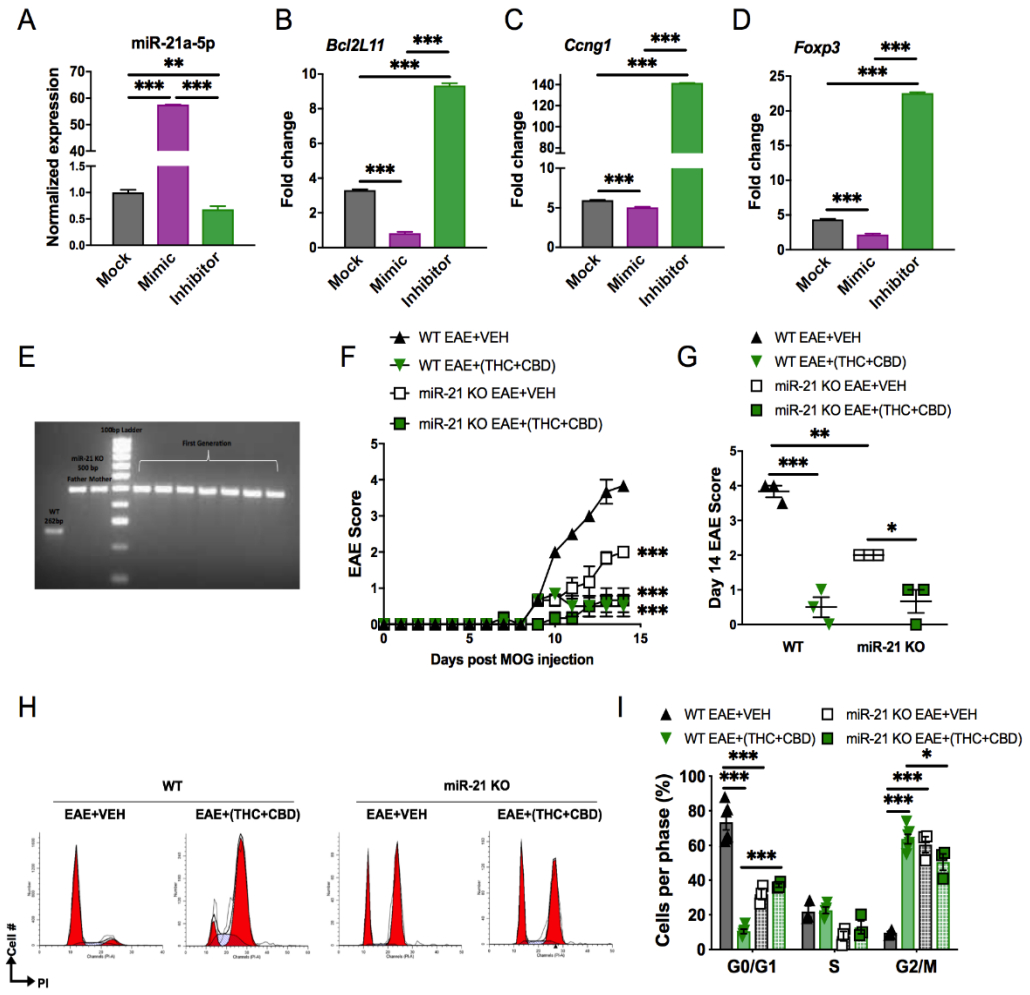

Figure 2.6 Role of miR-21a-5p downregulation on THC+CBD-mediated amelioration of EAE. For (A-D), miR-21a-5p transfection assays were performed in CD4+ T cells purified from naïve WT C57BL6 mice. Cells were cultured for 24h and transfected with miR-21a-5p mimic, inhibitor, or mock (transfection reagent only). For (E-F) EAE was induced in WT and Mir21-/- mice as described in Methods then treated with Veh or THC+CBD upon development of EAE symptoms. (A-D) qRT-PCR validation for miR-21 and the target genes. (E) Agarose gel electrophoresis of genotyping for the parents and the first generation of Mir21-/- mice (miR-21 KO). (F) EAE scoring in WT and Mir21-/- mice. (G) Quantification of the clinical scores. (H) Representative flow cytometry histograms of brain MNCs stained with PI study cell cycle analysis. (I) Quantification of cell cycle phases. Data are expressed as the mean ± S.E.M. and statistical significance is indicated as ***p<0.001, **p<0.01, *p<0.05. For (F), statistical significance is vs. WT EAE+Veh. Significance was determined by one- or two-way ANOVA with Tukey post hoc corrections.

Table 2.1 3'UTR alignments and scores of miRNAs and their target genes

CCNG1		
3' guuugugguaacagUGUGAGGu 5' mmu-miR-122 ||||||| 1796:5' uuaggcuugauaaaACACUCCa 3' Ccng1	mirSVR score: PhastCons score:	-1.0549 0.5536
3' uuggguacCUUAAG---UCAAGAGu 5' mmu-miR-146a ||| || |||||| 921:5' agaacgaaGAACUCCCAAGUUCUCu 3' Ccng1	mirSVR score: PhastCons score:	-0.1505 0.4986
3' cgcCUUGAAUCGGUGACACUu 5' mmu-miR-27a ||| | | |||||| 1306:5' uguGAAAUAA--AACUGUGAa 3' Ccng1	mirSVR score: PhastCons score:	-1.0267 0.5944
3' guguuugguaauacACGACGAu 5' mmu-miR-15a ||||||| 1682:5' aaauuugucagaacUGCUGCUu 3' Ccng1	mirSVR score: PhastCons score:	-0.4111 0.5536
3' guGACCAUGUUCCCAACCCUCu 5' mmu-miR-150 ||| | | | |||||| 1226:5' ucCUGAUUCUAAGCUUGGGAGa 3' Ccng1	mirSVR score: PhastCons score:	-0.2496 0.5917
CDKN1b		

3' aguUGUAGUCAGACUAUUCGAu 5' mmu-miR-21 |:| :|||:| ||||||| 1093:5' cuuAUAAUAGUUU-AUAAGCUc 3' Cdkn1b	mirSVR score: PhastCons score:	-0.5432 0.537
3' gugUUUA-AGC-CUA-GAUGUCCCAu 5' mmu-miR-10a :||| | | ||| |||||| 1236:5' aagGAAUAUAGAGAUGGCACAGGGUu 3' Cdkn1b	mirSVR score: PhastCons score:	-0.1534 0.537
3' gugACCAUGUU-CCCAACCCUCu 5' mmu-miR-150 | || || || ||||| 1376:5' aagUUGUCGAAUUGGAUGGGAGu 3' Cdkn1b	mirSVR score: PhastCons score:	-0.0062 0.5328
3' ugGGGAUAGUGUUAAUCGUAAUu 5' mmu-miR-155 :::|| |:: ||:||||| 1811:5' caUUUUAGAAUGUUUGGCAUUAu 3' Cdkn1b	mirSVR score: PhastCons score:	-0.0055 0.5372
3' gucGAUACGGUCGUAGAACGGa 5' mmu-miR-31 | | || || | ||||| 232:5' uucCCAAGCAAG-AACUUGCCa 3' Cdkn1b	mirSVR score: PhastCons score:	-0.0062 0.5482
Bcl2l11		
3' gugagucguGGUCCUAUAACAa 5' mmu-miR-338-5p | || :||||| 803:5' ggguaucuuCAAGUGUAUUGUg 3' Bcl2l11	mirSVR score: PhastCons score:	-0.0008 0.5603

3' aguUGUAGUCAGACUAUUCGAu 5' mmu-miR-21 |:||:| || ||||||| 1814:5' uguAUAUUA-CCU-AUAAGCUu 3' Bcl2l11	mirSVR score: PhastCons score:	-0.1597 0.546
3' guguuuaagccuagauGUCCCAu 5' mmu-miR-10a |||||| 785:5' augcgcagcuucagccCAGGGUa 3' Bcl2l11	mirSVR score: PhastCons score:	-0.0017 0.5603
IL10		
3' gugaccauguucccaACCCUCu 5' mmu-miR-150 |||||| 290:5' gauuauauuauaugaUGGGAGg 3' Il10	mirSVR score: PhastCons score:	-0.0295 0.6418
3' uuGGGUACCUUAAGUCAAGAgu 5' mmu-miR-146a | | | |||| ||||| 578:5' acCACCUAAAAUU-AGUUCUaa 3' Il10	mirSVR score: PhastCons score:	-0.586 0.7581
3' aguuguagucagacuAUUCGAu 5' mmu-miR-21 |||||| 233:5' uuuuuaaccuguguuUAAGCUg 3' Il10	mirSVR score: PhastCons score:	-0.155 0.6617
3' uccGUAUCCUACUGUUUCCCUu 5' mmu-miR-204 :|||| || :||||||| 270:5' cuuUAUAGUAU-UUAAAGGGAg 3' Il10	mirSVR score: PhastCons score:	-1.2036 0.6418

3' uuGGGUACCUUAAGUCAAGAgu 5' mmu-miR-146a | | | |||| |||||| 578:5' acCACCUAAAAUU-AGUUCUaa 3' Il10	mirSVR score: PhastCons score:	-0.586 0.7581
3' cgccuUGAAUCG--GUGACACUu 5' mmu-miR-27a ||| ||| | ||||| 165:5' uauucACUGAGCUUCUCUGUGAa 3' Il10	mirSVR score: PhastCons score:	-0.0968 0.6709
Foxp3		
3' uccguaUCCUACUGUUUC-CCUu 5' mmu-miR-204 || | || |||| ||| 896:5' gaucccAGCAGGAGAAAGCGGAu 3' Foxp3	mirSVR score: PhastCons score:	-0.194 0.5948
3' gucgauacggucguaGAACGGa 5' mmu-miR-31 |||||| 695:5' guaccccacgucucaCUUGCCa 3' Foxp3	mirSVR score: PhastCons score:	--- 0.6807 0.7094
3' guGUUUGGUAAUACAC-GACGAu 5' mmu-miR-15a |:::| || ||||| ||||| 97:5' acCGGGCGAUGAUGUGCCUGCUa 3' Foxp3	mirSVR score: PhastCons score:	-0.1344 0.5291
3' guuugugguaacaguGUGAGGu 5' mmu-miR-122 |||||| 	mirSVR score: PhastCons score:	-0.0057 0.5172

1243:5' guauguccuucccucCACUCCa 3' Foxp3		
IL17a		
3' aaaaaacucuguccCAAAGAGa 5' mmu-miR-706 ||||||| 23:5' uaagaaacccccacGUUUCUCa 3' Il17a	mirSVR score: PhastCons score:	-0.6735 0.4105
TNF		
5' ...CCCAGUGUGGGAAGCUGUCUUCA… (Position 529-535) |||||| 3' AAAAAAAAGGACUACAGAAGU mmu-miR-7116-5p	Targetscan context score :-0.17 Targetscan context++ score percentile: 86	
IL6		
5' ...UUAUAAUGUUUAGAC-UGUCUUCA… (Position 390-397) ||| |||||| 3' AAAAAAAAGGACUACAGAAGU mmu-miR-7116-5p	Targetscan context score :-0.57 Targetscan context++ score percentile: 99	

Table 2.2 miRNAs with their seed sequences and fold changes

MicroRNA Identification	MicroRNA Sequence 5`-3`	Seed Sequence	Fold Change
miR-7116-5p	UGAAGACAUCAGGAAAAAAAA	GAAGACA	6.8
miR-706	AGAGAAACCCUGUCUCAAAAAA	GAGAAAC	10.4
miR-122-5p	UGGAGUGUGACAAUGGUGUUUG	GGAGUGU	-25.8
miR-21a-5p	UAGCUUAUCAGACUGAUGUUGA	AGCUUAU	-2.4
miR-155-5p	UUAAUGCUAAUUGUGAUAGGGGU	UAAUGCU	-2.5
miR-338-5p	AACAAUAUCCUGGUGCUGAGUG	ACAAUAU	-1.8
miR-146a-5p	UGAGAACUGAAUUCCAUGGGUU	GAGAACU	-1.7
miR-31-5p	AGGCAAGAUGCUGGCAUAGCUG	GGCAAGA	-4.7
miR-27-5p	AGGGCUUAGCUGCUUGUGAGCA	GGGCUUA	-1.8
miR-204-5p	UUCCCUUUGUCAUCCUAUGCCU	UCCCUUU	-6.5

Table 2.3 mRNA quantitative RT-PCR primer sequences

Genes	Primers Sequence (5′–3′)
Il10	Forward: CCCATTCCTCGTCACGATCTC Reverse: TCCCATTCCTCGTCACGATCTC
Tgfβ	Forward: ATGTCACGGTTAGGGGCTC Reverse: GGCTTGCATACTGTGCTGTATAG
Il4	Forward: GGTCTCAACCCCCAGCTAGT Reverse: GCCGATGATCTCTCTCAAGTGAT
Gata3	Forward: CTCGGCCATTCGTACATGGAA Reverse: GGATACCTCTGCACCGTAGC
Il17a	Forward: TTTAACTCCCTTGGCGCAAAA Reverse: CTTTCCCTCCGCATTGACAC
Ifng	Forward: TCCTCGCCAGACTCGTTTTC Reverse: GTCTTGGGTCATTGCTGGAAG
Tbx21	Forward: AGCAAGGACGGCGAATGTT Reverse: GGGTGGACATATAAGCGGTTC
Il6	Forward: CCAAGAGGTGAGTGCTTCCC Reverse: CTGTTGTTCAGACTCTCTCCCT
TNF-α	Forward: GGAACACGTCGTGGGATAATG Reverse: GGCAGACTTTGGATGCTTCTT
Foxp3	Forward: CCCATCCCCAGGAGTCTTG Reverse: ACCATGACTAGGGGCACTGTA
SOCS1	Forward: CTGCGGCTTCTATTGGGGAC Reverse: AAAAGGCAGTCGAAGGTCTCG
Bcl2L11	Forward: GACAGAACCGCAAGGTAATCC Reverse: ACTTGTCACAACTCATGGGTG
CCNG1	Forward: ACAACTGACTCTCAGAAACTGC Reverse: CATTATCATGGGCCGACTCAAT
CDKN2B	Forward: CCCTGCCACCCTTACCAGA Reverse: CAGATACCTCGCAATGTCACG
Cacul1	Forward: AACACCTCCACCTCCAAGTT Reverse: AGACTCGCTCTAAGTGGCTG
Cdca4	Forward: GTAGAGGGTTTTGGCACTGTC Reverse: TGGGCTCCACTAGCATGTGA
GAPDH	Forward: TGGATTTGGACGCATTGGTC Reverse: TTTGCACTGGTACGTGTTGAT

CHAPTER 3

COMBINATION OF CANNABINOIDS, Δ9-TETRAHYDROCANNABINOL (THC) AND CANNABIDIOL (CBD), MITIGATES EXPERIMENTAL AUTOIMMUNE ENCEPHALOMYELITIS (EAE) BY DIMINISHING THE GUT MUCINS DEGRADER BACTERIA

3.1 ABSTRACT

Multiple Sclerosis (MS) is one of the most common autoimmune diseases that affects the central nervous system (CNS). Currently there is no cure for patients suffering from MS, and most treatments involve the use of immunosuppressive drugs that can have adverse side effects or increased toxicity. Cannabis, traditionally known as marijuana, is a product of the *Cannabis sativa*, an annual herbaceous plant, and for several centuries, marijuana has been used as an alternative medicine in many cultures. *Cannabis sativa* has over 421 chemical compounds, including about 80 terpenophenol compounds named phytocannabinoids, which includes both delta-9-tetrahydrocannabinol (THC) and cannabidiol (CBD). In the currently study, we show a combination therapy of THC and CBD (THC+CBD) results in amelioration of experimental autoimmune encephalomyelitis (EAE), an animal model of MS, by reducing hind limb paralysis, decreasing immune cellular infiltration into the brain, and preventing the presence of inflammatory biomarkers. We performed 16S rRNA sequencing on bacterial DNAs extracted from the experimental groups to investigate the gut microbiome compositions after using a combination of THC and CBD after EAE induction. Interestingly, we found

that EAE mice showed a high abundance of mucin degrading bacterial species, such as *Akkermansia muciniphila (A.muc)*, which was significantly reduced after THC+CBD treatment. Fecal Material Transfer (FMT) experiments confirmed that THC+CBD-mediated changes in the microbiome helped attenuate EAE clinical scores. Collectively, our data suggests that THC+CBD can ameliorate disease by preventing EAE-associated microbial dysbiosis which is characterized by an accumulation of mucin-degrading bacteria such as *A.muc*.

3.2 INTRODUCTION

Multiple sclerosis (MS) is a chronic neuroinflammatory and demyelinating autoimmune disorder of the central nervous system (CNS) mainly affecting young adults worldwide and it is more common in women than men (145). The pathogenesis of this disease includes development lead to demyelination. Although the complete etiology and the pathogenesis of MS remains unclear, there is evidence that increased migration of autoreactive lymphocytes across the blood-brain barrier (BBB) may be responsible for axonal demyelination of neurons, which results in axonal injury, oligodendrocyte loss, neuronal damage, and glial plaques (99). Experimental autoimmune encephalomyelitis (EAE), an animal model of MS, is often used to study disease development and is characterized by neurological dysfunction and demyelination closely mimicking conditions in the human MS patient population (146-148). Most current treatments of MS, such as interferon (IFN)-β, fingolimod, and glatiramer acetate act by regulating the immune response (99, 149, 150), however these drugs are only partially effective in many cases (20-30% successful in MS patients) and can have negative side-effects and increased toxicity (151, 152). Since current treatments present many challenges to the

patient population, new treatments are needed to improve the outcomes of patients who are affected by MS.

Cannabis is a product of *Cannabis sativa*, an annual herbaceous plant, and for several centuries this plant product has been used as an alternative medicine in many countries (153). *Cannabis sativa* produces over 421 chemical compounds, including about 80 terpenophenolic compounds named phytocannabinoids, which include both THC and CBD (14). Research has shown cannabinoids are effective treatment options against neurodegenerative diseases, including MS, because these plant products can reduce disease-associated effects such as oligodendrocyte death and axonal damage (15, 154). In addition, THC+CBD combination therapy has been shown to effectively reduce MS-associated tremors and spasticity, leading to ongoing human clinical trials (155-158). Cannabinoids have also been shown to exert potent anti-inflammatory activities, particularly through regulating immune cells involved in the innate and adaptive immune response (15-17, 22, 159). More recent reports are exploring the role cannabinoids have in regulating the gut microbiome, a major player in overall human host health and disease (160-163).

The microbiome, consisting of a large population of commensal microbes, plays such an important role in the health of the host it has been referred to as the "forgotten organ" (164). Studies of MS patients and the EAE mouse model of MS have shown the gut microbiome plays a significant role in disease both progression and severity (46, 165, 166). For example, it was found that germ-free mice developed a less severe EAE disease with a reduction in pro-inflammatory IFN-γ and IL-17A T cell responses accompanied with increase production of anti-inflammatory regulatory T cell (Tregs) (167). A more

recent study has shown that unaltered commensal bacteria can trigger a spontaneous form of EAE after exposure to myelin oligodendrocytes glycoprotein (MOG) (168). Interestingly, studies also found that the microbiome influences the development of the BBB, as germ-free mice had disrupted formation of this important barrier protecting the host CNS (169). Among the factors related to the microbiome which influence the host immune system response, short chain fatty acids (SCFAs) are some of the most significant functioning metabolites synthesized by the gut microbiome. SCFAs were found to be critical modulators in the gastrointestinal tract capable of regulating the pro-inflammatory Th1/Th17 and anti-inflammatory Treg responses during autoimmune neuroinflammation (170).

In the current study, we investigated the use of combination cannabinoid treatment (THC+CBD) during EAE to determine how this treatment effects the gut microbiome and whether these alterations influenced THC+CBD-mediated protective effects. The results showed THC+CBD treatment of EAE results in reduction in disease severity and alterations in the pro-inflammatory immune response. 16S rRNA sequencing of colon contents revealed THC+CBD treatment altered the gut microbiome during EAE, particularly by reducing the abundance of *Akkermansia muciniphila* (*A.muc*) which was increased during the disease state. In addition to the alterations in the microbial phylogenetic profile, THC+CBD treatment during EAE resulted in changes in the gut metabolome, specifically leading to increases in SCFAs such as anti-inflammatory butyrate. Lastly, fecal transfer experiments revealed that the protective effects of THC+CBD during EAE was at least partly due to the alterations of the microbiome during treatment with these combined cannabinoids.

3.3 MATERIAL AND METHODS

Mice

6-8-week-old female C57BL/6 mice were purchased from the Jackson laboratories (Bar Harbor, ME). Mice were housed in the Animal Resource Facility (ARF) at the University of South Carolina, School of Medicine. All animal experiments were performed in accordance with National Institutes of Health (NIH) guidelines under protocols approved by the Institutional Animal Care and Use Committee (IACUC) of the University of South Carolina.

Reagents

The following reagents were used during the experiments and purchased as follows: THC and CBD were from Cayman Chemical (Ann Arbor, MI); red blood cell (RBC) lysis buffer and β-mercaptoethanol were from Sigma-Aldrich (St. Louis, MO); percoll was purchased from GE Healthcare Life Sciences (Pittsburgh, PA); RPMI 1640, l-glutamine, HEPES, phosphate-buffered saline, and fetal bovine serum (FBS) were from VWR (West Chester, PA); myelin oligodendrocyte glycoprotein (MOG35-55) peptide and H-MEVGWYRSPFSRVVHLYRNGK-OH were from PolyPeptide Laboratories (San Diego, CA); Mycobacterium tuberculosis (strain H37Ra) and complete Freund's adjuvant were purchased from Difco (Detroit, MI); pertussis toxin was purchased from List Biological Laboratories (Campbell, CA); Neural Tissue Dissociation Kit (P) was purchased from Miltenyi Biotech Inc. (Auburn, CA); QIAamp DNA Stool mini kit was purchased from Qiagen (Germantown, MD); Illumina MiSeq reagents were purchased from Illumina, Inc. (San Diego, CA) except The Agencourt AMPure XP system beads were purchased from Beckman Coulter Life Science (Indianapolis, IN);

Lipopolysaccharide (LPS) ELISA Kit (Sandwich ELISA) was purchased from LifeSpan Biosciences, Inc. (Seattle, WA. USA). Besides, the following mouse-specific ELISA kits were purchased from BioLegend (San Diego, CA): IL-10, IL-17A, IFN-γ, and TGF-β.

EAE induction and treatment with THC+CBD

To investigate the effect of the THC+CBD combination, EAE was induced as described previously (104, 105). Briefly, mice were given a subcutaneous injection with 100 µl of 150 µg MOG35-55 peptide emulsified in complete Freund's adjuvant containing 8 mg/ml killed Mycobacterium tuberculosis (strain H37Ra), followed by an intraperitoneal injection (i.p.) of 200 ng of pertussis toxin on day 0. These injections were repeated with 400 ng pertussis toxin on day 2. For treatment, EAE mice were randomized and treated with an i.p. injection of 10 mg/kg THC+CBD or vehicle (2% dimethylsulfoxide, DMSO; 20% ethanol diluted in PBS) on day 10 after the induction of EAE, and this treatment regimen continued once daily until the end of the experiment. Animals were monitored, and clinical scores were observed and evaluated daily.

EAE clinical scoring

The measured parameters for clinical EAE scores were recorded as follow: 0 = normal; 1 = partial loss of tail tonicity/inability to curl the distal end of the tail; 2 = tail atony/ moderately clumsy/impaired righting; 3 = hind limbs weakness/partial paralysis; 4 = complete hind limp paralysis/fore limb weakness; 5 = tetraplegia/moribund (106). The mean score was calculated for each group every day. Proper care of paralytic animals unable to access food and water was ensured by providing supplementary DietGel Boost and Hydrogel from Daily H_2O (Portland, ME) on a daily basis. Death was not used as an index for clinical scores, and any mice that were moribund were immediately euthanized

with an overdose anesthetic isoflurane (%5), a method approved by the American Association for Laboratory Animal Science and university IACUC.

Histopathological analysis

For histopathological evaluation, brain tissues from experimental mice were isolated at day 15 after EAE induction during the peak of disease. Prior to brain isolation, euthanized mice were perfused with 10 mL heparinized PBS to flush out vascular circulating cells. Isolated brain tissues obtained after perfusion were immersed in 4% paraformaldehyde (PFA) overnight prior to embedding in paraffin. Microtome sections (7 μm) were obtained, and tissue sections were stained with Hematoxylin and Eosin (H&E) to evaluate damage and cellular infiltration into the CNS.

Analysis of cytokine production

Pro-inflammatory (IFNγ and IL17A) and anti-inflammatory (IL-10 and transforming growth factor-β, TGF-β) cytokines were evaluated in the serum and ex vivo splenocyte supernatants from experimental groups using ELISA kits as previously described (104). For serum, blood was collected on day 15 and serum was separated and stored at -80°C until analysis. For evaluation of the peripheral response in the spleen during EAE, spleens from experimental mice were excised at the end of the experiment and processed into a cell single suspension. Isolated splenocytes were seeded ($1x10^6$ cells/ml) cultured for 24 hours at 37°C and 5% CO2 overnight in complete RPMI 1640 media supplemented with 10% fetal bovine serum, 10 mM l-glutamine, 10 mM HEPES, 50 μM β-mercaptoethanol, and 100 μg/ml penicillin/streptomycin. After 24 hours, cell culture supernatants were cultured and stored at -80°C until further analysis.

Flow cytometry analysis for myeloid-derived suppressor cells (MDSCs)

To determine peripheral MDSC induction, spleens were excised prior to perfusion in experimental mice. Whole splenocyte tissues were homogenized into a single cell suspension and subjected to red blood cell (RBS) lysis. Cells suspensions from experimental groups were tagged with fluorescently-labeled monoclonal antibodies (mAbs) purchased from Biolegend. Specifically, PE-labeled Gr-1 and AlexaFluro700-labeled CD11b were used to identify MDSC populations in the spleen. Antibody-tagged samples were run a BD FACs Celesta flow cytometer and analyzed using FlowJo software from BD Biosciences (San Jose, CA).

Bacterial phylogenetic and metabolomic profiling by 16S rRNA analysis

16S rRNA sequencing using the Illumina MiSeq platform and analysis with Nephele were performed as previously described (171). Briefly, cecal flushes were collected from Naïve, EAE-VEH and EAE-(THC+CBD) mice under antiseptic conditions, and collected samples were kept frozen at - 80 °C until DNA extraction. Isolation of DNA from stool was performed using the QIAamp DNA Stool Mini Kit from Qiagen as per the instructions from the manufacturer. 200 mg of cecal contents was collected per experimental mouse. Sequencing was performed on the Illumina MiSeq platform to generate reads, and all further downstream analysis was performed using the Nephele platform from the National Institute of Allergy and Infectious Diseases (NIAID) Office of Cyber Infrastructure and Computational Biology (OCICB) in Bethesda, MD (172). To analyze phylogenetic and possible metabolomic alterations within samples, Nephele-based analysis using the Phylogenetic Investigation of Communities by Reconstruction of Unobserved States (PiCRUSt) option was used which requires a closed

reference against the Greengenes database (Greengene_99) at taxa levels 2 and 3 (Phylum and Class) for KEGG annotations. In order to determine significantly altered bacteria and processes within the samples, linear discrimination analysis of effect size (LefSE) was performed operational taxonomic unit (OTU) tables generated from Nephele (173). To validate *A.muc* (F 5′GACTAGAGTAATGGAGGGGGAA 3′ R 5′GTATCTAATCCCTTTCGCTCCC 3′) expression, PCR was performed using Qiagen miScript cDNA synthesis kit and Biorad SSO advanced SYBR Green PCR reagents for analysis on a CFX96 qPCR system. Fold change of *A.muc* was determined using the delta-delta-CT method expressed relatively to a Eubacteria (Forward: 5′ACTCCTACGGGAGGCAGCAGT; 3′ Reverse: 5′ATTACCGCGGCTGCTGGC 3′) control.

Quantification of SCFAs

Quantification of SCFAs was performed as previously described (166, 171). Briefly, 100mg of cecal contents was weighted and suspended in dIH2O to a final concentration of 250 mg/mL. Samples were vortexed until completely homogenized, then acidified with 1:4 volumes of 25% metaphosphoric acid. Acidified samples were vortexed and placed on ice for 30 min. Cold acidified samples were centrifuged at 12,000xg for 15 minutes at 4°C. Supernatants were filtered over ultra-free MC columns (0.22 um GVDurapore, UFC30GV0S, ThermoFisher Scientific) and centrifuge at 12,000xg for 4 minutes at 4°C. Samples were stored until later downstream quantification at -80°C. To quantify SCFAs and determine their concentrations within experimental samples, standards were prepared as shown in Table 1. Ethylbutyric acid (0.10 mM) was added as an internal standard (IS) for all samples and standards tubes. The acidified

samples were thawed and 100µL was transferred to a new microfuge tube, along with 100µL of the standards. For the IS-blank, 100µL ddH_2O was transferred to a new microcentrifuge tube. Then, 60µL of 0.1mM IS was added to each sample, standard, and IS-blank for a final volume of 160 µL. Two sets of glass GC vials (Supelco 29056-U) were labeled for each sample, standard, and IS-blank. Approximately 400µL of methyl tert-butyl ether (MTBE) was added to one set of glass vials using a 2mL glass serological pipette. Samples, standards, and IS-blank from the tubes that had final volume of 160µL(100µL ddH_2O+60µL of 0.1mM IS) were added into the glass vials containing MTBE. Samples were vortexed ~5-10 seconds, then spun down at 1.300 rpm for 5 minutes at room temperature. Lastly, 100µL of the top organic layer from the samples was placed into the other set of glass vials for analysis. Samples were stored at -20°C until analyzed with the gas chromatography flame-ionized detection (GC-FID) instrument (174).

Lipopolysaccharide (LPS) Detection in brain lysates

Brain tissues were collected from naïve, EAE-VEH and EAE-(THC+CBD), rinsed with 1X PBS, and minced into a single cell suspension. Cells were collected and pelleted by centrifugation, and the supernatant was removed. Cells were washed 3 times with 1X cold-PBS and suspended in 1X PBS to be lysed by freezing the cells at -20°C and allowing to thaw at room temperature 3 times. Cells were centrifuged at 1500×g for 10 minutes at 4°C to remove cellular debris. The collected cell supernatants were analyzed for detection of LPS by using a LPS ELISA Kit (Sandwich ELISA) for LifeSpan Biosciences, Inc. (Seattle, WA) according to the manufacturer's instructions.

Fecal microbial transplantation (FMT)

In order to perform FMT experiments, the EAE model was induced as described above. Cecal flushes from experimental groups, Naïve, EAE-VEH, and EAE-(THC+CBD), were harvested aseptically at the peak of the disease (day 15) using an anaerobic chamber were suspended in sterile PBS containing 30% glycerol for storage at -80C until used. To prepare mice for FMTs, 6-week-old C57Bl/6J mice we administered antibiotics (streptomycin 1g/L and ampicillin 1g/L, referred to as "Abx") by oral gavage (100μL) daily for 4 weeks. Abx-treated mice were kept in autoclaved cages with autoclaved water and chow. To ensure depletion of the microbiome, PCR validation (DNA collected from stool) using a primer for Eubacteria (Forward: 5′ACTCCTACGGGAGGCAGCAGT; 3′ Reverse: 5′ATTACCGCGGCTGCTGGC 3′) and bacterial culture plates were performed. EAE was induced in mice treated with Abx for 4 weeks and after symptoms started, mice were randomized into 4 groups: FMT EAE+Control (PBS only), FMT EAE+Naive, FMT EAE+VEH, FMT EAE+(THC+CBD). We performed daily FMTs (50mg) by oral gavage starting at day 10 until the end of the experiment (day 18).

Statistics

We performed our statistical analysis using GraphPad Prism 6 (GraphPad Inc, La Jolla, CA). The data shown in this study represents at least three independent experiments unless otherwise stated. Average values ± standard error mean (SEM) are shown for experiments to determine to significance. The statistical differences between two experimental groups were calculated using ANOVA and student *t* test. For comparisons of three or more groups, one-way ANOVA and Tukey's multiple comparisons posthoc

test were performed. EAE clinical scores over a period of time were evaluated using groups of at least five mice and significance was determined using two-way ANOVA and Tukey's multiple comparisons test in order to determine significance during each individual time point (e.g. days). A P value <0.05 was considered significant for all experiments.

3.4 RESULTS

Combination THC+CBD treatment reduces EAE disease and promotes anti-inflammatory response

In order to determine the effectiveness of THC+CBD treatment in the EAE model, disease induction and treatment were performed as outlined in Figure 1A, initially comparing the following groups: EAE mice treated with vehicle (EAE-VEH) and EAE mice treated with cannabinoid combination (EAE-(THC+CBD)). Clinical EAE scores showed EAE-(THC+CBD) had reduced disease severity when compared to EAE-VEH disease controls (Figure 1B). Histological results from the brains taken at day 15 of the experimental model revealed that as expected, when compared to naïve wild-type (WT) mice, EAE-VEH mice had high number of infiltrating cells and signs of tissue damage, however, EAE-(THC+CBD) brain tissues showed similar naïve group morphology (Figure 1C). Serum samples also showed EAE-(THC+CBD) mice had a decrease in the pro-inflammatory cytokines levels for IL-17A (Figure 1D) and IFN-γ (Figure 1E) when compared to the disease controls. However, EAE-(THC+CBD) serum had increases in the levels of anti-inflammatory cytokines TGF-β (Figure 1F) and IL-10 (Figure 1G) compared to EAE-VEH groups. In the periphery, splenic levels of pro-inflammatory cytokines IL-17A (Figure 1H) and IFN-γ (Figure 1I) were also reduced with THC+CBD treatment, and this correlated with an increase in anti-inflammatory myeloid-derived

suppressor cells (MDSCs) when compared to disease controls. Collectively, this data showed that THC+CBD treatment was able to reduce EAE disease severity and promote and anti-inflammatory response.

Combination THC+CBD treatment alters the gut microbiome during EAE induction

16S rRNA gene sequencing was performed on cecal flushes from the following groups: Naïve, EAE-VEH, and EAE-(THC+CBD). The Illumina MiSeq platform using primers targeting the V3 and V4 variable regions was used. Sequences were translated by using the 16S QIIME Paired-End pipeline implemented in Nephele platform (release 1.6 which uses QIIME 1.9.1) (175). OTUs were picked with QIIME's unclust-based (176), open-reference OTU picking protocol (177), and the taxonomic assignment was done against Greengenes-99 reference sequence set at 99% similarity, as previously described (178). Alpha diversity, as assessed using Chao1 rarefraction measure, showed that EAE-induced mice had slightly lower abundances of bacteria in the gut (Figure 2A). Beta diversity, depicted in a 3D principle coordinate analysis (PCOA) plot, showed that three experimental groups clustered together well within their own groups, suggesting there was divergence in the gut microbiome population (Figure 2B). At the phylum level (Figure 2C), there were notable differences in the taxa. EAE-induced mice had significantly lower abundances of Bacteriodetes when compared to Naïve mice (Figure 2D), whereas EAE-treated with THC+CBD had higher levels of Firmicutes when compared to the disease controls (Figure 2E). Both EAE groups had a significant drop in Tenericutes when compared to the controls (Figure 2F), but had increased abundance of Verrucomicrobia, although EAE-(THC+CBD) had reduced levels compared to EAE-VEH (Figure 2G). Interestingly, Proteobacteria was significantly higher in EAE-VEH

mice compared to controls, but the abundance of this phylum was reduced to normal levels after treatment with THC+CBD (Figure 2H). Significant alterations in the gut microbiome were observed throughout the various taxa levels from class to genus among the experimental groups with an interesting consistent trend showing EAE-associated increase in Verrucomicrobia sub-levels was decreased after THC+CBD treatment (Supplementary Figures 1-4).

In order to ascertain the most significantly altered bacteria between naïve and disease controls and identify any potential microbial biomarkers of disease, LefSE was performed on the OTU output data (Figure 3A). When examining microbial disruption between the Naïve and EAE-VEH groups, the bacterial species *Akkermansia muciniphilia* (*A.muc)* within the Verrucomicrobiae class had the highest LDA score in EAE-induced mice (Figure 3B). When considering the levels in treated groups, EAE-(THC+CBD) mice had significantly reduced levels of this EAE-associated bacteria (Figure 3C). The sequencing data was validated using primers specific for *A.muc*, reinforcing the observation that THC+CBD treatment reduced the levels of this bacteria that were significantly higher in EAE mice when compared to naïve controls (Figure 3D).

Treatment with THC+CBD during EAE alters gut bacterial metabolite production

In addition to the phylogenetic data from 16s rRNA sequencing, *in silico* computational metabolomics was performed using the PICRUSt method. LefSE analysis of the output data showed that when comparing disease controls (EAE-VEH) to EAE-(THC+CBD) treated groups, several KEGG pathways had high LDA scores in the disease state (Figure 4A). For example, LPS biosynthesis, a key component in gram-negative bacteria such as *A.muc* was found to be elevated in disease controls compared to

naïve mice, but this was greatly reduced after treatment with THC+CBD (Figure 4B). In order to corroborate this *in silico* data, brain lysates from experimental groups were analyzed for detection of LPS levels. When comparing all the experimental groups, lysates from the brains of EAE-VEH mice had significantly higher levels of LPS compared to controls, however, EAE-(THC+CBD) mice reduced this level significantly (Figure 4C). Production of known SCFAs was also evaluated from cecal flushes. Compared to Naïve controls, EAE-induced mice (untreated or untreated) had higher levels of acetic (Figure 4D) and propionic acids (Figure 4E), though only EAE-(THC+CBD) mice appeared to have increased isobutyric acid (Figure 4F). In addition, EAE-(THC+CBD) samples had significantly higher levels of butyric (Figure 4G), isovaleric (Figure 4H), and valeric (Figure 4I) acids compared to naïve or disease controls. Collectively, data showed EAE-(THC+CBD) mice had global increases in SCFA production, in addition to altering other bacterial metabolomic pathways such as LPS production.

FMT of THC+CDB-altered microbiome attenuates EAE disease severity

In order to determine if the alterations in the microbiome by THC+CBD treatment mediated any protective effects against EAE induction, FMT experiments were performed as described in Figure 5A. To deplete the microbiome, mice were treated with Abx for 4 weeks, and confirmation of this depletion was confirmed with PCR (Figure 5B) and bacterial culturing (Figure 5C). For FMTs, EAE-induced mice were fed either controls (FMT EAE Control), or fecal material from Naïve (FMT EAE-Naïve), disease controls (FMT EAE-VEH), or disease mice treated with THC+CBD (FMT EAE-(THC+CBD)). When assessing the clinical scores after EAE induction, all mice treated

with Abx had reduced disease severity compared to normal EAE experiments (Figure 5D), more than likely due to the dependency of EAE induction on the microbiota. However, FMT EAE-(THC+CBD) mice had significantly reduced scores compared to the other groups. This data confirms that alterations in the microbiome by combination THC+CBD leads to protection against EAE-induction, thus providing another interesting mechanism by when cannabinoids are capable of protecting against inflammatory diseases.

3.5 DISCUSSION

MS is a neurological autoimmune disease caused by a combination of genetic and environmental exposures which has increased in incidence in the past several decades suggesting a changes in environmental risk factors (179), and gut microbiota might be one of these environmental factors (50). Our study demonstrated a mixture of cannabinoids (THC and CBD) in EAE resulted in alleviation of the clinical symptoms. A previous report from our lab also found that treatment with CBD alone was able to attenuate EAE-induced disease (16). Such findings were observed even 20 years ago when it was reported that a MS patient who smoked marijuana had decreased incident of MS-associated ataxia and spasticity (180), and since then several reports have shown cannabinoids are effective at lessening MS disease burden (181, 182). There is even a oromucosal pharmaceutical cannabinoid spray (Sativex) available to reduce spasticity and pain attributed to MS (183). In fact, there is a reported increase in use of *cannabis* by MS patients in the United States (184). Such an increase in use is not surprising given the evidence of benefits available from research.

Several mechanisms have been attributed to the beneficial effects of cannabinoids like THC and CBD, to include those that affect the immune system. In the current report, treatment with THC+CBD resulted in reduction of pro-inflammatory cytokines production and increase in anti-inflammatory cytokines production. In early reports, Kozela et al found that CBD was found to suppress microglial activity and prevent T cell proliferation associated with inducible EAE (185). The same research group later reported that separately THC and CBD were able to suppress Th17 cells and proinflammatory cytokines such as TNFα and IFNγ during EAE (19), consistent with our combination treatment findings. In addition to suppressing the pro-inflammatory phenotype, our lab has also shown that cannabinoids are able to increase abundance and activity of anti-inflammatory immune cell phenotypes, such as Tregs and MDSCs, in various inflammatory models of disease (16, 18, 22, 121, 159, 186). Therapeutic agents that can reduce pro-inflammatory Th1/Th17 subsets and increase anti-inflammatory Th2/Treg/MDSC subsets can potential help patients suffering from MS, reinforcing the case that these cannabinoids are a good source of alternative therapy for the patient population. Despite a continuing field of research in cannabinoids and MS, few have yet to study another possible mechanism linked to the disease, which consists of examining the effects occurring in the microbiome.

Current research has noted that MS is characterized by alterations in amount, composition, and metabolomic profile of the microbiome (187). Of particularly note in this study was during EAE induction and treatment significant changes were observed in *A. Muc* which is reported to be involved in exacerbation of both the human MS patients and animal models of MS, like EAE (187, 188). For example, it was found that increased

A. Muc in MS patients was capable of increasing the severity of EAE when transplanted into mice (189). In a study done by Jangi et al., researchers found that the genus Akkermansia increased in patients with MS (50). In another study, researchers found that untreated MS subjects showed increase of Akkermansia as well (190). The current report suggests that cannabinoid treatment may be able to regulate *A. Muc*, which is certainly possible given that blocking cannabinoid receptors lead to a significant increase in *A. Muc* in an model of obesity (161). Interestingly, use of another natural product (resveratrol) was found to regulate the endocannabinoid system to decrease *A. Muc* in high-fat diet-induced non-alcoholic steatohepatitis (191).

Microbial dysbiosis in MS/EAE hosts characterized by increased gram-negative bacteria, such as *A.Muc*, could be linked to increased LPS, which was observed in brain lysates from EAE mice in the current study. Elevated LPS levels suggest a shift to increased presence of gram negative bacterial endotoxin and a study has shown LPS results in degeneration of myelin and results in white matter damage (192). This makes sense as LPS is linked to a proinflammatory response in the host capable of activating microglia, disrupting the BBB, and making Tregs act in a defective manner (193). In addition, the current study shows THC+CBD treatment results in widespread increases in SCFAs. SCFAs play a very important role in regulating the inflammatory response and preventing autoimmune diseases such as MS by suppressing the production of Th17 cells and promoting the production of Treg cells from CD4 naïve T cells (194). In fact, a recent report showed that gut dysbiosis and lack of SCFAs were present in Chinese MS patients (195). The results of all these aforementioned studies, combined with the results in EAE treated with THC+CBD, provide an interesting therapeutic approach and target in

the future treatment of MS patients, by way of altering the gut microbiome and preventing MS-associated microbial dysbiosis.

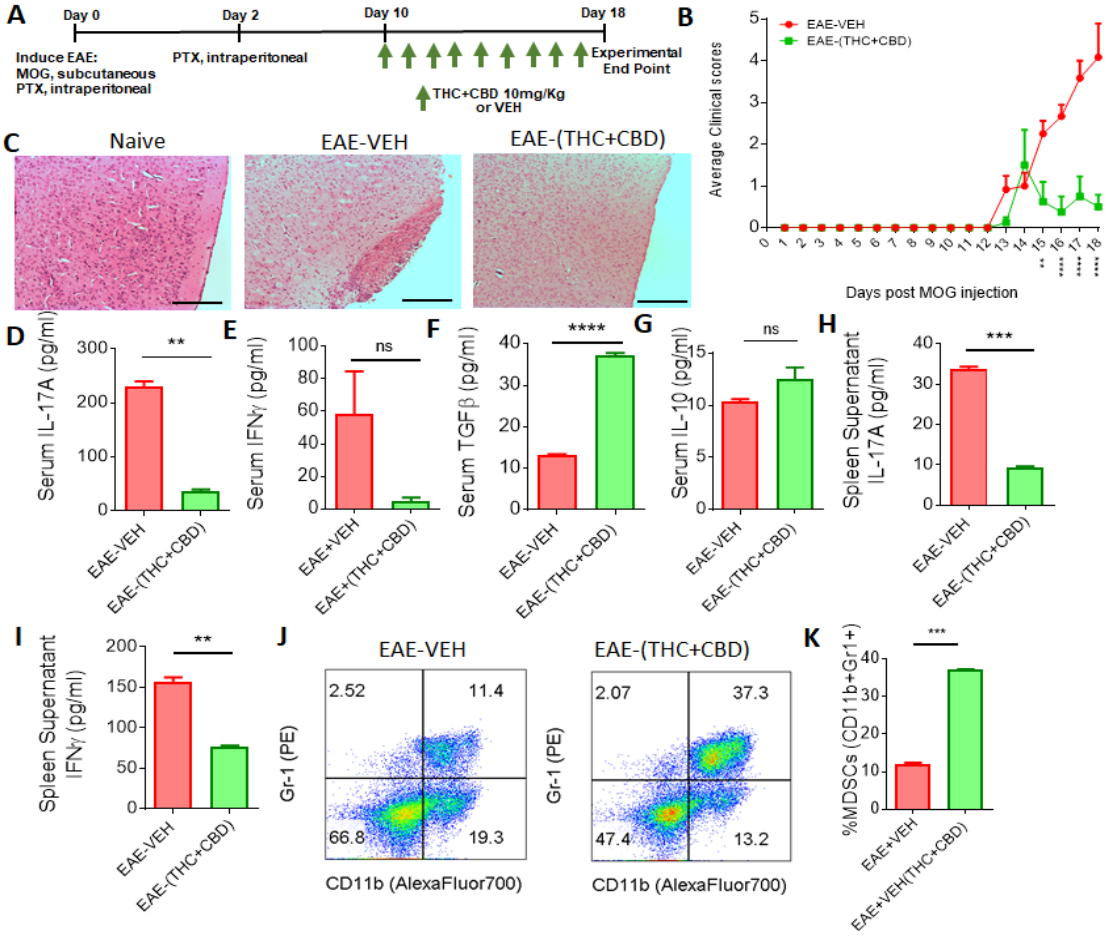

Figure 3.1 Combination THC+CBD treatment attenuates EAE disease severity and promotes anti-inflammatory immune response. (A) Experimental design of EAE experiments using combined treatment of THC+CBD (10mg/kg). (B) Clinical scores, outlined in the Materials and Methods section, of EAE mice treated with VEH (n = 10) or THC+CBD (n = 10). Significance was determined using two-way ANOVA and Tukey's multiple comparisons test to evaluate significance at each day. Significant p values (*P < 0.05, **P < 0.01, ***P < 0.001 and ****P < 0.0001) are indicated below respective days after EAE induction. (C) Representative images of brain histopathology stained with H&E (10×) at day 15 from experimental groups: Naïve, EAE+VEH, and EAE+THC; scale bars, 100 µM. (D-G) Serum was collected at the peak of the disease (day 15) to determine levels of IL-17A (D), IFN-γ (E), TGF-β (F), and IL-10 (G). (H-I) Supernatants from cultured splenocytes were collected after 24hrs to analyze IL-17A (H) and IFN-γ (I) by ELISA. (J-K) Representative flow cytometry plots (J) to determine MDSC (Gr-1+CD11b+) percentages (K). Bar graph data are expressed as the mean ± SEM and statistical significance is indicated as *P < 0.05, **P < 0.01, ***P < 0.001 and ****P < 0.0001 when compared between EAE-VEH and EAE-(THC+CBD) unless otherwise stated.

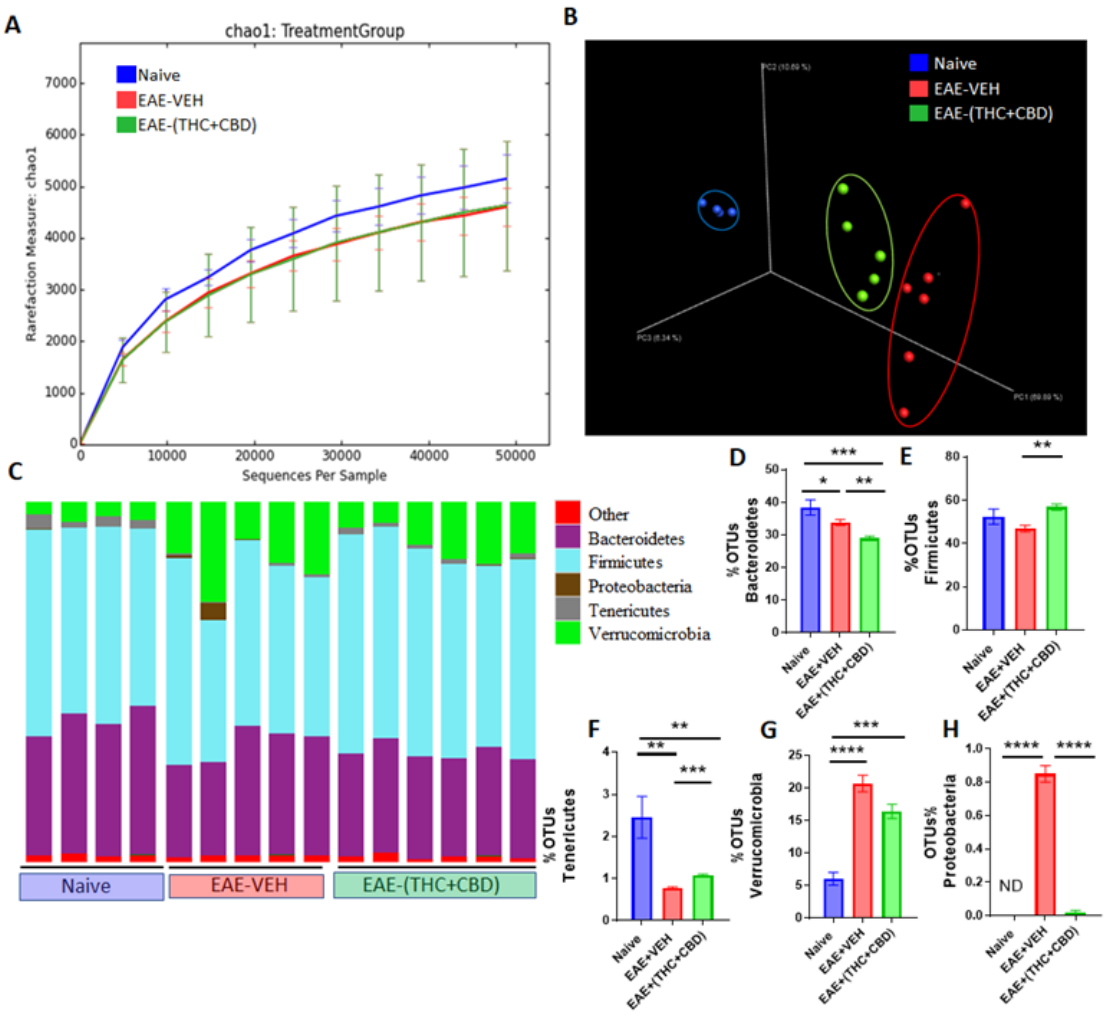

Figure 3.2 Combination THC+CBD treatment alters the gut microbiome during EAE disease. (A-B) 16S rRNA sequencing from the cecal flushes was performed on Naive (n=4), EAE-VEH (n=5), and EAE-(THC+CBD) (n=6) experimental mice and data are representative of one experiment. Sequenced reads were analyzed using Nephele to generate chao1 alpha diversity (A) and beta diversity PCOA (B) plots. (C) Depicted stacked bar graphs of percent OTUs at the phylum level. (D-H) Individual bar graphs are depicted for the following phylum level: Bacteriodetes (D), Firmicutes (E), Tenericutes (F), Verrucomicrobia (G), and Proteobacteria (H). Bar graph data are expressed as the mean ± SEM and statistical significance is indicated as *P < 0.05, **P < 0.01, ***P < 0.001 and ****P < 0.0001. Significance was determined using one-way ANOVA and Tukey's multiple comparisons test

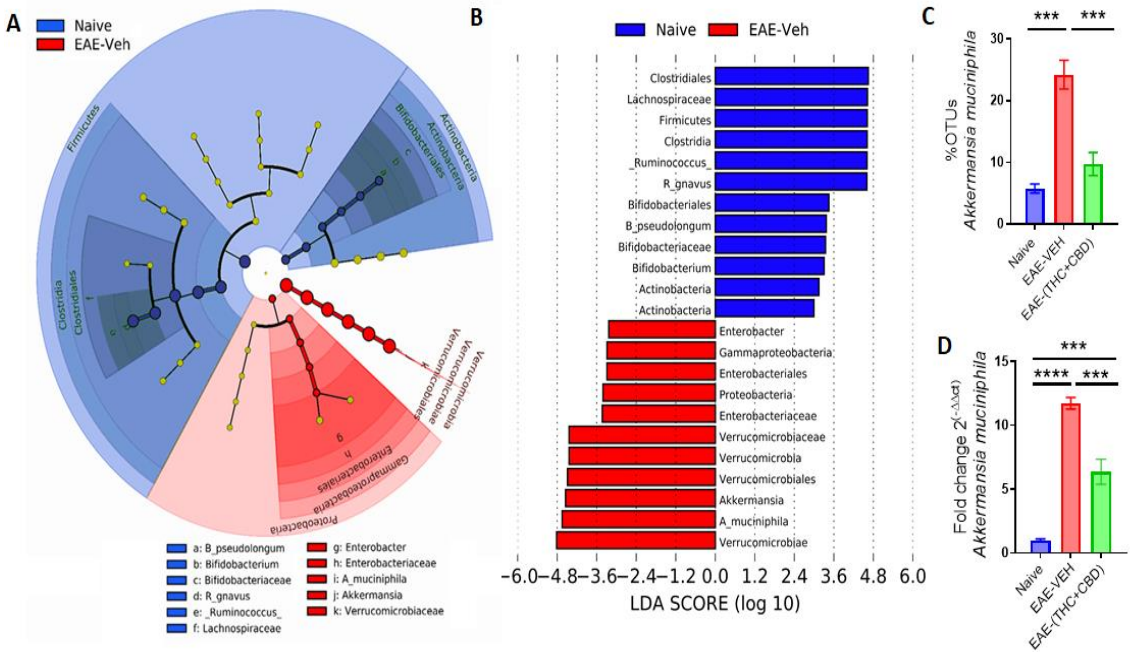

Figure 3.3 LefSE analysis identifies *A.Muc* as a potential biomarker of EAE disease which is reduced after THC+CBD treatment. (**A-B**) 16S rRNA sequencing from the cecal flushes was performed on Naive (n=4), EAE-VEH (n=5), and EAE-(THC+CBD) (n=6) experimental mice and OTU data was subjected to LefSE analysis to generate cladogram (**A**) and LDA scores (**B**) between Naïve and EAE-VEH groups. For LefSe data, the alpha factorial Kruskal-Wallis test among classes was set to 0.05, and the threshold on the logarithmic LDA score for discriminative features was set at3. (**C**) Bar graph depicting the percent OTUs of *A.Muc* generated from 16S rRNA sequencing in Naïve, EAE-VEH, and EAE-(THC+CBD) groups. (**D**) Bar graph depicting PCR validation and fold change of *A.Muc* in Naïve (n=5), EAE-VEH (n=5), and EAE-(THC+CBD) (n=5) groups. Bar graph data are expressed as the mean ± SEM and statistical significance is indicated as *P < 0.05, **P < 0.01, ***P < 0.001 and ****P < 0.0001. Significance was determined using one-way ANOVA and Tukey's multiple comparisons test.

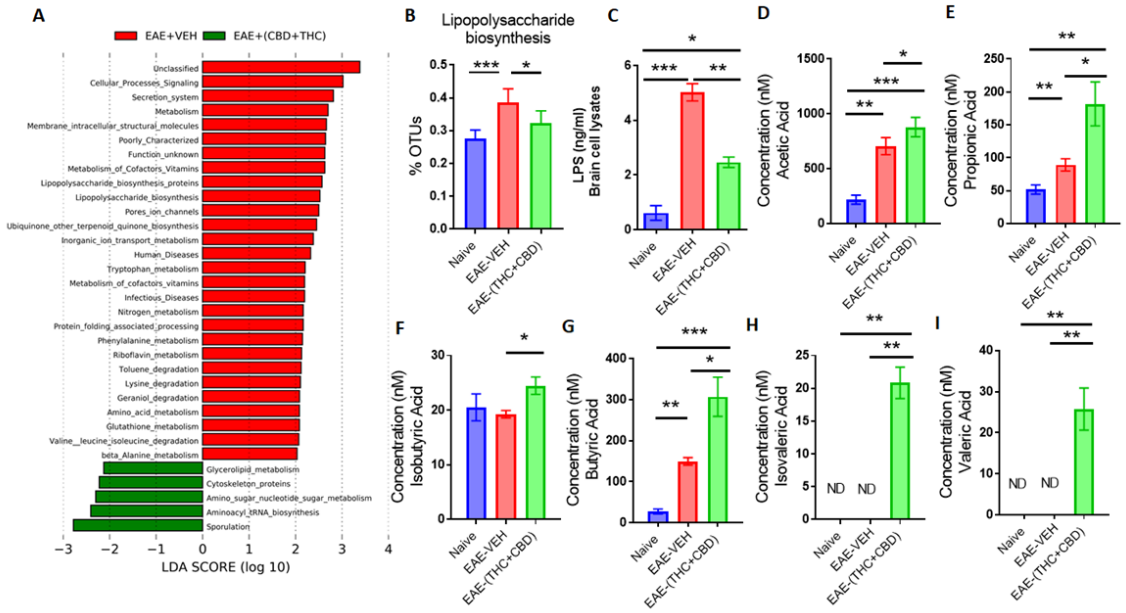

Figure 3.4 Combination THC+CBD treatment alters the gut microbiome metabolome during EAE disease. (**A**) LDA scores between EAE-VEH and EAE-(THC+CBD) groups using PICRUSt-generated Level 3 (L3) KEGG pathways of 16S rRNA sequencing data from Naive (n=4), EAE-VEH (n=5), and EAE-(THC+CBD) (n=6) experimental mice. (**B**) Individual bar graph depicting percent OTUs attributed to LPS biosynthesis from Naive (n=4), EAE-VEH (n=5), and EAE-(THC+CBD) (n=6) experimental mice after PICRUSt analysis. (C) Concentration of LPS levels from cultured brain lysates detected by ELISA for Naive (n=5), EAE-VEH (n=5), and EAE-(THC+CBD) (n=5) samples. (**D-I**) Concentrations of SCFAs from cecal flushes of Naive (n=5), EAE-VEH (n=5), and EAE-(THC+CBD) (n=5) samples. Bar graph data are expressed as the mean ± SEM and statistical significance is indicated as *P < 0.05, **P < 0.01, ***P < 0.001 and ****P < 0.0001. Significance was determined using one-way ANOVA and Tukey's multiple comparisons test.

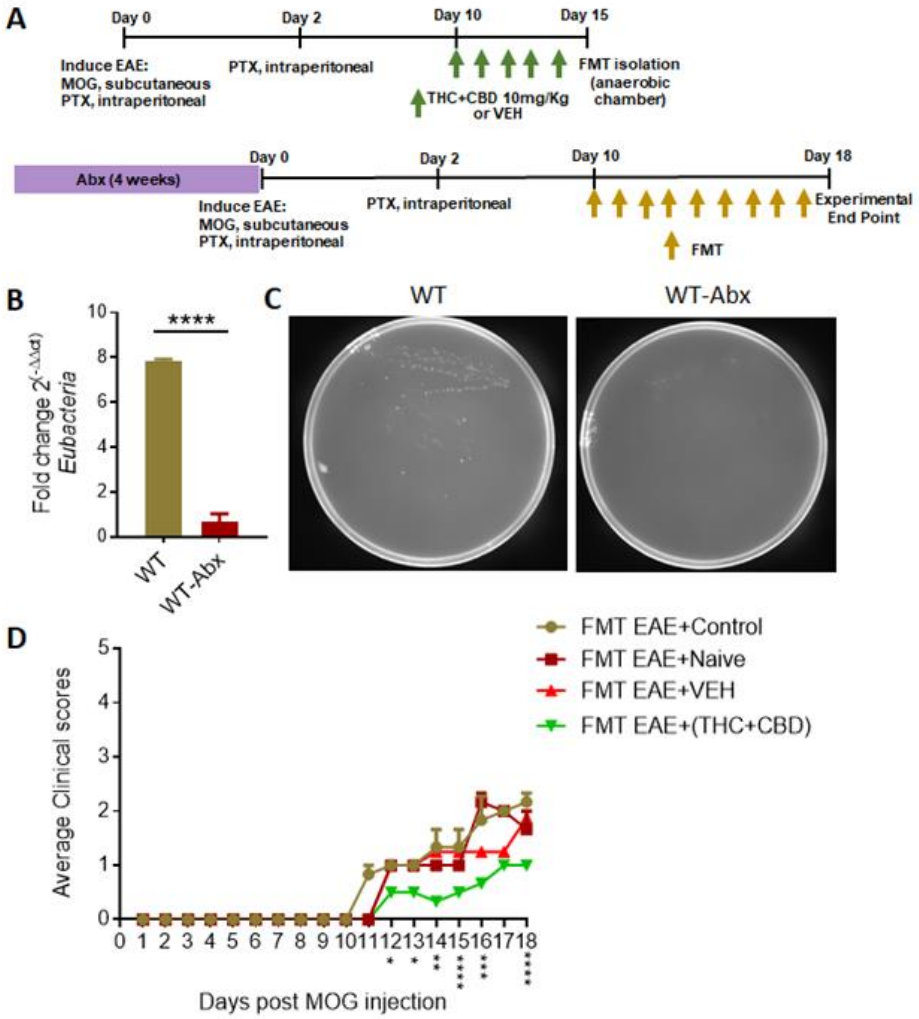

Figure 3.5 FMT of THC+CBD altered microbiome attenuates EAE severity. (**A**) Experimental design of FMT EAE experiments where 4-week Abx-treated mice received FMTs (50mg) from either Control PBS (n=3), Naïve (n=3), EAE-VEH (n=5), or EAE-(THC+CBD) (n=5) mice. (**B**) PCR validation confirming Abx mice had depleted microbiome. Depicted is the fold change of Eubacteria normalized to 18S compared between WT(n=5) and WT+Abx (n=5). Bar graph data are expressed as the mean ± SEM and statistical significance is indicated as *P < 0.05, **P < 0.01, ***P < 0.001 and ****P < 0.0001 (C) Representative feces cultured plates from WT (n=4) and WT+Abx (n=4) mice to confirm depletion of microbiome. (**D**) Clinical scores, outlined in the Materials and Methods section, of FMT EAE mice treated with Control PBS (n=3), Naïve (n=3), EAE-VEH (n=5), or EAE-(THC+CBD) (n=5) fecal material. Significance was determined using two-way ANOVA and Tukey's multiple comparisons test to evaluate significance at each day. Significant p values (*P < 0.05, **P < 0.01, ***P < 0.001 and ****P < 0.0001) are indicated below respective days after EAE induction.

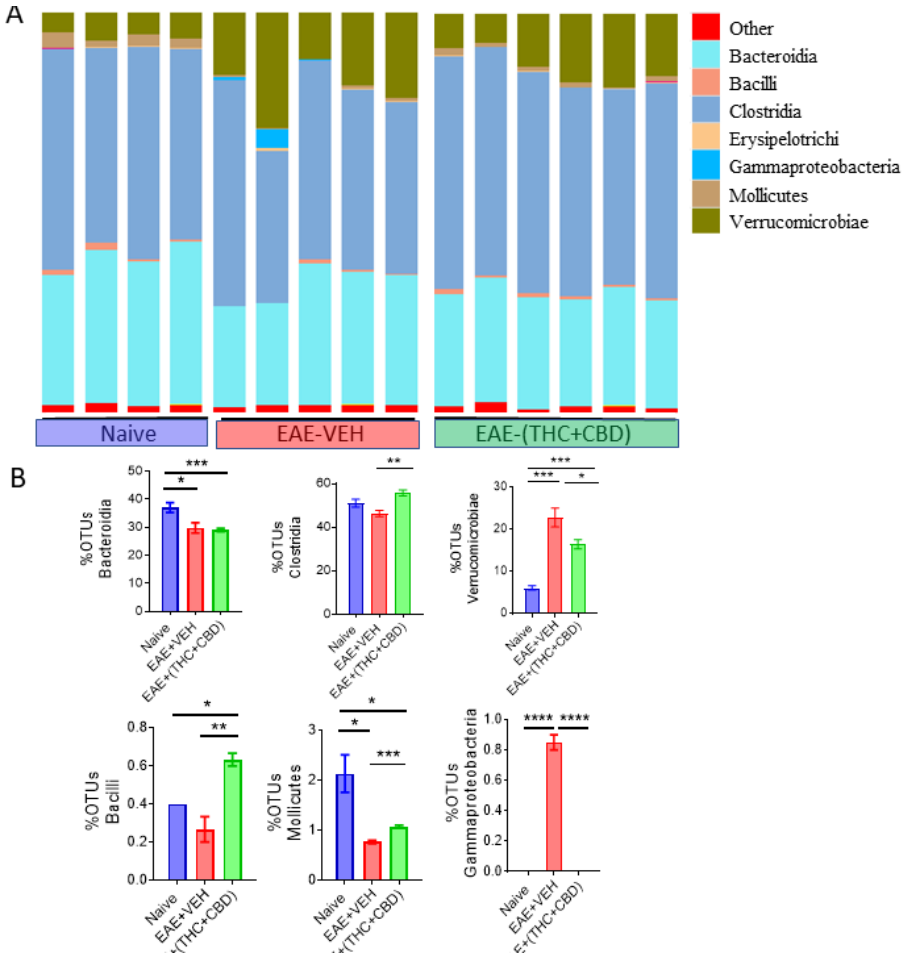

Figure 3.6 16S rRNA analysis of EAE treated with THC+CBD at the class level. (**A-B**) Induction of EAE and treatment with THC+CBD, followed by Nephele 16S rRNA analysis was performed as described in Figure 2 legend and Materials and Methods for Naïve (n=4), EAE+VEH (n=5), and EAE+(THC+CBD) (n=6) experimental groups. (**A**) Depicted are stacked bar graphs for percent OTUs at the class level. (**B**) Significantly altered bacteria at the class level depicted as bar graphs. Bar graph data are expressed as the mean ± SEM and statistical significance is indicated as *P < 0.05, **P < 0.01, ***P < 0.001 and ****P < 0.0001. Significance was determined using one-way ANOVA and Tukey's multiple comparisons test. Data are representative of one independent experiment.

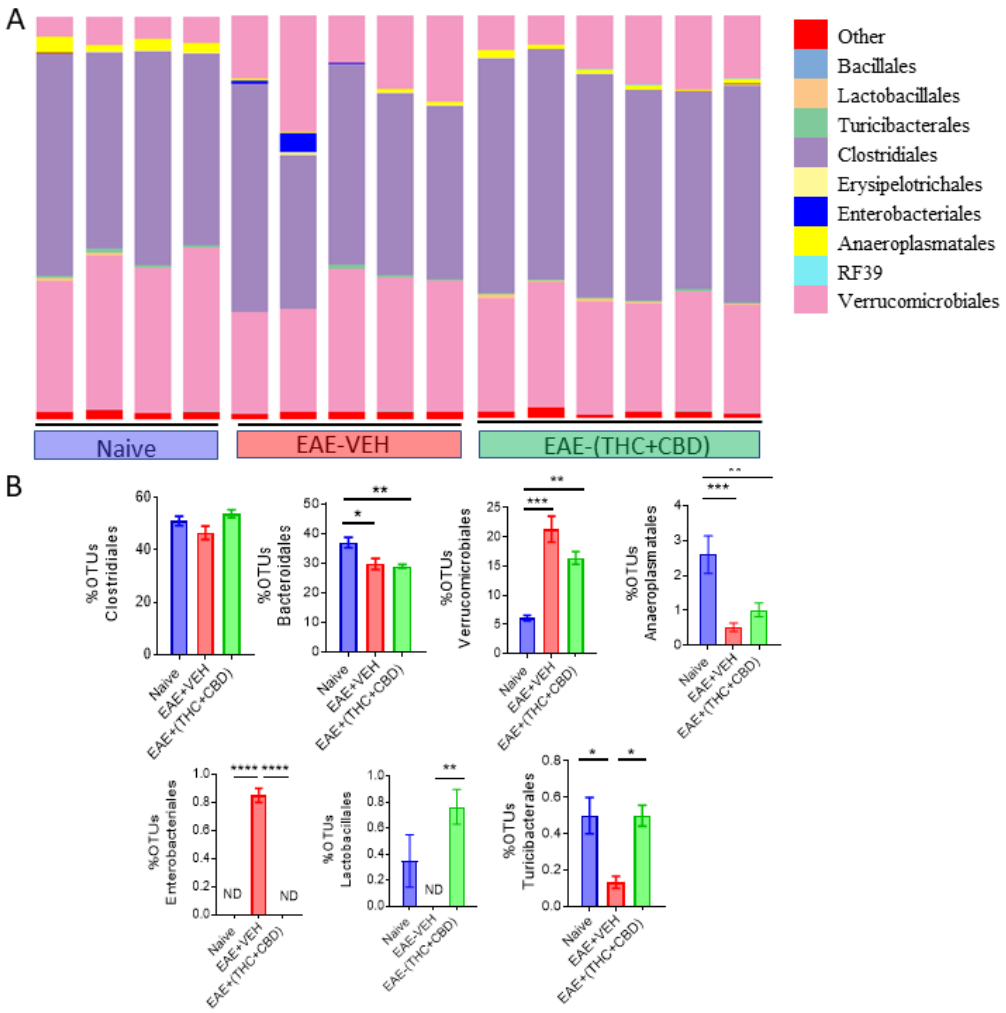

Figure 3.7 16S rRNA analysis of EAE treated with THC+CBD at the order level. (**A-B**). Induction of EAE and treatment with THC+CBD, followed by Nephele 16S rRNA analysis was performed as described in Figure 2 legend and Materials and Methods for Naïve (n=4), EAE+VEH (n=5), and EAE+(THC+CBD) (n=6) experimental groups. (**A**) Depicted are stacked bar graphs for percent OTUs at the order level. (**B**) Significantly altered bacteria at the order level depicted as bar graphs. Bar graph data are expressed as the mean ± SEM and statistical significance is indicated as *P < 0.05, **P < 0.01, ***P < 0.001 and ****P < 0.0001. Significance was determined using one-way ANOVA and Tukey's multiple comparisons test. Data are representative of one independent experiment.

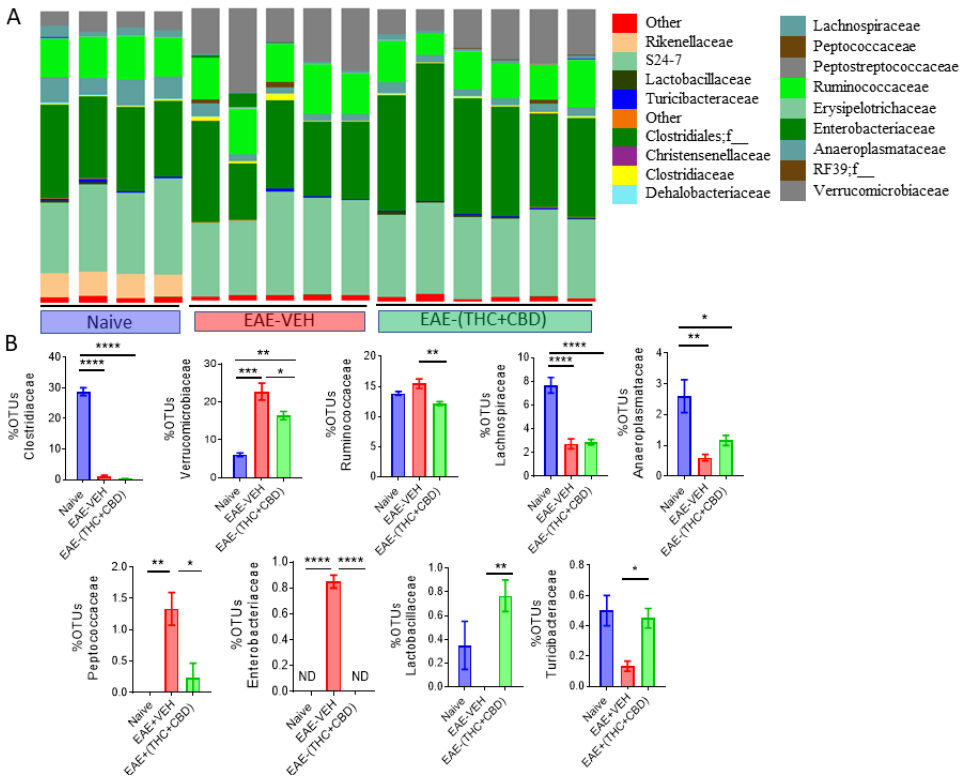

Figure 3.8 16S rRNA analysis of EAE treated with THC+CBD at the family level. (**A-B**). Induction of EAE and treatment with THC+CBD, followed by Nephele 16S rRNA analysis was performed as described in Figure 2 legend and Materials and Methods for Naïve (n=4), EAE+VEH (n=5), and EAE+(THC+CBD) (n=6) experimental groups. (**A**) Depicted are stacked bar graphs for percent OTUs at the family level. (**B**) Significantly altered bacteria at the family level depicted as bar graphs. Bar graph data are expressed as the mean ± SEM and statistical significance is indicated as *P < 0.05, **P < 0.01, ***P < 0.001 and ****P < 0.0001. Significance was determined using one-way ANOVA and Tukey's multiple comparisons test. Data are representative of one independent experiment.

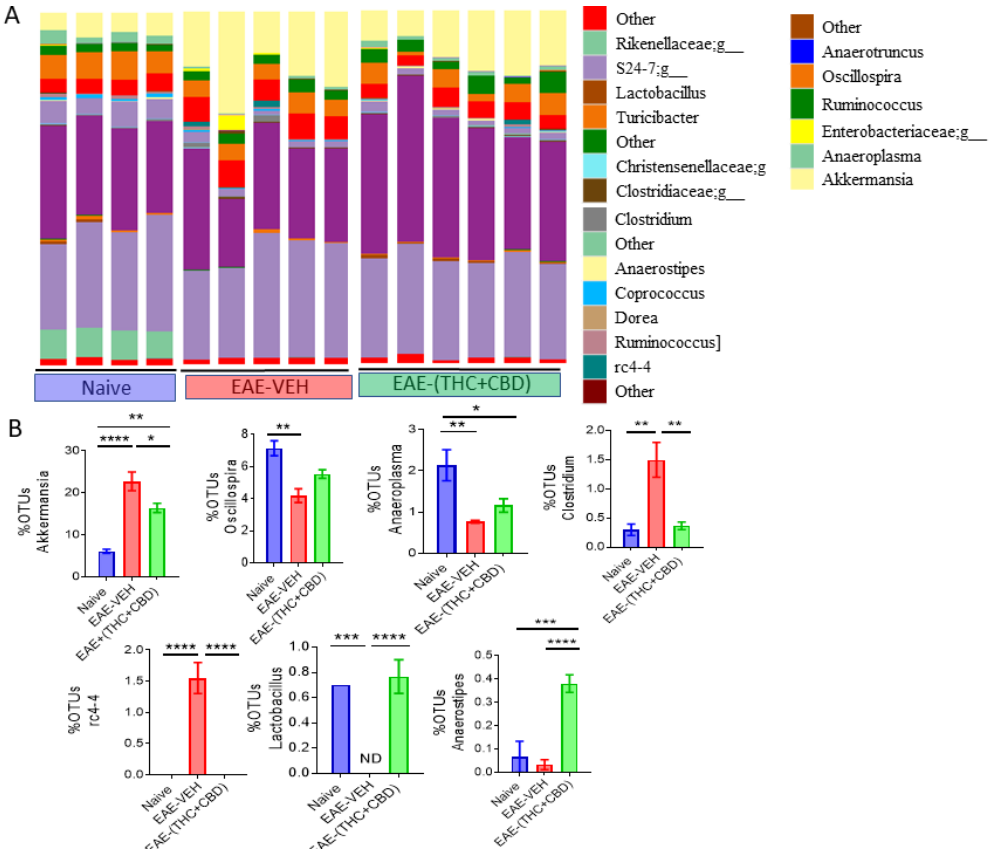

Figure 3.9 16S rRNA analysis of EAE treated with THC+CBD at the genus level. (**A-B**) Induction of EAE and treatment with THC+CBD, followed by Nephele 16S rRNA analysis was performed as described in Figure 2 legend and Materials and Methods for Naïve (n=4), EAE+VEH (n=5), and EAE+(THC+CBD) (n=6) experimental groups. (**A**) Depicted are stacked bar graphs for percent OTUs at the genus level. (**B**) Significantly altered bacteria at the genus level depicted as bar graphs. Bar graph data are expressed as the mean ± SEM and statistical significance is indicated as *P < 0.05, **P < 0.01, ***P < 0.001 and ****P < 0.0001. Significance was determined using one-way ANOVA and Tukey's multiple comparisons test. Data are representative of one independent experiment.

Table 3.1 Source and concentration of SCFAs standards

Acid	Vendor (Cat. No.)	Concentration(mM)	μL
Water(ddH_2O)	-	-	422.3
Acetic	Acros Organics (64-19-7)	400	11.5
Propionic	Sigma (402907)	400	14.9
n-Butyric	Sigma (B103500)	400	18.3
Isovaleric	Sigma (129542)	200	11.0
Valeric	Sigma (240370)	200	10.9
Isobutyric	Sigma (58360)	100	4.6
Caproic	MP Biomedicals (101242)	50	3.0
n-Heptanoic	Sigma (75190)	50	3.5

CHAPTER 4

AHR ACTIVATION BY TCDD (2,3,7,8-TETRACHLORODIBENZO-P-DIOXIN) ATTENUATES PERTUSSIS TOXIN-INDUCED INFLAMMATORY RESPONSES BY DIFFERENTIAL REGULATION OF TREGS AND TH17 CELLS THROUGH SPECIFIC TARGETING OF MICRORNA

4.1 ABSTRACT

TCDD (2,3,7,8-Tetrachlorodibenzo-*p*-dioxin), a halogenated aromatic hydrocarbon, is an environmental contaminant and potent ligand for Aryl hydrocarbon hydroxylase (AhR) ligand. Pertussis Toxin (PTX) is a virulence factor found in *Bordetella pertussis,* a human respiratory pathogen that causes whooping cough. PTX promotes colonization and disease promotion by triggering heightened inflammatory response. In the current study, we investigated if AhR activation by TCDD can attenuate PTX-mediated systemic inflammation. To this end, C57BL/6 mice were injected i.p. with TCDD (25 μg/kg body weight) or vehicle (VEH, corn oil) followed by an i.p. injection of PTX (400 ng/mouse) Twenty-four hours later, mice were rechallenged with the same dose of PTX and 3 days later, mice were euthanized for immunological studies. PTX+VEH group has elevated levels of pro-inflammatory cytokines (IL-17A, IL-6, and IFNγ) in serum and increased proportions of CD4+ Th1 and Th17 cells in spleens. In contrast, PTX+TCDD group had significantly lower levels of these inflammatory cytokines and decreased proportions of Th1 and Th17 cells but increased proportions of Th2 and FoxP3+Tregs when compared to PTX+VEH group. PTX+TCDD treated mice

also had elevated levels of IL-10, and TFG-□, potent anti-inflammatory cytokines. microRNAs (miRs) analysis of CD4+ T cells from the spleens of PTX+TCDD treated mice revealed significant alterations in their expression and several of these miRs targeted cytokines and signaling molecules involved in inflammation. Specifically, PTX+TCDD group had significantly enhanced expression of miR-3082-5p that targeted IL-17, and decreased expression of miR-1224-5p, which targeted FoxP3. Transfection studies with these miR mimics and inhibitors confirmed that this was indeed the mechanism through which TCDD suppressed Th17 while inducing Tregs. Together, the current study demonstrates that AhR activation by TCDD suppresses PTX-induced inflammation through miR regulation that trigger reciprocal differentiation of Tregs and Th17 cells. These studies also suggest that AhR activation may serve as a treatment modality to suppress heightened inflammation induced during *B. pertussis* infection.

4.2 INTRODUCTION

TCDD (2,3,7,8-Tetrachlorodibenzo-p-dioxin), also known as dioxin, is one of the polyhalogenated aromatic hydrocarbons compounds (196). TCDD is a potent agonist with high binding affinity to aryl hydrocarbon receptor (AhR) because which it is extensively used to study the impact of AhR activation on various physiological and immune functions (197, 198). AhR is a basic helix-loop-helix/PAS transcription factor localized in the cytoplasm. More recent studies have shown that AhR activation can not only cause toxicity but also regulate the immune response, specifically the regulation of T cell differentiation (199, 200) Activation of AhR by TCDD or other ligands leads to translocation to the nucleus where it binds to its dimerization partner, aryl hydrocarbon receptor nuclear translocator (ARNT). The AhR-ARNT complex

initiates transcription of genes with promoters containing a dioxin-responsive element (DRE) consensus sequence.(201, 202) In addition to the well characterized ligand, TCDD, a variety of other compounds including tryptophan derivatives, dietary flavonoids and biphenyls have been shown to bind to AhR with varying affinities (203). While AhR was initially discovered in the context of activation by environmental chemicals leading to induction of xenobiotic metabolizing enzymes, and regulating the toxicity mediated by such chemicals, more recent studies have shown that AhR activation plays diverse roles in cellular functions, especially in the regulation of T cell differentiation (204).

Pertussis Toxin (PTX) is one of the most important virulence associated factors of *Bordetella pertussis*, the gram-negative bacterium that is responsible of whooping cough. PTX belongs to the A-B structure class of bacterial toxins (205). Its B subunit binds to a cell surface receptor, and the enzymatically active A subunit interrupts intracellular signaling via irreversible ADP ribosylation of the Gi subclass of G protein (206). PTX exerts its effects through binding to G protein coupled receptors, and since they are present in several mammalian cell types, it affects most cells types (207). One of the $G_{i/o}$ protein dependent effects of PTX is lymphocytosis (208, 209). Moreover, PTX also acts via a phosphokinase C pathway to increase the permeability of the blood-brain barrier resulting in neurological effects (210). Studies have shown that PTX can trigger the development of Th17 cells that promote inflammation (61, 64, 211). Today, PTX is also recognized as a major contributor to autoimmune pathogenesis (212). Previous studies have reported increased interferon gamma (IFN-γ) secretion by immune cells in response to PTX (213), (214), (215). In addition, at the peak of *B. pertussis* infection, PTX enhances neutrophil influx into the airways through the upregulation of interleukin-17

(IL-17). Several studies comparing wild-type and PTX-deficient *B. pertussis* strains have revealed that PTX plays an important role in promoting infection in the respiratory tract, through initial phase of immune suppression followed by enhanced inflammation leading to lung pathogenesis. Thus, agents that suppress inflammation induced by PTX may serve as treatment modalities.

MicroRNAs (miRs) are short non-coding single stranded RNAs, about 19-25 nucleotides long, that negatively regulate the target genes expression at the post transcriptional level (216, 217). A connection between microRNAs and different diseases, such as inflammatory bowel disease, autoimmune diseases, and cancers, is being investigated (216, 218, 219). Recent studies have shown that exposure to chemicals can cause alteration in miRNAs and gene expression that lead to different health problems and diseases (217, 220). The evidence linking between the environmental chemical contaminants like dioxin and miRNAs functions to human diseases is rapidly growing (221). However, it is not clear yet how AhR activation by TCDD alters miRNAs or the possibility that TCDD-induced miRNAs may control mRNA that regulate inflammation. Some studies have confirmed an association between deregulation of miRNAs and exposure to environmental chemicals and the dioxins are among them (222). It has been found that the toxic effects of TCDD may also be controlled by certain epigenetic mechanisms like DNA methylation or histones modification (223). The involvement of PTX in miRNAs dysregulation is also not fully understood and studies in this field still limited. Ge *et al*. 2013, indicating that miR-202, 342-5p, 206, 487b, 576-5p were upregulated and linked to the pathogenesis of inflammatory diseases and significantly increased in the peripheral blood of pertussis patients (224, 225).

In this study, we investigated whether AhR activation by TCDD can attenuate PTX-induced inflammation in mice and if so, whether such anti-inflammatory action is mediated by miRNA. Our studies demonstrate that TCDD does alter the expression of several miRNA that target various cytokine and transcription factors in T cells leading to suppression of PTX-mediated inflammation.

4.3 MATERIALS AND METHODS

Mice

Female C57BL/6 mice (6–8 weeks old) were purchased from Jackson Laboratories (Indianapolis, Indiana). Animals were housed in AALAC approved animal facility at the School of Medicine, University of South Carolina. Use of mice for experiments and their maintenance were approved by the University of South Carolina Institutional Animal Care and Use Committee.

Ethical statement

Animals used in the experiments of this study were approved by Institutional Animal Use and Care committee of University of South Carolina.

PTX and TCDD Administration

TCDD was kindly provided by Dr. Steve Safe (Institute of Biosciences & Technology, Texas A&M Health Sciences Center, College Station, Texas). TCDD dissolved in DMSO (Sigma, St. Louis, MO) City, State?) was further diluted with corn oil (CO), (Sigma. St. Louis, MO) before administration (212). The mice were first injected intraperitoneal (ip) with vehicle (CO) or TCDD (25 µg/kg body weight) and then injected intraperitoneal(ip) with 400 ng/mouse PTX (List Biological Laboratories,

Campbell, CA) Twenty-four hours later, the mice were rechallenged with the same dose of PTX, as described (16).

Determination of cytokines Expression by performing ELISA

To examine the expression of pro- and anti-inflammatory cytokines post PTX and Vehicle or TCDD treatments, blood was collected from the portal vein of PTX+VEH and PTX+TCDD mice. Sera from mice of both groups were either used immediately or stored at -20 °C until further use. Cytokines of interest, such as IL-17A, IL-6, IFNγ and IL-10 were determined by performing ELISA using BioLegend ELISA Max kits (BioLegend, San Diego, CA) and following the protocol of the company and as described in detail previously by Busbee *et al*. (226).

Flow Cytometry Analysis of splenic cells post PTX and TCDD treatments

We performed flow cytometry to determine various cell types present in spleens of mice treated with PTX + Vehicle and PTX+TCDD. In brief, single cell suspensions of spleens from both groups were first prepared. The splenic cells were then treated with GolgiPlug purchased from BD (BD Biosciences, San Jose, CA) for at least 6 hrs at 37°C to enhance cytokine staining. These cells were then stained using PE-conjugated anti-mouse CD4 (clone GK1.5) for 30 min at 4°C. Next, the cells were washed with cold PBS twice and then stained using following Abs: anti-FoxP3, anti-IL-10, anti-TGF-β, anti-IL-17, and anti-IFN-γ (Biolegend, San Diego, *C*A). For MDSCs, splenocytes were stained with MDSCs fluorescent conjugated antibodies: CD11b and Gr-1. Stained cells were analyzed using Beckman Coulter FC500 flow cytometer (Indianapolis, IN, USA) and their software or BD FACSCelesta (BD Biosciences, San Jose, CA) and DIVA software or FlowJo software.

Investigation of miRNA profile in splenic CD4+ T cells

To investigate miRNAs profile in CD4+ splenic cells, CD4+ cells were isolated from the splenocytes of PTX+VEH and PTX+TCDD groups of mice using the EasySep PE Positive Selection Kit (StemCell Technologies, Cambridge, MA) and anti-CD4 mAb (Biolegend, San Diego, CA). The isolated CD4 cells were washed with cold PBS and then Qiazol Lysis Reagent (Qiagen, Germantown, MD) was added and either used immediately for total RNA including miRNA or stored at -80°C for future use. Total RNA including miRNAs were extracted using miRNeasy micro kit (Qiagen, Germantown, MD) and according to the manufacturer's instructions. The concentration and purity of the extracted RNAs were determined using the NanoDrop 2000 spectrophotometer (Thermo Scientific, Wilmington, DE). The expression profile of miRNAs was determined by performing microRNA Arrays using the Affymetrix miRNA array version 4 (JHMI deep sequencing and microarray core) and GeneChip miRNA 3.0-array platform. miRNAs data were analyzed using Inguinety Pathway Analysis (IPA, Qiagen) as describe (227) . In this study, a > 1.5-fold change in miRNAs expression was considered positive (228).

Validation of miRNAs in splenic CD4+ T cells treated with vehicle or TCDD

Next, we validated several of miRNA that were selected based on their expression and corresponding genes expression. For miRNA expression analysis, cDNA synthesis was performed from total RNA using miScript II cDNA Synthesis Kit (# 218161, Qiagen, Germantown, MD). Two step miRNA qRT-PCR was carried out using SsoAdvanced SYBR green Mix (#1725270 Bio-Rad, Hercules, CA) with mouse primers for SNORD96A (#MS00033733 Qiagen, Germantown, MD), miR-141-3p

(#MS00001610 Qiagen, Germantown, MD), miR-142-3p (# MS00012201 Qiagen, Germantown, MD), and miR-211-3p (# MS00024563 Qiagen, Germantown, MD). Expression levels for miRNA were normalized to SNORD96A. All PCR experiments used a CFX96 Touch Real-Time PCR Detection System (Bio-Rad, Hercules, CA). Fold changes were calculated using the $2^{-\Delta\Delta CT}$ method.

Validation of miRNAs-specific gene expression in splenic CD4+ T cells treated with vehicle or TCDD

Next, we evaluated the expression of target genes (IL-10, TGF-β1, TGFβ2, TGFβR3, TGFβR1, GATA3, SMAD2, IL-6, and RORγt), as described (229). For gene expression analysis, cDNAs was generated as described above from total RNA using miScript II cDNA synthesis kit. A two-step amplification with a 60° annealing temperature for qRT-PCR was carried out using SsoAdvanced SYBR green supermix from Bio-Rad with mouse primers for IL-10, TGF-β1, TGFβ2, TGFβR3, TGFβR1, GATA3, SMAD2, IL-6, and RORγt customized and ordered from IDT (Coralville,IA). All PCR experiments used a CFX96 Touch Real-Time PCR Detection System (Bio-Rad, Hercules, CA), and expression levels were normalized to GAPDH mRNA levels. Fold changes were calculated using the $2^{-\Delta\Delta CT}$ method.

Transfection of splenic cells with miR-1224-5p and miR-3082-5p mimic or inhibitor

Two miRNAs (miR-3082-5p and miR-1224-5p) were selected based on their alignments with mouse IL-17 and FoxP3 genes. For transfection, we used T cells purified from naïve splenocytes and maintained for 24 hours in complete RPMI 1640 medium supplemented with 10% heat-inactivated fetal bovine serum, 10 mM L-glutamine, 10 mM HEPES, 50 μM β-mercaptoethanol, and 100 μg/ml penicillin/streptomycin at 37°C and 5% CO_2 (32). Prior to transfection, T cells were seeded at a density of

$2x10^5$ cells/well in a 24-well plate. The following day, the cells were transfected with scrambled miRNA (Mock) control or mature miR-1224-5p mimic (Qiagen # MSY0005460), miR-1224-5p inhibitor (Qiagen # MSY0005460), mature miR-3082-5p mimic or miR-3082-5p inhibitor (Qiagen # YI04103580) using HiPerFect transfection reagent (Qiagen, Germantown, MD) and following the protocol of the company.

Quantitative Real-Time PCR (qRT-PCR) to determine the expression of miRNAs and target genes

We performed Q-RT-PCR to determine the expression of miRNAs that target FoxP3 and IL17 genes respectively. The selection of these two miRNAs was based on their alignment with highly conserved regions of their target genes using miRNA.org, miRNAWalk, TargetScan software. As described above, cDNA synthesis was performed from total RNAs using miScript II cDNA Synthesis Kit (Qiagen # 218161) and Two step miRNA QRT-PCR were carried out using SsoAdvanced SYBR green Mix (BioRad #1725270) with mouse primers for SNORD96A (Qiagen #MS00033733), miR-3082-5p (Qiagen # MS00025102), miR-1224-5p (Qiagen # MS00011074), Expression levels for miRNAs were normalized to SNORD96A. All PCR experiments used a CFX96 Touch Real-Time PCR Detection System (Bio-Rad. Fold changes were calculated using the $2^{-\Delta\Delta CT}$ method.

Next, we evaluated the expression of target genes (FoxP3 and IL17) by performing QRT-PCR as described above. All qRT-PCRs were performed using a CFX96 Touch Real-Time PCR Detection System (Bio-Rad, Hercules, CA), and expression levels were normalized to GAPDH mRNA levels. Fold changes were calculated using the $2^{-\Delta\Delta CT}$ method. Specific primers sequences of genes are provided in table 2. Furthermore, we also performed QRT-PCR to determine the expression of miR-

3082-5p and miR-1224-5p and their respective target genes IL17 and FoxP3 in miR-3082-5p and miR-1224-5p mimic and inhibitor-transfected T cells treated with PTX+Vehicle and PTX+TCDD as described above.

Statistical analysis

We used GraphPad Prism6 software to perform statistical analyses. The statistical analyses were performed using Student's t-test and/or ANOVA. p value <0.05 was considered significant.

4.4 RESULTS

TCDD suppresses PTX-induced inflammation in mice

In this study, we investigated the effect of AhR activation by TCDD on PTX-mediated inflammatory response in C57BL/6 mice. To that end, mice received PTX+TCDD or PTX+Veh on day 0 and 24 hr later, all mice received a second dose of PTX. On day 4, the mice were euthanized and studied for inflammation (Fig 1A). First, we performed ELISA using sera from PTX+VEH and PTX+TCDD groups. The data showed significant decrease in pro-inflammatory cytokines IL-17A, IFN-γ, and IL-6 in PTX+TCDD mice, when compared to PTX+VEH mice (Figure 1B-D). In contrast, there was significant increase in IL-10, an anti-inflammatory cytokine in PTX+TCDD group, when compared to PTX+VEH group (Figure 1E). These data demonstrated that TCDD may suppress pro-inflammatory cytokine response by upregulating the generation of anti-inflammatory cytokine, IL-10.

TCDD promotes differential regulation of Tregs and Th17 cells and generation of MDSCs in vivo

Next, we investigated the phenotypic changes in spleens harvested from PTX+VEH and PTX+TCDD mice. We analyzed for the following cell types: Tregs:

CD4+FoxP3+, Th17: CD4+IL17+, Th1: CD4+IFNγ+, and Th2:CD4+IL10+ and CD4+TGFβ+ cells. When we compared Th1 vs Th2 cells, we noted that the percentages of Th2 cells (CD4+IL10+ cells and CD4+TGFβ+) were significantly increased in PTX+TCDD group, when compared to PTX+VEH group (Figure 2A, B). In contrast, the proportions of Th1 cells was significantly decreased in PTX+TCDD group when compared to controls (Figure 2 C). Th17 and Tregs are reciprocally regulated and thus when we analyzed these cells in the two groups and found that the percentages of Th17 cells (CD4+IL17+) were increased while that of Tregs (CD4+FoxP3+) were decreased in PTX+VEH group and interestingly, this pattern was completely reversed in PTX+TCDD group (Figure 3 A, B).

We also examined myeloid-derived suppressor cells (MDSCs; CD11b+/Gr1+) in spleens of PTX+VEH and PTX+TCDD groups of mice because these cells are also highly immunosuppressive and have been known to induce Tregs (230), (231). There was significant increase in both the percentage and numbers of MDSCs in the mice exposed to PTX+TCDD group when compared to controls (Figure 4A-C).

TCDD dysregulates expression of miRNAs in splenic cells in vivo

To understand anti-inflammatory/immunosuppressive effects of TCDD, we investigated the molecular mechanisms that TCDD may regulate to affect gene expression. To this end, we performed miRNA arrays using total RNA from splenic CD4+ T cells from PTX +VEH and PTX+TCDD groups as described in Methods. Of approximately 1111 miRNAs tested, 157 miRNAs were differentially expressed (Fold change > +/- 1.5) (Figure 5A). Proportional Venn diagram was generated to represent the fold change Of 1111 miRNA in CD4+ T cells examined, there were 48 miRNA that were

upregulated (>1.5-fold) and 58 miRNA that were downregulated (>1.5-fold) in splenic CD4 T cells of PTX+TCDD group of mice, when compared to PTX+VEH group of mice (Figure 5B). Next, 106 miRNA that showed altered expression in PTX+TCDD group were analyzed using Ingenuity Pathway Analysis (IPA) software from QIAGEN. IPA pathway analysis showed several miRNAs that targeted the expression of cytokines, transcription factors, and signaling molecules related to inflammation (Figure 5C). Using Affymatrix Expression Console software, heat map of miRNAs of both groups was generated (Figure 5D). In addition, we analyzed miRNA-specific target genes using TargetScan and microRNA.org (www.microRNA.org) analytical tools available online. A list of target genes and their putative 3'UTRs (mRNAs/miRNAs) has been presented in Table 3. We identified miR-142-3p to target FoxP3, TGFβ2 and TGFβR1, miR-141-3p to target TGFβ2 and TGFβR1, miR-211-3p to target TGFβ1, TGFβ2, TGFβR1 and Smad2 (Table 3). These data suggested that TCDD causes dysregulation of miRNA in T cells that target genes involved in inflammatory pathways.

Validation of miRNAs by Quantitative Real-Time PCR (QRT-PCR)

After analyzing miRNAs profile obtained from miRNA arrays, we selected several miRNAs, particularly that target cytokines production and Tregs proliferation, to validate their expression by QRT-PCR. We used the same RNAs from CD4+ T cells that we used for miRNA arrays. We validated the microarray data by using QRT-PCR of some select miRs that were up or down-regulated following TCDD treatment. The data demonstrated that there was significant downregulation, miR-141-3p (Figure 5E, miR142-3p (Figure 5F), and miR-211-3p (Figure 5G) in splenic CD4 T cells from PTX+TCDD group when compared to PTX+VEH group.

qRT-PCR to determine the expression miRNA target genes

Next, we validated the gene expression of some of the targets of miRs disrupted by TCDD. We noted significant upregulation of IL-10 (Figure 6A), TGF-β1 (Figure 6B), TGF-β2 (Figure 6C), TGF-βR3 (Figure 6D), TGF-βR1 (Figure 6E), GATA3 (Figure 6F), SMAD2 (Figure 6G) in cells from mice exposed to PTX+TCDD, when compared to PTX+VEH group. Additionally, there was significant downregulation of IL-6 (Figure 6H), and RORγT (Figure 6I) in PTX+TCDD group when compared to PTX+VEH group.

Transfection studies to demonstrate the specificity of miR and their inflammatory target genes.

During IPA analysis and using target scan, we observed that miR-1224-5p and miR-3082-5p had strong binding affinity with 3'UTRs of FoxP3 and IL-17, respectively (Table 3). To confirm that miR-1224 and miR-3082 specifically targeted FoxP3 and IL-17 gene expression, respectively, we first performed QRT-PCR analysis of the expression of both miRs and potential targets from the same cell population namely, splenic CD4+ cells from PTX+VEH or PTX+TCDD. We noted significant upregulation of miR-3082-5p (Figure 7A) and downregulation of miR-1224 (Figure 7E) in PTX+TCDD group when compared to controls. Additionally, in the same cells, there was significant downregulation of IL-17 expression (Figure 7B) and increase in FoxP3 expression (Figure 7F) in PTX+TCDD groups when compared to controls. These data demonstrated that in the same cells, the miRNA expression induced by TCDD correlated with the expression of respective target genes involved in inflammation.

To further confirm the role of miR-1224-5p and miR-3082-5p in the regulation of FoxP3 and IL-17, respectively, CD4+ T cells were transfected with either miR-1224-5p or miR-3082-5p mimics or their respective inhibitors. Expression of miR-1224-5p and

miR-3082-5p was determined by QRT-PCR. There was significant increase in the expression of miR-3802-5p and miR-1224-5p in cells transfected with miR-3082-5p mimic or miR-1224-5p mimic when compared to mock controls (Figure 7C, G). Inhibitors of miR-3082-5p and miR1224-5p completely blocked the expression of these miRs respectively (Figure 7C, G). In these cells, transfection with miR-3082-5p mimic led to significant downregulation of IL-17 while the inhibitor caused upregulation of IL-17 (Figure 7D). Furthermore, transfection of these cells with miR-1224-5p mimic led to downregulation of FoxP3 while the inhibitor caused increased expression of FoxP3 (Figure 7H). The data obtained from transfection experiment demonstrated a clear role of miR-1224-5p and miR-3082-5p in the expression of FoxP3 and IL-17 mediated by exposure to TCDD.

4.5 DISCUSSION

Bordetella pertussis is a human respiratory pathogen that causes whooping cough, and its virulence factor, pertussis toxin (PTX), promotes colonization leading to systemic disease (232). Experimentally, PTX is well characterized as an adjuvant that promotes development of tissue-specific experimental autoimmune diseases such as experimental autoimmune encephalomyelitis (EAE), experimental autoimmune uveitis (EAU), and the like (233),(234). PTX in these models, is known to enhance vascular permeability, damage to blood-brain barrier and induce Th1 responses (235), (236). More recent studies suggested that PTX can induce a robust Th17 response while inhibiting Tregs (64). While the precise mechanisms through which PTX serves as a virulence factor in promoting *B. pertussis* infection is unclear, it is believed that the ability of PTX, at peak of *B. pertussis* growth in the airways, to trigger increased inflammation leads to

pathology in the airways(60). Thus, agents that suppress such inflammation induced by PTX may help attenuate the pathogenesis. In the current study, therefore, we tested the effect of TCDD, a potent AhR ligand on PTX-mediated inflammation. Because the effect of TCDD on a potent toxin such as PTX known for its ability to promote Th1 and Th17 response while suppressing Tregs, has not been studies previously, we were interested to see if TCDD would reverse these effects and if so, identify the mechanisms.

TCDD is described as the worst and most toxic human made environmental contaminant. TCDD is an environmental pollutant that mediates toxicity through activation of AhR, a ligand-dependent transcription factor and member of the basic helix-loop-helix–Per/Arnt/Sim gene family (237, 238). It is well characterized for its toxicity against the cells of the immune system (239-241). More recently, activation of AhR by TCDD has been shown to regulate differential expression of FoxP3 and IL-17 causing generation of more Tregs but suppression of Th17 cells (239), (242). The study from our lab has shown that TCDD suppressed EAE in mice (212). We have shown that TCDD modulated differential expression of IL-17 and FoxP3 in mice with EAE through epigenetic modifications (212). PTX, on the other hand, has been shown to promote the generation of Th17 cells (64). Because of opposite molecular functions of PTX and TCDD, we investigated whether TCDD can suppress PTX-induced inflammation in mice and examined the molecular mechanisms involved in TCDD-induced suppression of PTX-induced inflammation.

In this study, we noted that injection of PTX triggered significant systemic inflammation in mice as evidenced by detection of several inflammatory cytokines in the serum including IL-17, IL-6, and IFN-γ. These cytokine expressing cells were also

detected in CD4+ T cells in the spleen. Interestingly, the serum levels of IL-17 or proportion of Th17 cells in the spleens of PTX-treated mice was higher than that of IFN-γ or Th1 cells in the spleen, thereby demonstrating that PTX is a more potent inducer of Th17 cells than Th1 cells. These data were consistent with the observation that PTX generates a cytokine storm associated with inflammation in mice by inducing IL-6 that promotes IL-17 production in CD4+ T cells (64). Also, our findings agree with previous observation that administration of PTX stimulates the development of pathogenic Th17 cells in mice of immune-mediated ocular inflammation more than other TLR ligands, such as LPS, and polyinosinic-polycytidylic acid (243). In another study, it was reported that immunization with whole cell pertussis vaccination in mice resulted in the generation of Th17 cells (244). Previous studies, using mice infected with pertussis toxin (PTX)–producing *B. pertussis* strain or an isogenic PTX-deficient strain (ΔPT), had shown that PTX activity was associated with upregulated expression of proinflammatory cytokines and chemokines (61) (232). Studies on immunomodulation by *B. pertussis* have also shown that the host immune response may be tilted towards development Th17 cells, that produce IL-17A (64).

In the current study, we noted that TCDD caused significant decrease in inflammatory (IL-17, IL-6, and IFN-γ) cytokines but an increase in anti-inflammatory (IL-10) cytokine in PTX-injected mice. These data demonstrated that TCDD was able to suppress PTX-induced inflammation in mice. We noted increased switch from Th1 to Th2 phenotype with increased induction of IL-10 and TGF-□□following TCDD treatment. IL-10 is an anti-inflammatory cytokine that is known to inhibit the activity of Th1 cells (245). TGF-□□inhibits Th1 differentiation by blocking the expression of T-

bet, the master regulator of Th1 cell differentiation (246). We also noted that TCDD was able to induce a switch from Th17 to Tregs in PTX-immunized mice. This may result from decreased IL-6 seen in PTX+TCDD treated mice because IL-6-mediated STAT3 signaling is essential for Th17 differentiation and plays a central role in the pathogenesis of certain autoimmune diseases such as rheumatoid arthritis (247). The second mechanism through which TCDD may suppress Th17 cells may result from its ability to increase the expression of FoxP3 and induce more Tregs as seen in the current study using PTX and seen in other models autoimmune disease (248), (249). For example, TCDD was shown to suppress diabetes in NOD mice by increasing Foxp3+ T cells in pancreatic lymph nodes (249). Also, TCDD inhibited the clinical symptoms in an experimental autoimmune encephalomyelitis (EAE) model by inducing Tregs (68). Because EAE mouse models use PTX along with myelin oligodendrocyte glycoprotein (MOG) to enhance clinical signs of EAE, our studies raise an interesting question on whether TCDD-mediated suppression of EAE results from suppression of PTX effects or direct action on MOG-specific T cells. Previous studies from our laboratory has also shown that activation of AhR led to reciprocal epigenetic regulation of FoxP3 and IL-17 expression and amelioration of experimental Colitis (239). In this study, we noted that there was decreased methylation of CpG islands of Foxp3 and increased methylation of IL-17 promoters, which led to increased induction of Tregs while suppressing Th17 generation (239). In the current study, we noted that TCDD induced MDSC in PTX-treated mice. Because Tregs have also been shown to be induced by MDSCs 30103447,(250) this may constitute another additional mechanism through which Tregs were induced in PTX+TCDD administered mice. As there were more Tregs in

PTX+TCDD-treated mice, it is possible that the increased IL-10 seen in these mice may have resulted from such Tregs that produce IL-10 (251). Previous studies from our lab reported TCDD-induced MDSCs generation in different tissues/organs like spleen and peritoneal cavity. Myeloid-derived suppressor cells (MDSCs) are a heterogeneous population of immature myeloid cells that play a major role in immunosuppression in inflammation, cancer, and other diseases (252).

In recent years, miRs have been shown to play an important role in the regulation gene expression and potentially may control majority of the molecular and cellular pathways (253-255). Also, specific miRs may play important roles in T cell and MDSCs development and functions by regulating target genes involved in their proliferation and differentiation (230). Previous studies from our lab have shown that AhR activation by dietary ligands such as indole-3-carbinol (I3C) or 3,3'-diindolylmethane (DIM) leads to decreased the expression of several miRs (miR-31, miR-219, and miR-490) that target Foxp3, while incresinga the expression of miR-495 and miR-1192 that target IL-17 (240). This leads to increased induction of Tregs and decreased differentiation of Th17 cells consequently suppressing delayed-type hypersensitivity (DTH) response to methylated BSA (240) In another study, we noted that miRNA-466a-3p targeted TGF-β2 and regulated Treg differentiation (256). In the current study, we observed that PTX+TCDD group showed significant alterations in the expression of a numbers of miRNA and pathway analysis showed that some of these altered miRNAs targeted inflammatory cytokines or signaling pathways. Interestingly, we were able to narrow down to some specific miRs that seemed to target FoxP3 and IL-17 gene expression through target scanning. Specifically, we found that miR-1224-5p and miR-3082-5p had strong binding

affinity with 3'UTRs of FoxP3 and IL-17, respectively. We confirm the role of miR-1224-5p and miR-3082-5p in the regulation of FoxP3 and IL-17, respectively, we performed transfection studies which conclusively demonstrated that miR-1224-5p and miR-3082-5p were involved in the upregulation of FoxP3 and down regulation of IL-17 following exposure to TCDD. The role of miR-1224-5p in the regulation of immune response has not been previously studied. MiR-1224-5p has been shown to act as a tumor suppressor by targeting CREB1 in malignant gliomas (257). Similarly, the role of miR-3082-5p has not been reported in any disease model. Thus, our studies are unique in identifying for the first time that miR-1224-5p and miR-3082-5p play a role in the regulation of inflammation.

In summary, our studies suggest that during PTX-induced inflammation, activation of AhR by TCDD may promote anti-inflammatory activity primarily through regulation of miRNA that target Foxp3 and IL-17 gene. Because PTX plays a critical role in the pathogenesis of *B. pertusis* infection by inducing cytokine storm and exaggerated inflammatory response, our studies suggest that AhR ligands may serve as therapeutic modality to treat such inflammatory response

.

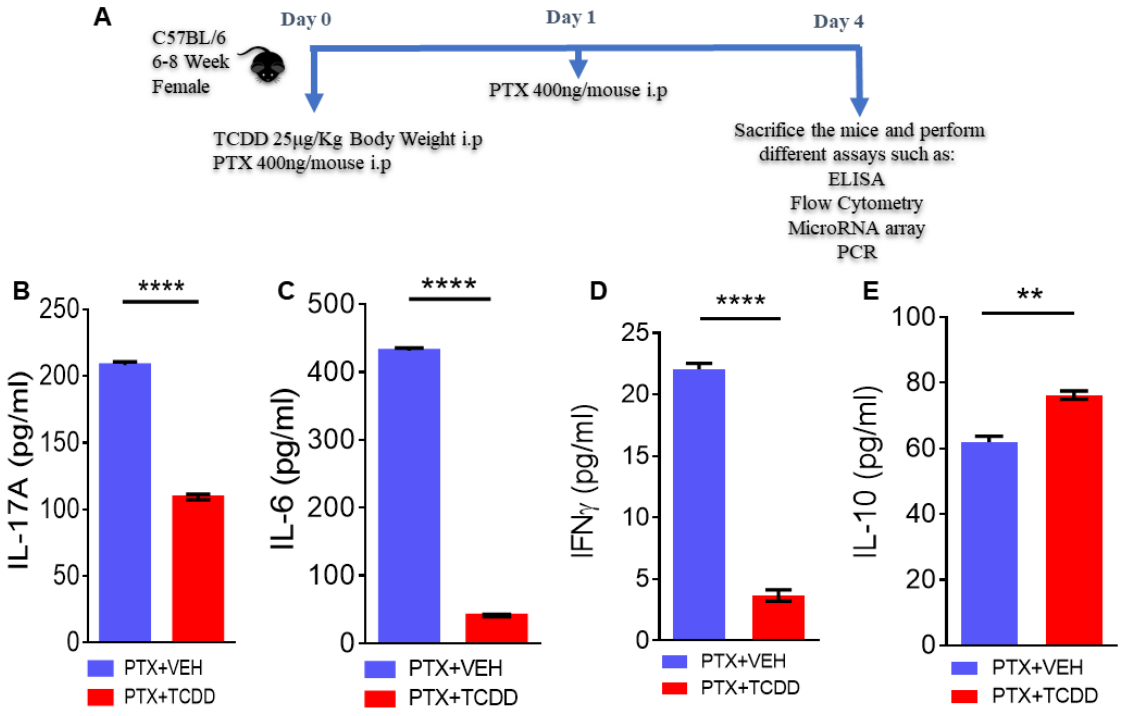

Figure 4.1 TCDD suppresses PTX-induced inflammation in mice. Mice were injected with PTX and TCDD as described in panel A and 4 days later, PTX+VEH or PTX+TCDD groups were investigated for inflammation. (**B**) ELISA was performed using sera collected from PTX+VEH and PTX+TCDD group of mice. Cytokines IL-17A (**B**), IL-6 (**C**), IFNγ (**D**), and IL-10 (**E**) were measured. Data are expressed as the mean ± S.E.M. and statistical significance is indicated as **p < 0.01, ***p< 0.001 and ****P < 0.0001 between the two groups.

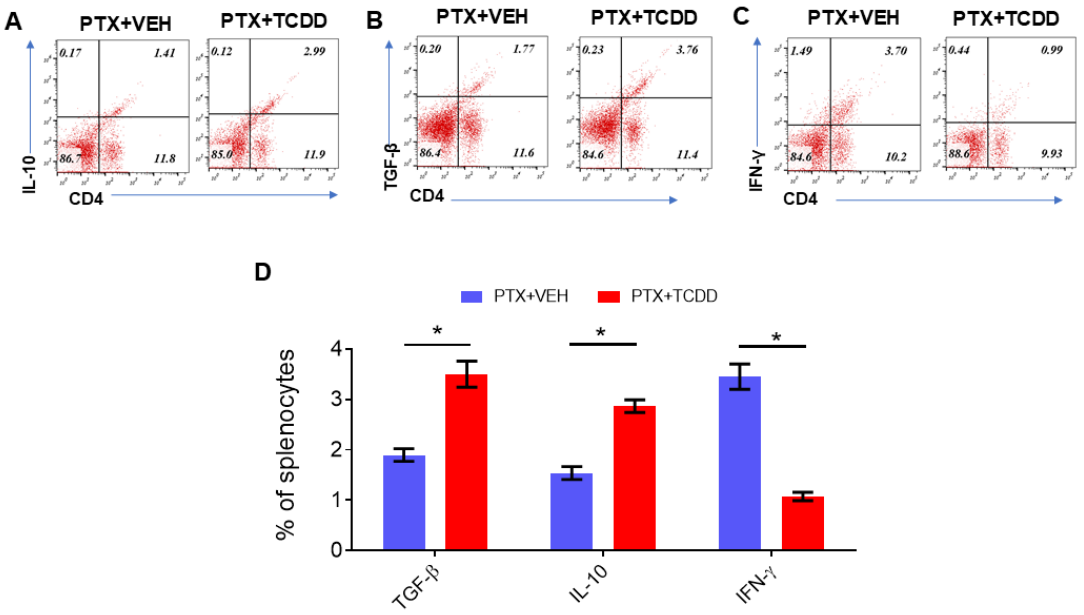

Figure 4.2 TCDD suppresses PTX-induced Th1 cells and promotes Th2 cells. Mice were immunized with PTX and injected with TCDD as described in Fig 1 legend. Splenocytes were double-stained for CD4 and various cytokines and analyzed by flow cytometry: (A) IL-10; (B)TGF-β; (C) IFN-□. Panels A-C show a representative experiment and data from multiple mice plotted in Panel D. Statistical analysis using Student's t-test. Data are expressed as the mean ± S.E.M. and statistical significance between the two groups is indicated as *$p < 0.05$.

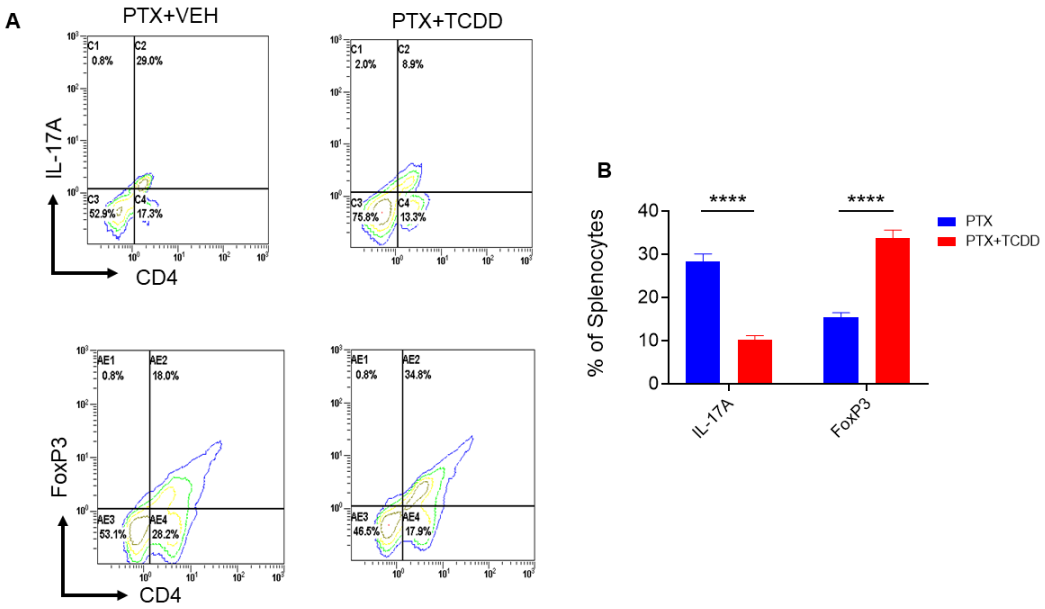

Figure 4.3 TCDD promotes Treg while inhibiting Th17 induction. Mice were immunized with PTX and injected with TCDD as described in Fig 1 legend. Splenocytes were double-stained for CD4 and FoxP3 or CD4 and IL-17 markers and analyzed using Flow cytometry. Panel A shows a representative experiment while data from multiple mice plotted in Panel B, showing reciprocal regulation of Th17 vs Tregs between the two groups. Statistical analysis between the two groups showing ****$p < 0.0001$.

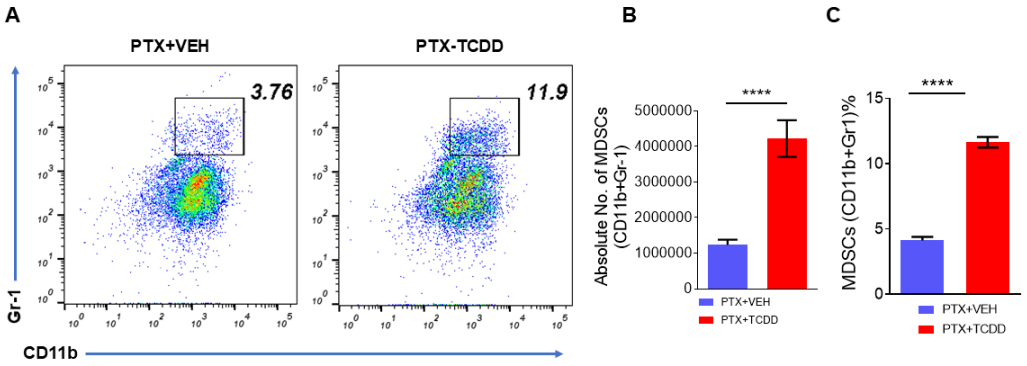

Figure 4.4 TCDD promotes MDSCs production. Mice were immunized with PTX and injected with TCDD as described in Fig 1 legend. Spleen cells were double-stained for Gr-1+CD11b+ cells. Panel A shows a representative experiment while data from multiple mice is plotted in Panel B-C. Statistical analysis using Student's t-test. In Panel B-C data are expressed as the mean ± S.E.M. and statistical significance is indicated as ****$p < 0.0001$ when the two groups are compared.

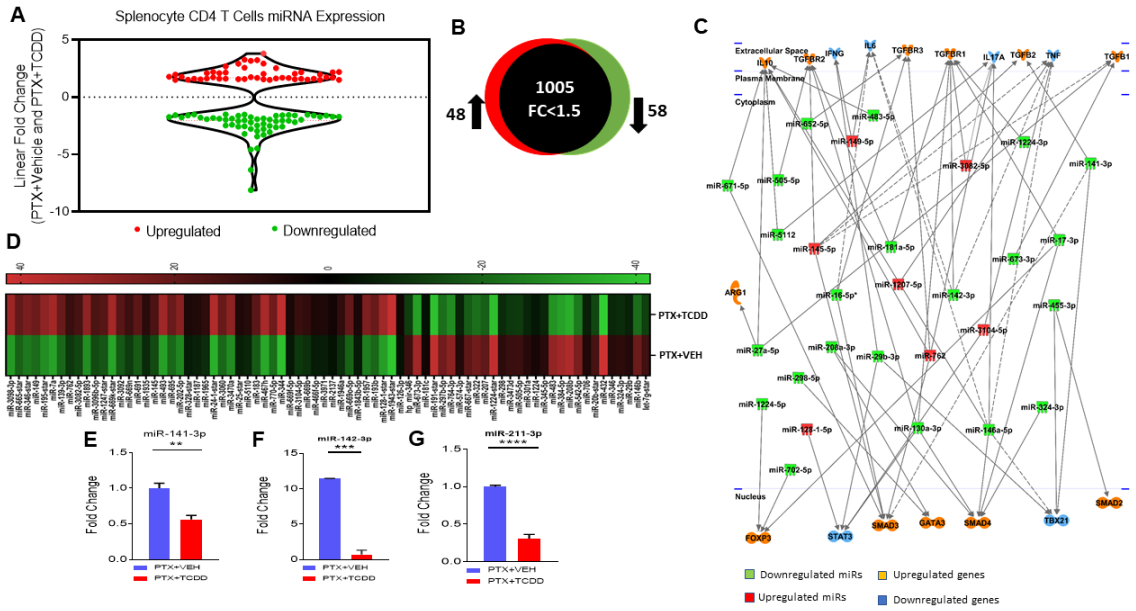

Figure 4.5 MicroRNAs Analysis. Mice were immunized with PTX and injected with TCDD as described in Fig 1 legend. Differentially expressed miRNA were analyzed in splenic CD4+ T cells. Total RNA was isolated and pooled from CD4+ T cells obtained from the spleen of PTX+VEH or PTX+TCDD groups (n = 5). miRNA microarray assay was performed to test differentially expressed miRNA. (**A**) The fold change distribution of the miRNAs found within CD4+ T cells from the spleen of PTX+Vehicle and PTX +TCDD mice. (**B**) Proportional Venn diagram illustrating fold change (>1.5) of miRNAs between the two groups. (**C**) Pathway analysis of miR mediating dysregulation in gene expression in PTX+TCDD group. (**D**) Heat map of hierarchical clustering of the relative expression of miRNA alterations. The color scale denotes those miRNAs that were upregulated (red) and downregulated (green). (**E-G**) Expression levels of select downregulated miRNAs analyzed by qRT-PCR using Snord96a as a control.

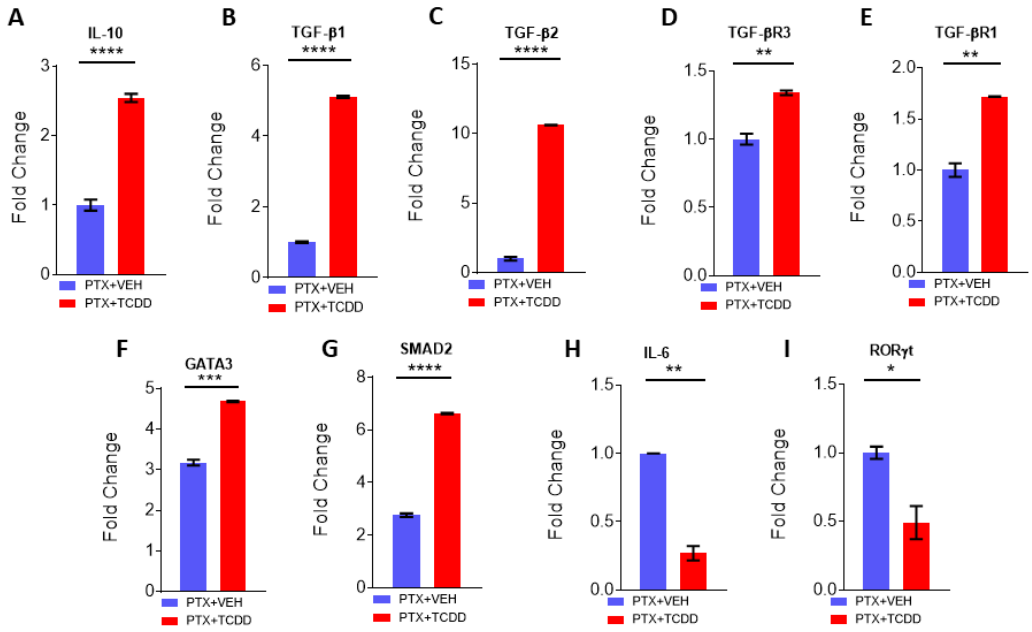

Figure 4.6 qRT-PCR validation of gene expression. Mice were immunized with PTX and injected with TCDD as described in Fig 1 legend. Expression of target genes was studied using qRT-PCR in CD4+ Tcells: (**A**) IL-10, (**B**) TGF-β1, (**C**)TGFβ2, (**D**)TGFβR3, (**E**) TGFβR1, (**F**) GATA3, (**G**) SMAD2, (**H**) IL-6 and (**I**) RORγt are shown, using GAPDH as a control. Data present mean ±SEM of 3 tests and statistical significance between the two groups was tested by Student's t-test and p values were indicated as follows: $*p < 0.05$; $**p < 0.01$ and ****p< 0.000.

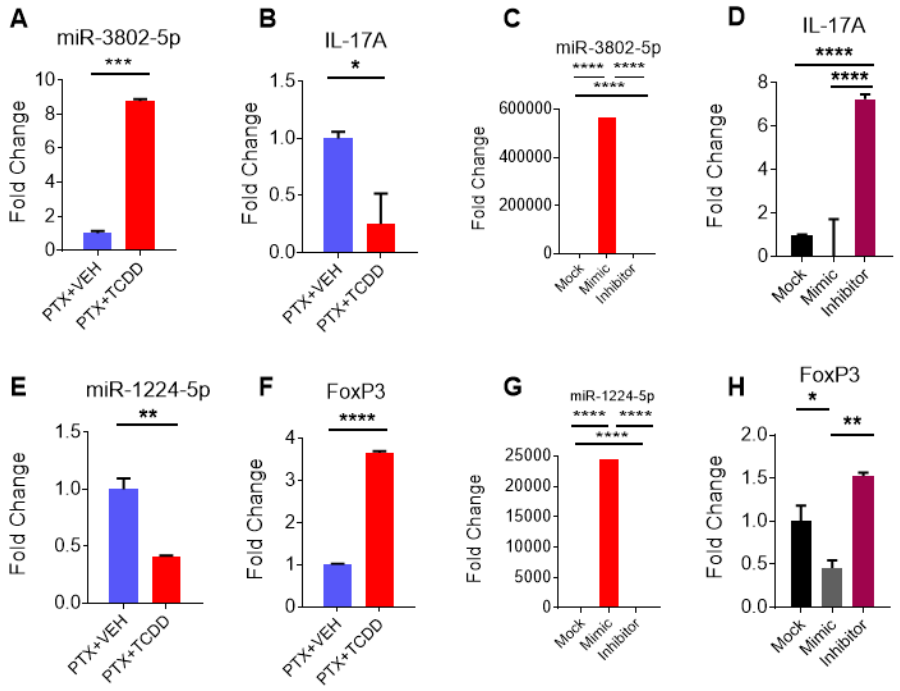

Figure 4.7 Role of miR-3082-5p and miR-1224-5p in regulating expression of IL-17A and FoxP3 respectively. T cells purified from splenocytes were analyzed as described in Fig 6: (**A, B, E, F**): miRNA and target gene expression were analyzed by qRT-PCR. For transfection studies (**C, D, G, H**), splenic T cells were purified from naive B6 mice were cultured for 24 h transfected by nucleofection with miR-3082 inhibitor or mimic, and the expression of miRNA and target genes was analyzed using qRT-PCR. Data are presented as the mean ±SEM. Of experiments performed 3 times. Statistical significance between the two groups was compared by Student's t-test with p values indicated as follows: *p< 0.05, **p< 0.01, **p< 0.001 and ****p< 0.0001.

Table 4.1 Up-regulated and down-regulated miRNAs upon TCDD exposure

microRNA Identification	microRNA Sequence (5'-3')
miR-211-3p	GCAAGGACAGCAAAGGGGGGC
miR-142-3p	UGUAGUGUUUCCUACUUUAUGGA
miR-141-3p	UAACACUGUCUGGUAAAGAUGG
miR-3082-5p	GACAGAGUGUGUGUCUGUGU
miR-1224-5p	GUGAGGACUGGGGAGGUGGAG

Table 4.2 mRNA related oligonucleotides that used in this study

Gene	Forward Sequence (5′–3′)	Reverse Sequence (5′–3′)
Tgfβ1	CTCCCGTGGCTTCTAGTGC	GCCTTAGTTTGGACAGGATCTG
Tgfβ2	CTTCGACGTGACAGACGCT	GCAGGGGCAGTGTAAACTTATT
Tgfβr1	TCTGCATTGCACTTATGCTGA	AAAGGGCGATCTAGTGATGGA
Tgfβr3	GGTGTGAACTGTCACCGATCA	GTTTAGGATGTGAACCTCCCTTG
Il10	CCCATTCCTCGTCACGATCTC	TCAGACTGGTTTGGGATAGGTTT
Foxp3	CCCATCCCCAGGAGTCTTG	ACCATGACTAGGGGCACTGTA
Smad2	ATGTCGTCCATCTTGCCATTC	AACCGTCCTGTTTTCTTTAGCTT
Gata3	CTCGGCCATTCGTACATGGAA	GGATACCTCTGCACCGTAGC
IL17a	TTTAACTCCCTTGGCGCAAAA	CTTTCCCTCCGCATTGACAC
RORγt	GACCCACACCTCACAAATTGA	AGTAGGCCACATTACACTGCT
Il6	CCAAGAGGTGAGTGCTTCCC	CTGTTGTTCAGACTCTCTCCCT
GAPDH	TGGATTTGGACGCATTGGTC	TTTGCACTGGTACGTGTTGAT

Table 4.3 3'UTR alignments and scores of miRNAs and their target genes

IL-17A	
5' ...AUAAUUUAGCUCCCUACUCUGUU... (Position 585-591)	Targetscan context++ score: -0.26
|||||||	
3' UGUGUCUGUGUGUGUGAGACAG mmu-miR-3082-5p	Targetscan context++ score percentile: 97
IL-17AR	
5' ...GAGGGUGUAUAUUGUACUCUGUG... (Position 38-44)	Targetscan context++ score: -0.04
|||||||	
3' UGUGUCUGUGUGUGUGAGACAG mmu-miR-3082-5p	Targetscan context++ score percentile: 81
FoxP3	
5' ...CAUGAUAGUGCCUGUGUCCUCAA... (Position 1529-1536)	Targetscan context++ score: -0.16
|||||||	
3' GAGGUGGAGGGGUCAGGAGUG mmu-miR-1224-5p	Targetscan context++ score percentile: 91
3' agguauuucauccuuuGUGAUGu 5' mmu-miR-142-3p	mirSVR score:-0.0083
|||||||	
1737:5' gccauuccccccuuuucCACUACu 3' FoxP3	PhastCons score: 0.4973

TGFβ1	
5' ...GUCAGGUGUGUGGCUGUCCUUGA... (Position 1529-1536)	Targetscan context++ score: -0.03
|||||||||	
3' CGGGGGGAAACGACAGGAACG mmu-miR-211-3p	Targetscan context++ score percentile: 68
TGFβR1	
5' ...UGACAUUUUUCCACUUCCUUGAG... (Position 1529-1536)	Targetscan context++ score: - 0.02
||||||	
3' CGGGGGGAAACGACAGGAACG mmu-miR-211-3p	Targetscan context++ score percentile: 45
5' ...UUAAAUUUCAUCCUAACACUACA... (Position 1529-1536)	Targetscan context++ score: - 0.44
|||||||	
3' AGGUAUUUCAUCCUUUGUGAUGU mmu-miR-142-3p	Targetscan context++ score percentile: 95
5' ...UUUAUUUGAUCAAAGCAGUGUUU... (Position 1050-1056)	Targetscan context++ score: - 0.47
|||||||	
3' GGUAGAAAUGGUCUGUCACAAU mmu-miR-142-3p	Targetscan context++ score percentile: 98
TGFβ2	
5' ...GGAGUUUUGAUUCAUCAGUGUUU... (Position 106-112)	Targetscan context++ score: - 0.3

||||||	
3' GGUAGAAAUGGUCUGUCACAAU mmu-miR-141-3p	Targetscan context++ score percentile: 93
5' ...CUAGAUUUUGACUUGCACUACAA...(Position 1222-1228)	Targetscan context++ score: - 0.17
|||||	
3' AGGUAUUUCAUCCUUUGUGAUGU mmu-miR-142-3p	Targetscan context++ score percentile: 76
5' ...CUUAUCUGAGGAGCUGUCCUUGA.. (Position 2098-2105)	Targetscan context++ score: - 0.13
||||||||	
3' CGGGGGGAAACGACAGGAACG mmu-miR-211-3p	Targetscan context++ score percentile: 89
Smad2	
5' ...UGGAUUAACUUGGAAGUCCUUGA... (Position 581-588)	Targetscan context++ score: - 0.15
||| ||||||	
3' CGGGGGGAAACGACAGGAACG mmu-miR-211-3p	Targetscan context++ score percentile: 91

CHAPTER 5

SUMMARY AND CONCLUSION

Inflammation is involved in the pathogenesis of several clinical disorders including autoimmune, cardiovascular, and neurological diseases, obesity and cancer. Thus, identifying agents that suppress inflammation can have significant impact on human health. In the current study, we used two unique models of inflammatory disease: 1) Chronic inflammatory mouse model of EAE that mimics human MS, and 2) Acute mouse model of inflammation using PTX, a toxin produced by *Bordetella pertussis* that causes whooping cough. In these models, we tested the role of activation of CB receptors and AhR, using select agonists such as cannabinoids (THC and CBD), or TCDD, respectively, to suppress inflammation. THC+CBD combination (Sativex) has been used to treat patients with MS for muscle spasticity. However, whether it can also suppress neuro-inflammation and if so, the mechanism of action remains obscure. We demonstrate the effectiveness of these cannabinoids to ameliorate chronic inflammation, through unique mechanisms. The current study demonstrates for the first time that THC+CBD-mediated suppression of neuroinflammation in EAE stems from alterations in miRNA expression and changes in microbiota. Specifically, THC+CBD reduced cellular infiltration into the brain and spinal cord, decreased pro-inflammatory cytokines such as IL-17A, IFNγ, IL-6, TNF-α and IL-1β levels, while increasing anti-inflammatory IL-10 and TGF-β. Also, THC+CBD prevented T cell expansion through induction of cell cycle arrest and apoptosis. Collectively, we showed that the combination of THC and CBD

suppresses neuro-inflammation and that this may be regulated by certain miRNA as well as alterations in the gut microbiota. Importantly, these studies form the basis of targeting such miRNA and microbiota to treat MS. We also demonstrated that AhR activation by TCDD led to suppression of acute inflammation induced by Pertussis Toxin (PTX). PTX is an exotoxin that promotes bacterial invasion into the lungs and cause lung toxicity. Such toxicity results from cytokine storm involving pro-inflammatory cytokines such as IL-17A, IFNγ, and IL-6. AhR activation decreased the production of these cytokines potentially through induction of immunosuppressive cells such as Tregs and MDSCs. AhR activation was also associated with alterations in the expression of miRNAs that promoted anti-inflammatory pathways. It is interesting that activation of both CB receptors and AhR caused alterations in the expression of miRNA that targeted anti-inflammatory pathways. Thus, the current study, by using CB and AhR signaling pathways, has identified new epigenetic pathways that can be targeted to suppress inflammation and thus treat inflammatory diseases.

REFERENCES

1. Matute-Blanch C, Montalban X, Comabella M. Multiple sclerosis, and other demyelinating and autoimmune inflammatory diseases of the central nervous system. Handb Clin Neurol. 2017;146:67-84. doi: 10.1016/B978-0-12-804279-3.00005-8. PubMed PMID: 29110780.

2. Wootla B, Eriguchi M, Rodriguez M. Is multiple sclerosis an autoimmune disease? Autoimmune Dis. 2012;2012:969657. doi: 10.1155/2012/969657. PubMed PMID: 22666554; PMCID: PMC3361990.

3. Compston A, Coles A. Multiple sclerosis. Lancet. 2008;372(9648):1502-17. doi: 10.1016/S0140-6736(08)61620-7. PubMed PMID: 18970977.

4. Kaminska J, Koper OM, Piechal K, Kemona H. Multiple sclerosis - etiology and diagnostic potential. Postepy Hig Med Dosw (Online). 2017;71(0):551-63. PubMed PMID: 28665284.

5. Denison MS, Pandini A, Nagy SR, Baldwin EP, Bonati L. Ligand binding and activation of the Ah receptor. Chem Biol Interact. 2002;141(1-2):3-24. PubMed PMID: 12213382.

6. Christogianni A, Bibb R, Davis SL, Jay O, Barnett M, Evangelou N, Filingeri D. Temperature sensitivity in multiple sclerosis: An overview of its impact on sensory and cognitive symptoms. Temperature (Austin). 2018;5(3):208-23. doi: 10.1080/23328940.2018.1475831. PubMed PMID: 30377640; PMCID: PMC6205043.

7. Zwibel HL, Smrtka J. Improving quality of life in multiple sclerosis: an unmet need. Am J Manag Care. 2011;17 Suppl 5 Improving:S139-45. PubMed PMID: 21761952.

8. Hedstrom AK, Lima Bomfim I, Barcellos L, Gianfrancesco M, Schaefer C, Kockum I, Olsson T, Alfredsson L. Interaction between adolescent obesity and HLA risk genes in the etiology of multiple sclerosis. Neurology. 2014;82(10):865-72. doi: 10.1212/WNL.0000000000000203. PubMed PMID: 24500647; PMCID: PMC3959752.

9. Siegel SR, Mackenzie J, Chaplin G, Jablonski NG, Griffiths L. Circulating microRNAs involved in multiple sclerosis. Mol Biol Rep. 2012;39(5):6219-25. doi: 10.1007/s11033-011-1441-7. PubMed PMID: 22231906.

10. Feinstein A, Pavisian B. Multiple sclerosis and suicide. Mult Scler. 2017;23(7):923-7. doi: 10.1177/1352458517702553. PubMed PMID: 28327056.

11. Gourraud PA, Harbo HF, Hauser SL, Baranzini SE. The genetics of multiple sclerosis: an up-to-date review. Immunol Rev. 2012;248(1):87-103. doi: 10.1111/j.1600-065X.2012.01134.x. PubMed PMID: 22725956; PMCID: PMC5967887.

12. Kular L, Needhamsen M, Adzemovic MZ, Kramarova T, Gomez-Cabrero D, Ewing E, Piket E, Tegner J, Beck S, Piehl F, Brundin L, Jagodic M. Neuronal methylome reveals CREB-associated neuro-axonal impairment in multiple sclerosis. Clin Epigenetics. 2019;11(1):86. doi: 10.1186/s13148-019-0678-1. PubMed PMID: 31146783.

13. Venkatesha SH, Dudics S, Song Y, Mahurkar A, Moudgil KD. The miRNA Expression Profile of Experimental Autoimmune Encephalomyelitis Reveals Novel Potential Disease Biomarkers. Int J Mol Sci. 2018;19(12). doi: 10.3390/ijms19123990. PubMed PMID: 30544973; PMCID: PMC6321564.

14. Andre CM, Hausman JF, Guerriero G. Cannabis sativa: The Plant of the Thousand and One Molecules. Front Plant Sci. 2016;7:19. doi: 10.3389/fpls.2016.00019. PubMed PMID: 26870049; PMCID: PMC4740396.

15. Nagarkatti P, Pandey R, Rieder SA, Hegde VL, Nagarkatti M. Cannabinoids as novel anti-inflammatory drugs. Future medicinal chemistry. 2009;1(7):1333-49. doi: 10.4155/fmc.09.93. PubMed PMID: 20191092; PMCID: 2828614.

16. Elliott DM, Singh N, Nagarkatti M, Nagarkatti PS. Cannabidiol Attenuates Experimental Autoimmune Encephalomyelitis Model of Multiple Sclerosis Through Induction of Myeloid-Derived Suppressor Cells. Front Immunol. 2018;9:1782. doi: 10.3389/fimmu.2018.01782. PubMed PMID: 30123217; PMCID: PMC6085417.

17. Yang X, Bam M, Nagarkatti PS, Nagarkatti M. RNA-seq Analysis of delta9-Tetrahydrocannabinol-treated T Cells Reveals Altered Gene Expression Profiles That Regulate Immune Response and Cell Proliferation. J Biol Chem. 2016;291(30):15460-72. doi: 10.1074/jbc.M116.719179. PubMed PMID: 27268054; PMCID: PMC4957033.

18. Hegde VL, Nagarkatti PS, Nagarkatti M. Role of myeloid-derived suppressor cells in amelioration of experimental autoimmune hepatitis following activation of TRPV1 receptors by cannabidiol. PLoS One. 2011;6(4):e18281. doi: 10.1371/journal.pone.0018281. PubMed PMID: 21483776; PMCID: PMC3069975.

19. Kozela E, Juknat A, Kaushansky N, Rimmerman N, Ben-Nun A, Vogel Z. Cannabinoids decrease the th17 inflammatory autoimmune phenotype. J Neuroimmune Pharmacol. 2013;8(5):1265-76. doi: 10.1007/s11481-013-9493-1. PubMed PMID: 23892791.

20. Sido JM, Nagarkatti PS, Nagarkatti M. Delta(9)-Tetrahydrocannabinol attenuates allogeneic host-versus-graft response and delays skin graft rejection through activation of cannabinoid receptor 1 and induction of myeloid-derived suppressor cells. J Leukoc Biol. 2015;98(3):435-47. doi: 10.1189/jlb.3A0115-030RR. PubMed PMID: 26034207; PMCID: PMC4541500.

21. Atakan Z. Cannabis, a complex plant: different compounds and different effects on individuals. Ther Adv Psychopharmacol. 2012;2(6):241-54. doi: 10.1177/2045125312457586. PubMed PMID: 23983983; PMCID: PMC3736954.

22. Sido JM, Jackson AR, Nagarkatti PS, Nagarkatti M. Marijuana-derived Delta-9-tetrahydrocannabinol suppresses Th1/Th17 cell-mediated delayed-type hypersensitivity through microRNA regulation. J Mol Med (Berl). 2016;94(9):1039-51. doi: 10.1007/s00109-016-1404-5. PubMed PMID: 27038180; PMCID: PMC4992583.

23. Wright MJ, Jr., Vandewater SA, Parsons LH, Taffe MA. Delta(9)Tetrahydrocannabinol impairs reversal learning but not extra-dimensional shifts in rhesus macaques. Neuroscience. 2013;235:51-8. doi: 10.1016/j.neuroscience.2013.01.018. PubMed PMID: 23333671; PMCID: PMC3595391.

24. McKallip RJ, Nagarkatti M, Nagarkatti PS. Delta-9-tetrahydrocannabinol enhances breast cancer growth and metastasis by suppression of the antitumor immune response. J Immunol. 2005;174(6):3281-9. doi: 10.4049/jimmunol.174.6.3281. PubMed PMID: 15749859.

25. Newton CA, Chou PJ, Perkins I, Klein TW. CB(1) and CB(2) cannabinoid receptors mediate different aspects of delta-9-tetrahydrocannabinol (THC)-induced T helper cell shift following immune activation by Legionella pneumophila infection. J Neuroimmune Pharmacol. 2009;4(1):92-102. doi: 10.1007/s11481-008-9126-2. PubMed PMID: 18792785.

26. Rao R, Rieder SA, Nagarkatti P, Nagarkatti M. Staphylococcal enterotoxin B-induced microRNA-155 targets SOCS1 to promote acute inflammatory lung injury. Infect Immun. 2014;82(7):2971-9. doi: 10.1128/IAI.01666-14. PubMed PMID: 24778118; PMCID: PMC4097622.

27. Pandey R, Hegde VL, Nagarkatti M, Nagarkatti PS. Targeting cannabinoid receptors as a novel approach in the treatment of graft-versus-host disease: evidence from an experimental murine model. J Pharmacol Exp Ther.

2011;338(3):819-28. doi: 10.1124/jpet.111.182717. PubMed PMID: 21673072; PMCID: PMC3164345.

28. Kogan NM, Mechoulam R. Cannabinoids in health and disease. Dialogues Clin Neurosci. 2007;9(4):413-30. PubMed PMID: 18286801; PMCID: PMC3202504.

29. Watt G, Karl T. In vivo Evidence for Therapeutic Properties of Cannabidiol (CBD) for Alzheimer's Disease. Front Pharmacol. 2017;8:20. doi: 10.3389/fphar.2017.00020. PubMed PMID: 28217094; PMCID: PMC5289988.

30. Oreja-Guevara C. Clinical efficacy and effectiveness of Sativex, a combined cannabinoid medicine, in multiple sclerosis-related spasticity. Expert Rev Neurother. 2012;12(4 Suppl):3-8. doi: 10.1586/ern.12.11. PubMed PMID: 22509985.

31. Juckel G, Roser P, Nadulski T, Stadelmann AM, Gallinat J. Acute effects of Delta9-tetrahydrocannabinol and standardized cannabis extract on the auditory evoked mismatch negativity. Schizophr Res. 2007;97(1-3):109-17. doi: 10.1016/j.schres.2007.08.015. PubMed PMID: 17884351.

32. Roser P, Juckel G, Rentzsch J, Nadulski T, Gallinat J, Stadelmann AM. Effects of acute oral Delta9-tetrahydrocannabinol and standardized cannabis extract on the auditory P300 event-related potential in healthy volunteers. Eur Neuropsychopharmacol.2008;18(8):569-77.doi:10.1016/j.euroneuro.2008.04.008. PubMed PMID: 18544469.

33. Dai R, Ahmed SA. MicroRNA, a new paradigm for understanding immunoregulation, inflammation, and autoimmune diseases. Transl Res. 2011;157(4):163-79. doi: 10.1016/j.trsl.2011.01.007. PubMed PMID: 21420027; PMCID: PMC3072681.

34. Davidson-Moncada J, Papavasiliou FN, Tam W. MicroRNAs of the immune system: roles in inflammation and cancer. Ann N Y Acad Sci. 2010;1183:183-94. doi: 10.1111/j.1749-6632.2009.05121.x. PubMed PMID: 20146715; PMCID: PMC2876712.

35. Gandhi R. miRNA in multiple sclerosis: search for novel biomarkers. Mult Scler. 2015;21(9):1095-103. doi: 10.1177/1352458515578771. PubMed PMID: 25921051.

36. Lytle JR, Yario TA, Steitz JA. Target mRNAs are repressed as efficiently by microRNA-binding sites in the 5' UTR as in the 3' UTR. Proc Natl Acad Sci U S A. 2007;104(23):9667-72. doi: 10.1073/pnas.0703820104. PubMed PMID: 17535905; PMCID: PMC1887587.

37. Esquela-Kerscher A, Slack FJ. Oncomirs - microRNAs with a role in cancer. Nat Rev Cancer. 2006;6(4):259-69. doi: 10.1038/nrc1840. PubMed PMID: 16557279.

38. Chen X, Ba Y, Ma L, Cai X, Yin Y, Wang K, Guo J, Zhang Y, Chen J, Guo X, Li Q, Li X, Wang W, Zhang Y, Wang J, Jiang X, Xiang Y, Xu C, Zheng P, Zhang J, Li R, Zhang H, Shang X, Gong T, Ning G, Wang J, Zen K, Zhang J, Zhang CY. Characterization of microRNAs in serum: a novel class of biomarkers for diagnosis of cancer and other diseases. Cell Res. 2008;18(10):997-1006. doi: 10.1038/cr.2008.282. PubMed PMID: 18766170.

39. O'Connell RM, Rao DS, Baltimore D. microRNA regulation of inflammatory responses. Annu Rev Immunol. 2012;30:295-312. doi: 10.1146/annurev-immunol-020711-075013. PubMed PMID: 22224773.

40. McCoy CE. miR-155 Dysregulation and Therapeutic Intervention in Multiple Sclerosis. Adv Exp Med Biol. 2017;1024:111-31. doi: 10.1007/978-981-10-5987-2_5. PubMed PMID: 28921467.

41. Martinelli-Boneschi F, Fenoglio C, Brambilla P, Sorosina M, Giacalone G, Esposito F, Serpente M, Cantoni C, Ridolfi E, Rodegher M, Moiola L, Colombo B, De Riz M, Martinelli V, Scarpini E, Comi G, Galimberti D. MicroRNA and mRNA expression profile screening in multiple sclerosis patients to unravel novel pathogenic steps and identify potential biomarkers. Neurosci Lett. 2012;508(1):4-8. doi: 10.1016/j.neulet.2011.11.006. PubMed PMID: 22108567.

42. Keller A, Leidinger P, Lange J, Borries A, Schroers H, Scheffler M, Lenhof HP, Ruprecht K, Meese E. Multiple sclerosis: microRNA expression profiles accurately differentiate patients with relapsing-remitting disease from healthy controls. PLoS One. 2009;4(10):e7440. doi: 10.1371/journal.pone.0007440. PubMed PMID: 19823682; PMCID: PMC2757919.

43. Galland L. The gut microbiome and the brain. J Med Food. 2014;17(12):1261-72. doi: 10.1089/jmf.2014.7000. PubMed PMID: 25402818; PMCID: PMC4259177.

44. Swidsinski A, Loening-Baucke V, Lochs H, Hale LP. Spatial organization of bacterial flora in normal and inflamed intestine: a fluorescence in situ hybridization study in mice. World J Gastroenterol. 2005;11(8):1131-40. doi: 10.3748/wjg.v11.i8.1131. PubMed PMID: 15754393; PMCID: PMC4250702.

45. Belkaid Y, Hand TW. Role of the microbiota in immunity and inflammation. Cell. 2014;157(1):121-41. doi: 10.1016/j.cell.2014.03.011. PubMed PMID: 24679531; PMCID: PMC4056765.

46. Chu F, Shi M, Lang Y, Shen D, Jin T, Zhu J, Cui L. Gut Microbiota in Multiple Sclerosis and Experimental Autoimmune Encephalomyelitis: Current

Applications and Future Perspectives. Mediators Inflamm. 2018;2018:8168717. doi: 10.1155/2018/8168717. PubMed PMID: 29805314; PMCID: PMC5902007.

47. Ayache SS, Chalah MA. Moral Judgment: An Overlooked Deficient Domain in Multiple Sclerosis? Behav Sci (Basel). 2018;8(11). doi: 10.3390/bs8110105. PubMed PMID: 30453483; PMCID: PMC6262463.

48. Shahi SK, Freedman SN, Mangalam AK. Gut microbiome in multiple sclerosis: The players involved and the roles they play. Gut Microbes. 2017;8(6):607-15. doi: 10.1080/19490976.2017.1349041. PubMed PMID: 28696139; PMCID: PMC5730390.

49. Chen J, Chia N, Kalari KR, Yao JZ, Novotna M, Paz Soldan MM, Luckey DH, Marietta EV, Jeraldo PR, Chen X, Weinshenker BG, Rodriguez M, Kantarci OH, Nelson H, Murray JA, Mangalam AK. Multiple sclerosis patients have a distinct gut microbiota compared to healthy controls. Sci Rep. 2016;6:28484. doi: 10.1038/srep28484. PubMed PMID: 27346372; PMCID: PMC4921909.

50. Jangi S, Gandhi R, Cox LM, Li N, von Glehn F, Yan R, Patel B, Mazzola MA, Liu S, Glanz BL, Cook S, Tankou S, Stuart F, Melo K, Nejad P, Smith K, Topcuolu BD, Holden J, Kivisakk P, Chitnis T, De Jager PL, Quintana FJ, Gerber GK, Bry L, Weiner HL. Alterations of the human gut microbiome in multiple sclerosis. Nat Commun. 2016;7:12015. doi: 10.1038/ncomms12015. PubMed PMID: 27352007; PMCID: PMC4931233.

51. Miyake S, Kim S, Suda W, Oshima K, Nakamura M, Matsuoka T, Chihara N, Tomita A, Sato W, Kim SW, Morita H, Hattori M, Yamamura T. Dysbiosis in the Gut Microbiota of Patients with Multiple Sclerosis, with a Striking Depletion of Species Belonging to Clostridia XIVa and IV Clusters. PLoS One. 2015;10(9):e0137429. doi: 10.1371/journal.pone.0137429. PubMed PMID: 26367776; PMCID: PMC4569432.

52. Rothhammer V, Quintana FJ. Environmental control of autoimmune inflammation in the central nervous system. Curr Opin Immunol. 2016;43:46-53. doi: 10.1016/j.coi.2016.09.002. PubMed PMID: 27710839; PMCID: PMC5125858.

53. Wang Y, Kasper LH. The role of microbiome in central nervous system disorders. Brain Behav Immun. 2014;38:1-12. doi: 10.1016/j.bbi.2013.12.015. PubMed PMID: 24370461; PMCID: PMC4062078.

54. Stathopoulou C, Nikoleri D, Bertsias G. Immunometabolism: an overview and therapeutic prospects in autoimmune diseases. Immunotherapy. 2019;11(9):813-29. doi: 10.2217/imt-2019-0002. PubMed PMID: 31120393.

55. Dalile B, Van Oudenhove L, Vervliet B, Verbeke K. The role of short-chain fatty acids in microbiota-gut-brain communication. Nat Rev Gastroenterol Hepatol. 2019. doi: 10.1038/s41575-019-0157-3. PubMed PMID: 31123355.

56. Melbye P, Olsson A, Hansen TH, Sondergaard HB, Bang Oturai A. Short-chain fatty acids and gut microbiota in multiple sclerosis. Acta Neurol Scand. 2019;139(3):208-19. doi: 10.1111/ane.13045. PubMed PMID: 30427062.

57. Feng W, Ao H, Peng C. Gut Microbiota, Short-Chain Fatty Acids, and Herbal Medicines. Front Pharmacol. 2018;9:1354. doi: 10.3389/fphar.2018.01354. PubMed PMID: 30532706; PMCID: PMC6265305.

58. Verma A, Burns DL. Requirements for assembly of PtlH with the pertussis toxin transporter apparatus of Bordetella pertussis. Infect Immun. 2007;75(5):2297-306. doi: 10.1128/IAI.00008-07. PubMed PMID: 17339350; PMCID: PMC1865746.

59. Verma A, Cheung AM, Burns DL. Stabilization of the pertussis toxin secretion apparatus by the C terminus of PtlD. J Bacteriol. 2008;190(21):7285-90. doi: 10.1128/JB.01106-08. PubMed PMID: 18723610; PMCID: PMC2580710.

60. Carbonetti NH. Contribution of pertussis toxin to the pathogenesis of pertussis disease. Pathog Dis. 2015;73(8):ftv073. doi: 10.1093/femspd/ftv073. PubMed PMID: 26394801; PMCID: PMC4626579.

61. Andreasen C, Powell DA, Carbonetti NH. Pertussis toxin stimulates IL-17 production in response to Bordetella pertussis infection in mice. PLoS One. 2009;4(9):e7079. doi: 10.1371/journal.pone.0007079. PubMed PMID: 19759900; PMCID: PMC2738961.

62. Munoz JJ, Bernard CC, Mackay IR. Elicitation of experimental allergic encephalomyelitis (EAE) in mice with the aid of pertussigen. Cell Immunol. 1984;83(1):92-100. PubMed PMID: 6607126.

63. Kugler S, Bocker K, Heusipp G, Greune L, Kim KS, Schmidt MA. Pertussis toxin transiently affects barrier integrity, organelle organization and transmigration of monocytes in a human brain microvascular endothelial cell barrier model. Cell Microbiol. 2007;9(3):619-32. doi: 10.1111/j.1462-5822.2006.00813.x. PubMed PMID: 17002784.

64. Chen X, Howard OM, Oppenheim JJ. Pertussis toxin by inducing IL-6 promotes the generation of IL-17-producing CD4 cells. J Immunol. 2007;178(10):6123-9. PubMed PMID: 17475838.

65. Komiyama Y, Nakae S, Matsuki T, Nambu A, Ishigame H, Kakuta S, Sudo K, Iwakura Y. IL-17 plays an important role in the development of experimental

autoimmune encephalomyelitis. J Immunol. 2006;177(1):566-73. doi: 10.4049/jimmunol.177.1.566. PubMed PMID: 16785554.

66. Millward JM, Caruso M, Campbell IL, Gauldie J, Owens T. IFN-gamma-induced chemokines synergize with pertussis toxin to promote T cell entry to the central nervous system. J Immunol. 2007;178(12):8175-82. doi: 10.4049/jimmunol.178.12.8175. PubMed PMID: 17548656.

67. Gonsiorek W, Lunn C, Fan X, Narula S, Lundell D, Hipkin RW. Endocannabinoid 2-arachidonyl glycerol is a full agonist through human type 2 cannabinoid receptor: antagonism by anandamide. Mol Pharmacol. 2000;57(5):1045-50. PubMed PMID: 10779390.

68. Quintana FJ, Basso AS, Iglesias AH, Korn T, Farez MF, Bettelli E, Caccamo M, Oukka M, Weiner HL. Control of T(reg) and T(H)17 cell differentiation by the aryl hydrocarbon receptor. Nature. 2008;453(7191):65-71. doi: 10.1038/nature06880. PubMed PMID: 18362915.

69. Knerr S, Schrenk D. Carcinogenicity of 2,3,7,8-tetrachlorodibenzo-p-dioxin in experimental models. Mol Nutr Food Res. 2006;50(10):897-907. doi: 10.1002/mnfr.200600006. PubMed PMID: 16977593.

70. Bock KW, Kohle C. Ah receptor- and TCDD-mediated liver tumor promotion: clonal selection and expansion of cells evading growth arrest and apoptosis. Biochem Pharmacol. 2005;69(10):1403-8. doi: 10.1016/j.bcp.2005.02.004. PubMed PMID: 15857604.

71. Ema M, Ohe N, Suzuki M, Mimura J, Sogawa K, Ikawa S, Fujii-Kuriyama Y. Dioxin binding activities of polymorphic forms of mouse and human arylhydrocarbon receptors. J Biol Chem. 1994;269(44):27337-43. PubMed PMID: 7961644.

72. Hahn ME. Aryl hydrocarbon receptors: diversity and evolution. Chem Biol Interact. 2002;141(1-2):131-60. PubMed PMID: 12213389.

73. Chiba T, Chihara J, Furue M. Role of the Arylhydrocarbon Receptor (AhR) in the Pathology of Asthma and COPD. J Allergy (Cairo). 2012;2012:372384. doi: 10.1155/2012/372384. PubMed PMID: 22500183; PMCID: PMC3303582.

74. Hahn ME, Karchner SI, Franks DG, Merson RR. Aryl hydrocarbon receptor polymorphisms and dioxin resistance in Atlantic killifish (Fundulus heteroclitus). Pharmacogenetics. 2004;14(2):131-43. PubMed PMID: 15077014.

75. Reitzel AM, Karchner SI, Franks DG, Evans BR, Nacci D, Champlin D, Vieira VM, Hahn ME. Genetic variation at aryl hydrocarbon receptor (AHR) loci in populations of Atlantic killifish (Fundulus heteroclitus) inhabiting polluted and

reference habitats. BMC Evol Biol. 2014;14:6. doi: 10.1186/1471-2148-14-6. PubMed PMID: 24422594; PMCID: PMC3899389.

76. Mezrich JD, Fechner JH, Zhang X, Johnson BP, Burlingham WJ, Bradfield CA. An interaction between kynurenine and the aryl hydrocarbon receptor can generate regulatory T cells. J Immunol. 2010;185(6):3190-8. doi: 10.4049/jimmunol.0903670. PubMed PMID: 20720200; PMCID: PMC2952546.

77. Peng L, Mayhew CN, Schnekenburger M, Knudsen ES, Puga A. Repression of Ah receptor and induction of transforming growth factor-beta genes in DEN-induced mouse liver tumors. Toxicology. 2008;246(2-3):242-7. doi: 10.1016/j.tox.2008.01.002. PubMed PMID: 18282651; PMCID: PMC2323453.

78. Iida K, Mimura J, Itoh K, Ohyama C, Fujii-Kuriyama Y, Shimazui T, Akaza H, Yamamoto M. Suppression of AhR signaling pathway is associated with the down-regulation of UDP-glucuronosyltransferases during BBN-induced urinary bladder carcinogenesis in mice. J Biochem. 2010;147(3):353-60. doi: 10.1093/jb/mvp169. PubMed PMID: 19880377.

79. Compston A, Coles A. Multiple sclerosis. Lancet. 2002;359(9313):1221-31. doi: 10.1016/S0140-6736(02)08220-X. PubMed PMID: 11955556.

80. Confavreux C, Vukusic S, Moreau T, Adeleine P. Relapses and progression of disability in multiple sclerosis. N Engl J Med. 2000;343(20):1430-8. doi: 10.1056/NEJM200011163432001. PubMed PMID: 11078767.

81. Hojsgaard Chow H, Schreiber K, Magyari M, Ammitzboll C, Bornsen L, Romme Christensen J, Ratzer R, Soelberg Sorensen P, Sellebjerg F. Progressive multiple sclerosis, cognitive function, and quality of life. Brain Behav. 2018;8(2):e00875. doi: 10.1002/brb3.875. PubMed PMID: 29484253; PMCID: PMC5822575.

82. Kurtzke JF. Epidemiology of multiple sclerosis. Does this really point toward an etiology? Lectio Doctoralis. Neurol Sci. 2000;21(6):383-403. PubMed PMID: 11441577.

83. Huang WJ, Chen WW, Zhang X. Multiple sclerosis: Pathology, diagnosis and treatments. Exp Ther Med. 2017;13(6):3163-6. doi: 10.3892/etm.2017.4410. PubMed PMID: 28588671; PMCID: PMC5450788.

84. Lassmann H, van Horssen J, Mahad D. Progressive multiple sclerosis: pathology and pathogenesis. Nat Rev Neurol. 2012;8(11):647-56. doi: 10.1038/nrneurol.2012.168. PubMed PMID: 23007702.

85. Trapp BD, Nave KA. Multiple sclerosis: an immune or neurodegenerative disorder? Annu Rev Neurosci. 2008;31:247-69. doi: 10.1146/annurev.neuro.30.051606.094313. PubMed PMID: 18558855.

86. Tramer MR, Carroll D, Campbell FA, Reynolds DJ, Moore RA, McQuay HJ. Cannabinoids for control of chemotherapy induced nausea and vomiting: quantitative systematic review. BMJ. 2001;323(7303):16-21. PubMed PMID: 11440936; PMCID: PMC34325.

87. Guzman M. Cannabinoids: potential anticancer agents. Nat Rev Cancer. 2003;3(10):745-55. doi: 10.1038/nrc1188. PubMed PMID: 14570037.

88. Turri M, Teatini F, Donato F, Zanette G, Tugnoli V, Deotto L, Bonetti B, Squintani G. Pain Modulation after Oromucosal Cannabinoid Spray (SATIVEX((R))) in Patients with Multiple Sclerosis: A Study with Quantitative Sensory Testing and Laser-Evoked Potentials. Medicines (Basel). 2018;5(3). doi: 10.3390/medicines5030059. PubMed PMID: 29933552; PMCID: PMC6163235.

89. Moreno-Martet M, Feliu A, Espejo-Porras F, Mecha M, Carrillo-Salinas FJ, Fernandez-Ruiz J, Guaza C, de Lago E. The disease-modifying effects of a Sativex-like combination of phytocannabinoids in mice with experimental autoimmune encephalomyelitis are preferentially due to Delta9-tetrahydrocannabinol acting through CB1 receptors. Mult Scler Relat Disord. 2015;4(6):505-11. doi: 10.1016/j.msard.2015.08.001. PubMed PMID: 26590655.

90. Feliu A, Moreno-Martet M, Mecha M, Carrillo-Salinas FJ, de Lago E, Fernandez-Ruiz J, Guaza C. A Sativex((R)) -like combination of phytocannabinoids as a disease-modifying therapy in a viral model of multiple sclerosis. Br J Pharmacol. 2015;172(14):3579-95. doi: 10.1111/bph.13159. PubMed PMID: 25857324; PMCID: PMC4507161.

91. Kendall DA, Yudowski GA. Cannabinoid Receptors in the Central Nervous System: Their Signaling and Roles in Disease. Front Cell Neurosci. 2016;10:294. doi: 10.3389/fncel.2016.00294. PubMed PMID: 28101004; PMCID: PMC5209363.

92. Karmaus PW, Chen W, Crawford R, Kaplan BL, Kaminski NE. Delta9-tetrahydrocannabinol impairs the inflammatory response to influenza infection: role of antigen-presenting cells and the cannabinoid receptors 1 and 2. Toxicol Sci. 2013;131(2):419-33. doi: 10.1093/toxsci/kfs315. PubMed PMID: 23152191; PMCID: PMC3551428.

93. Laprairie RB, Bagher AM, Kelly ME, Denovan-Wright EM. Cannabidiol is a negative allosteric modulator of the cannabinoid CB1 receptor. Br J Pharmacol. 2015;172(20):4790-805. doi: 10.1111/bph.13250. PubMed PMID: 26218440; PMCID: PMC4621983.

94. Alharris E, Singh NP, Nagarkatti PS, Nagarkatti M. Role of miRNA in the regulation of cannabidiol-mediated apoptosis in neuroblastoma cells. Oncotarget.

2019;10(1):45-59. doi: 10.18632/oncotarget.26534. PubMed PMID: 30713602; PMCID: PMC6343753.

95. Devinsky O, Cilio MR, Cross H, Fernandez-Ruiz J, French J, Hill C, Katz R, Di Marzo V, Jutras-Aswad D, Notcutt WG, Martinez-Orgado J, Robson PJ, Rohrback BG, Thiele E, Whalley B, Friedman D. Cannabidiol: pharmacology and potential therapeutic role in epilepsy and other neuropsychiatric disorders. Epilepsia. 2014;55(6):791-802. doi: 10.1111/epi.12631. PubMed PMID: 24854329; PMCID: PMC4707667.

96. Ambros V, Bartel B, Bartel DP, Burge CB, Carrington JC, Chen X, Dreyfuss G, Eddy SR, Griffiths-Jones S, Marshall M, Matzke M, Ruvkun G, Tuschl T. A uniform system for microRNA annotation. RNA. 2003;9(3):277-9. PubMed PMID: 12592000; PMCID: PMC1370393.

97. Pato ML. Role of ribonucleic acid synthesis in replication of deoxyribonucleic acid. J Bacteriol. 1975;121(3):1214-5. PubMed PMID: 1090599; PMCID: PMC246057.

98. Plank M, Maltby S, Mattes J, Foster PS. Targeting translational control as a novel way to treat inflammatory disease: the emerging role of microRNAs. Clin Exp Allergy. 2013;43(9):981-99. doi: 10.1111/cea.12170. PubMed PMID: 23957346.

99. Wu T, Chen G. miRNAs Participate in MS Pathological Processes and Its Therapeutic Response. Mediators Inflamm. 2016;2016:4578230. doi: 10.1155/2016/4578230. PubMed PMID: 27073296; PMCID: PMC4814683.

100. Junker A, Hohlfeld R, Meinl E. The emerging role of microRNAs in multiple sclerosis. Nat Rev Neurol. 2011;7(1):56-9. doi: 10.1038/nrneurol.2010.179. PubMed PMID: 21151203.

101. Li JS, Yao ZX. MicroRNAs: novel regulators of oligodendrocyte differentiation and potential therapeutic targets in demyelination-related diseases. Mol Neurobiol. 2012;45(1):200-12. doi: 10.1007/s12035-011-8231-z. PubMed PMID: 22218763.

102. Rezaei N, Talebi F, Ghorbani S, Rezaei A, Esmaeili A, Noorbakhsh F, Hakemi MG. MicroRNA-92a Drives Th1 Responses in the Experimental Autoimmune Encephalomyelitis. Inflammation. 2019;42(1):235-45. doi: 10.1007/s10753-018-0887-3. PubMed PMID: 30411211.

103. Guerau-de-Arellano M, Lovett-Racke AE, Racke MK. miRNAs in multiple sclerosis: regulating the regulators. J Neuroimmunol. 2010;229(1-2):3-4. doi: 10.1016/j.jneuroim.2010.08.025. PubMed PMID: 20888650; PMCID: PMC2991561.

104. Rouse M, Singh NP, Nagarkatti PS, Nagarkatti M. Indoles mitigate the development of experimental autoimmune encephalomyelitis by induction of reciprocal differentiation of regulatory T cells and Th17 cells. Br J Pharmacol. 2013;169(6):1305-21. doi: 10.1111/bph.12205. PubMed PMID: 23586923; PMCID: PMC3831710.

105. Singh NP, Hegde VL, Hofseth LJ, Nagarkatti M, Nagarkatti P. Resveratrol (trans-3,5,4'-trihydroxystilbene) ameliorates experimental allergic encephalomyelitis, primarily via induction of apoptosis in T cells involving activation of aryl hydrocarbon receptor and estrogen receptor. Mol Pharmacol. 2007;72(6):1508-21. doi: 10.1124/mol.107.038984. PubMed PMID: 17872969; PMCID: PMC4796949.

106. O'Neill JK, Baker D, Davison AN, Maggon KK, Jaffee BD, Turk JL. Therapy of chronic relapsing experimental allergic encephalomyelitis and the role of the blood-brain barrier: elucidation by the action of Brequinar sodium. J Neuroimmunol. 1992;38(1-2):53-62. PubMed PMID: 1577953.

107. Silva RBM, Greggio S, Venturin GT, da Costa JC, Gomez MV, Campos MM. Beneficial Effects of the Calcium Channel Blocker CTK 01512-2 in a Mouse Model of Multiple Sclerosis. Mol Neurobiol. 2018;55(12):9307-27. doi: 10.1007/s12035-018-1049-1. PubMed PMID: 29667130.

108. Espejo EF, Mir D. Structure of the rat's behaviour in the hot plate test. Behav Brain Res. 1993;56(2):171-6. PubMed PMID: 8240711.

109. Miranda K, Yang X, Bam M, Murphy EA, Nagarkatti PS, Nagarkatti M. MicroRNA-30 modulates metabolic inflammation by regulating Notch signaling in adipose tissue macrophages. Int J Obes (Lond). 2018;42(6):1140-50. doi: 10.1038/s41366-018-0114-1. PubMed PMID: 29899524; PMCID: PMC6195825.

110. Goldmann T, Wieghofer P, Muller PF, Wolf Y, Varol D, Yona S, Brendecke SM, Kierdorf K, Staszewski O, Datta M, Luedde T, Heikenwalder M, Jung S, Prinz M. A new type of microglia gene targeting shows TAK1 to be pivotal in CNS autoimmune inflammation. Nat Neurosci. 2013;16(11):1618-26. doi: 10.1038/nn.3531. PubMed PMID: 24077561.

111. Giacoppo S, Bramanti P, Mazzon E. Sativex in the management of multiple sclerosis-related spasticity: An overview of the last decade of clinical evaluation. Mult Scler Relat Disord. 2017;17:22-31. doi: 10.1016/j.msard.2017.06.015. PubMed PMID: 29055461.

112. Ardekani AM, Naeini MM. The Role of MicroRNAs in Human Diseases. Avicenna J Med Biotechnol. 2010;2(4):161-79. PubMed PMID: 23407304; PMCID: PMC3558168.

113. Su W, Aloi MS, Garden GA. MicroRNAs mediating CNS inflammation: Small regulators with powerful potential. Brain Behav Immun. 2016;52:1-8. doi: 10.1016/j.bbi.2015.07.003. PubMed PMID: 26148445; PMCID: PMC5030842.

114. De Angelis F, Plantone D, Chataway J. Pharmacotherapy in Secondary Progressive Multiple Sclerosis: An Overview. CNS Drugs. 2018;32(6):499-526. doi: 10.1007/s40263-018-0538-0. PubMed PMID: 29968175.

115. Wang J, Wang X, Chen X, Lu S, Kuang Y, Fei J, Wang Z. Gpr97/Adgrg3 ameliorates experimental autoimmune encephalomyelitis by regulating cytokine expression. Acta Biochim Biophys Sin (Shanghai). 2018;50(7):666-75. doi: 10.1093/abbs/gmy060. PubMed PMID: 29860267.

116. Love S. Demyelinating diseases. J Clin Pathol. 2006;59(11):1151-9. doi: 10.1136/jcp.2005.031195. PubMed PMID: 17071802; PMCID: PMC1860500.

117. Cannabis-based medicines--GW pharmaceuticals: high CBD, high THC, medicinal cannabis--GW pharmaceuticals, THC:CBD. Drugs R D. 2003;4(5):306-9. doi: 10.2165/00126839-200304050-00005. PubMed PMID: 12952500.

118. Lyman WD, Sonett JR, Brosnan CF, Elkin R, Bornstein MB. Delta 9-tetrahydrocannabinol: a novel treatment for experimental autoimmune encephalomyelitis. J Neuroimmunol. 1989;23(1):73-81. PubMed PMID: 2542370.

119. Wirguin I, Mechoulam R, Breuer A, Schezen E, Weidenfeld J, Brenner T. Suppression of experimental autoimmune encephalomyelitis by cannabinoids. Immunopharmacology. 1994;28(3):209-14. PubMed PMID: 7852052.

120. Pryce G, Riddall DR, Selwood DL, Giovannoni G, Baker D. Neuroprotection in Experimental Autoimmune Encephalomyelitis and Progressive Multiple Sclerosis by Cannabis-Based Cannabinoids. J Neuroimmune Pharmacol. 2015;10(2):281-92. doi: 10.1007/s11481-014-9575-8. PubMed PMID: 25537576.

121. Hegde VL, Singh UP, Nagarkatti PS, Nagarkatti M. Critical Role of Mast Cells and Peroxisome Proliferator-Activated Receptor gamma in the Induction of Myeloid-Derived Suppressor Cells by Marijuana Cannabidiol In Vivo. J Immunol. 2015;194(11):5211-22. doi: 10.4049/jimmunol.1401844. PubMed PMID: 25917103; PMCID: PMC4433789.

122. Ryan D, Drysdale AJ, Pertwee RG, Platt B. Interactions of cannabidiol with endocannabinoid signalling in hippocampal tissue. Eur J Neurosci. 2007;25(7):2093-102. doi: 10.1111/j.1460-9568.2007.05448.x. PubMed PMID: 17419758.

123. McPartland JM, Duncan M, Di Marzo V, Pertwee RG. Are cannabidiol and Delta(9) -tetrahydrocannabivarin negative modulators of the endocannabinoid

system? A systematic review. Br J Pharmacol. 2015;172(3):737-53. doi: 10.1111/bph.12944. PubMed PMID: 25257544; PMCID: PMC4301686.

124. Muller C, Morales P, Reggio PH. Cannabinoid Ligands Targeting TRP Channels. Front Mol Neurosci. 2018;11:487. doi: 10.3389/fnmol.2018.00487. PubMed PMID: 30697147; PMCID: PMC6340993.

125. Rossi S, Furlan R, De Chiara V, Muzio L, Musella A, Motta C, Studer V, Cavasinni F, Bernardi G, Martino G, Cravatt BF, Lutz B, Maccarrone M, Centonze D. Cannabinoid CB1 receptors regulate neuronal TNF-alpha effects in experimental autoimmune encephalomyelitis. Brain Behav Immun. 2011;25(6):1242-8. doi: 10.1016/j.bbi.2011.03.017. PubMed PMID: 21473912.

126. Maresz K, Pryce G, Ponomarev ED, Marsicano G, Croxford JL, Shriver LP, Ledent C, Cheng X, Carrier EJ, Mann MK, Giovannoni G, Pertwee RG, Yamamura T, Buckley NE, Hillard CJ, Lutz B, Baker D, Dittel BN. Direct suppression of CNS autoimmune inflammation via the cannabinoid receptor CB1 on neurons and CB2 on autoreactive T cells. Nat Med. 2007;13(4):492-7. doi: 10.1038/nm1561. PubMed PMID: 17401376.

127. Sisay S, Pryce G, Jackson SJ, Tanner C, Ross RA, Michael GJ, Selwood DL, Giovannoni G, Baker D. Genetic background can result in a marked or minimal effect of gene knockout (GPR55 and CB2 receptor) in experimental autoimmune encephalomyelitis models of multiple sclerosis. PLoS One. 2013;8(10):e76907. doi: 10.1371/journal.pone.0076907. PubMed PMID: 24130809; PMCID: PMC3793915.

128. Chitrala KN, Guan H, Singh NP, Busbee B, Gandy A, Mehrpouya-Bahrami P, Ganewatta MS, Tang C, Chatterjee S, Nagarkatti P, Nagarkatti M. CD44 deletion leading to attenuation of experimental autoimmune encephalomyelitis results from alterations in gut microbiome in mice. Eur J Immunol. 2017;47(7):1188-99. doi: 10.1002/eji.201646792. PubMed PMID: 28543188; PMCID: PMC5704912.

129. Chalah MA, Ayache SS. Is there a link between inflammation and fatigue in multiple sclerosis? J Inflamm Res. 2018;11:253-64. doi: 10.2147/JIR.S167199. PubMed PMID: 29922081; PMCID: PMC5995280.

130. Szabo SJ, Kim ST, Costa GL, Zhang X, Fathman CG, Glimcher LH. A novel transcription factor, T-bet, directs Th1 lineage commitment. Cell. 2000;100(6):655-69. PubMed PMID: 10761931.

131. Zhu J, Yamane H, Cote-Sierra J, Guo L, Paul WE. GATA-3 promotes Th2 responses through three different mechanisms: induction of Th2 cytokine production, selective growth of Th2 cells and inhibition of Th1 cell-specific factors. Cell Res. 2006;16(1):3-10. doi: 10.1038/sj.cr.7310002. PubMed PMID: 16467870.

132. Sellon RK, Tonkonogy S, Schultz M, Dieleman LA, Grenther W, Balish E, Rennick DM, Sartor RB. Resident enteric bacteria are necessary for development of spontaneous colitis and immune system activation in interleukin-10-deficient mice. Infect Immun. 1998;66(11):5224-31. PubMed PMID: 9784526; PMCID: PMC108652.

133. Gazzinelli RT, Wysocka M, Hieny S, Scharton-Kersten T, Cheever A, Kuhn R, Muller W, Trinchieri G, Sher A. In the absence of endogenous IL-10, mice acutely infected with Toxoplasma gondii succumb to a lethal immune response dependent on CD4+ T cells and accompanied by overproduction of IL-12, IFN-gamma and TNF-alpha. J Immunol. 1996;157(2):798-805. PubMed PMID: 8752931.

134. Klein TW, Lane B, Newton CA, Friedman H. The cannabinoid system and cytokine network. Proc Soc Exp Biol Med. 2000;225(1):1-8. PubMed PMID: 10998193.

135. Yang X, Hegde VL, Rao R, Zhang J, Nagarkatti PS, Nagarkatti M. Histone modifications are associated with Delta9-tetrahydrocannabinol-mediated alterations in antigen-specific T cell responses. J Biol Chem. 2014;289(27):18707-18. doi: 10.1074/jbc.M113.545210. PubMed PMID: 24841204; PMCID: PMC4081916.

136. O'Connell RM, Kahn D, Gibson WS, Round JL, Scholz RL, Chaudhuri AA, Kahn ME, Rao DS, Baltimore D. MicroRNA-155 promotes autoimmune inflammation by enhancing inflammatory T cell development. Immunity. 2010;33(4):607-19. doi: 10.1016/j.immuni.2010.09.009. PubMed PMID: 20888269; PMCID: PMC2966521.

137. Rouas R, Fayyad-Kazan H, El Zein N, Lewalle P, Rothe F, Simion A, Akl H, Mourtada M, El Rifai M, Burny A, Romero P, Martiat P, Badran B. Human natural Treg microRNA signature: role of microRNA-31 and microRNA-21 in FOXP3 expression. Eur J Immunol. 2009;39(6):1608-18. doi: 10.1002/eji.200838509. PubMed PMID: 19408243.

138. Zhang L, Ke F, Liu Z, Bai J, Liu J, Yan S, Xu Z, Lou F, Wang H, Zhu H, Sun Y, Cai W, Gao Y, Li Q, Yu XZ, Qian Y, Hua Z, Deng J, Li QJ, Wang H. MicroRNA-31 negatively regulates peripherally derived regulatory T-cell generation by repressing retinoic acid-inducible protein 3. Nat Commun. 2015;6:7639. doi: 10.1038/ncomms8639. PubMed PMID: 26165721; PMCID: PMC4510656.

139. McKallip RJ, Lombard C, Martin BR, Nagarkatti M, Nagarkatti PS. Delta(9)-tetrahydrocannabinol-induced apoptosis in the thymus and spleen as a mechanism of immunosuppression in vitro and in vivo. J Pharmacol Exp Ther. 2002;302(2):451-65. doi: 10.1124/jpet.102.033506. PubMed PMID: 12130702.

140. Do Y, McKallip RJ, Nagarkatti M, Nagarkatti PS. Activation through cannabinoid receptors 1 and 2 on dendritic cells triggers NF-kappaB-dependent apoptosis: novel role for endogenous and exogenous cannabinoids in immunoregulation. J Immunol. 2004;173(4):2373-82. PubMed PMID: 15294950.

141. Jia W, Hegde VL, Singh NP, Sisco D, Grant S, Nagarkatti M, Nagarkatti PS. Delta9-tetrahydrocannabinol-induced apoptosis in Jurkat leukemia T cells is regulated by translocation of Bad to mitochondria. Mol Cancer Res. 2006;4(8):549-62. doi: 10.1158/1541-7786.MCR-05-0193. PubMed PMID: 16908594.

142. Hayashi R, Goto Y, Ikeda R, Yokoyama KK, Yoshida K. CDCA4 is an E2F transcription factor family-induced nuclear factor that regulates E2F-dependent transcriptional activation and cell proliferation. J Biol Chem. 2006;281(47):35633-48. doi: 10.1074/jbc.M603800200. PubMed PMID: 16984923.

143. Begue T, Masquelet AC, Nordin JY. Anatomical basis of the anterolateral thigh flap. Surg Radiol Anat. 1990;12(4):311-3. PubMed PMID: 1982906.

144. Murugaiyan G, da Cunha AP, Ajay AK, Joller N, Garo LP, Kumaradevan S, Yosef N, Vaidya VS, Weiner HL. MicroRNA-21 promotes Th17 differentiation and mediates experimental autoimmune encephalomyelitis. J Clin Invest. 2015;125(3):1069-80. doi: 10.1172/JCI74347. PubMed PMID: 25642768; PMCID: PMC4362225.

145. Rogers KA, MacDonald M. Therapeutic Yoga: Symptom Management for Multiple Sclerosis. J Altern Complement Med. 2015;21(11):655-9. doi: 10.1089/acm.2015.0015. PubMed PMID: 26270955; PMCID: PMC4642819.

146. Bjelobaba I, Begovic-Kupresanin V, Pekovic S, Lavrnja I. Animal models of multiple sclerosis: Focus on experimental autoimmune encephalomyelitis. Journal of neuroscience research. 2018;96(6):1021-42. doi: 10.1002/jnr.24224. PubMed PMID: 29446144.

147. Glatigny S, Bettelli E. Experimental Autoimmune Encephalomyelitis (EAE) as Animal Models of Multiple Sclerosis (MS). Cold Spring Harbor perspectives in medicine. 2018;8(11). doi: 10.1101/cshperspect.a028977. PubMed PMID: 29311122.

148. Baxter AG. The origin and application of experimental autoimmune encephalomyelitis. Nature reviews Immunology. 2007;7(11):904-12. doi: 10.1038/nri2190. PubMed PMID: 17917672.

149. Scheu S, Ali S, Mann-Nuttel R, Richter L, Arolt V, Dannlowski U, Kuhlmann T, Klotz L, Alferink J. Interferon beta-Mediated Protective Functions of Microglia in

Central Nervous System Autoimmunity. International journal of molecular sciences. 2019;20(1). doi: 10.3390/ijms20010190. PubMed PMID: 30621022; PMCID: 6337097.

150. Fragoso YD, Adoni T, Gomes S, Goncalves MVM, Parolin LF, Rosa G, Ruocco HH. Severe Exacerbation of Multiple Sclerosis Following Withdrawal of Fingolimod. Clinical drug investigation. 2019. doi: 10.1007/s40261-019-00804-6. PubMed PMID: 31152369.

151. Freedman MS. Treatment options for patients with multiple sclerosis who have a suboptimal response to interferon-beta therapy. Eur J Neurol. 2014;21(3):377-87, e18-20. doi: 10.1111/ene.12299. PubMed PMID: 24237582.

152. Hocevar K, Ristic S, Peterlin B. Pharmacogenomics of Multiple Sclerosis: A Systematic Review. Frontiers in neurology. 2019;10:134. doi: 10.3389/fneur.2019.00134. PubMed PMID: 30863357; PMCID: 6399303.

153. Jensen B, Chen J, Furnish T, Wallace M. Medical Marijuana and Chronic Pain: a Review of Basic Science and Clinical Evidence. Current pain and headache reports. 2015;19(10):50. doi: 10.1007/s11916-015-0524-x. PubMed PMID: 26325482.

154. Kubajewska I, Constantinescu CS. Cannabinoids and experimental models of multiple sclerosis. Immunobiology. 2010;215(8):647-57. doi: 10.1016/j.imbio.2009.08.004. PubMed PMID: 19765854.

155. Izquierdo G. Multiple sclerosis symptoms and spasticity management: new data. Neurodegenerative disease management. 2017;7(6s):7-11. doi: 10.2217/nmt-2017-0034. PubMed PMID: 29143581.

156. Mallada Frechin J. Effect of tetrahydrocannabinol:cannabidiol oromucosal spray on activities of daily living in multiple sclerosis patients with resistant spasticity: a retrospective, observational study. Neurodegenerative disease management. 2018;8(3):151-9. doi: 10.2217/nmt-2017-0055. PubMed PMID: 29851356.

157. Maccarrone M, Maldonado R, Casas M, Henze T, Centonze D. Cannabinoids therapeutic use: what is our current understanding following the introduction of THC, THC:CBD oromucosal spray and others? Expert review of clinical pharmacology. 2017;10(4):443-55. doi: 10.1080/17512433.2017.1292849. PubMed PMID: 28276775.

158. Keating GM. Delta-9-Tetrahydrocannabinol/Cannabidiol Oromucosal Spray (Sativex((R))): A Review in Multiple Sclerosis-Related Spasticity. Drugs. 2017;77(5):563-74. doi: 10.1007/s40265-017-0720-6. PubMed PMID: 28293911.

159. Rao R, Nagarkatti PS, Nagarkatti M. Delta(9) Tetrahydrocannabinol attenuates Staphylococcal enterotoxin B-induced inflammatory lung injury and prevents mortality in mice by modulation of miR-17-92 cluster and induction of T-regulatory cells. Br J Pharmacol. 2015;172(7):1792-806. doi: 10.1111/bph.13026. PubMed PMID: 25425209; PMCID: PMC4376457.

160. Mestre L, Carrillo-Salinas FJ, Mecha M, Feliu A, Guaza C. Gut microbiota, cannabinoid system and neuroimmune interactions: New perspectives in multiple sclerosis. Biochemical pharmacology. 2018;157:51-66. doi: 10.1016/j.bcp.2018.08.037. PubMed PMID: 30171835.

161. Mehrpouya-Bahrami P, Chitrala KN, Ganewatta MS, Tang C, Murphy EA, Enos RT, Velazquez KT, McCellan J, Nagarkatti M, Nagarkatti P. Blockade of CB1 cannabinoid receptor alters gut microbiota and attenuates inflammation and diet-induced obesity. Scientific reports. 2017;7(1):15645. doi: 10.1038/s41598-017-15154-6. PubMed PMID: 29142285; PMCID: 5688117.

162. Cluny NL, Keenan CM, Reimer RA, Le Foll B, Sharkey KA. Prevention of Diet-Induced Obesity Effects on Body Weight and Gut Microbiota in Mice Treated Chronically with Delta9-Tetrahydrocannabinol. PloS one. 2015;10(12):e0144270. doi: 10.1371/journal.pone.0144270. PubMed PMID: 26633823; PMCID: 4669115.

163. Cluny NL, Reimer RA, Sharkey KA. Cannabinoid signalling regulates inflammation and energy balance: the importance of the brain-gut axis. Brain, behavior, and immunity. 2012;26(5):691-8. doi: 10.1016/j.bbi.2012.01.004. PubMed PMID: 22269477.

164. O'Hara AM, Shanahan F. The gut flora as a forgotten organ. EMBO Rep. 2006;7(7):688-93. doi: 10.1038/sj.embor.7400731. PubMed PMID: 16819463; PMCID: PMC1500832.

165. Gandy KAO, Zhang J, Nagarkatti P, Nagarkatti M. The role of gut microbiota in shaping the relapse-remitting and chronic-progressive forms of multiple sclerosis in mouse models. Scientific reports. 2019;9(1):6923. doi: 10.1038/s41598-019-43356-7. PubMed PMID: 31061496; PMCID: 6502871.

166. Chitrala KN, Guan H, Singh NP, Busbee B, Gandy A, Mehrpouya-Bahrami P, Ganewatta MS, Tang C, Chatterjee S, Nagarkatti P, Nagarkatti M. CD44 deletion leading to attenuation of experimental autoimmune encephalomyelitis results from alterations in gut microbiome in mice. Eur J Immunol. 2017. doi: 10.1002/eji.201646792. PubMed PMID: 28543188.

167. Lee YK, Menezes JS, Umesaki Y, Mazmanian SK. Proinflammatory T-cell responses to gut microbiota promote experimental autoimmune encephalomyelitis. Proceedings of the National Academy of Sciences of the

United States of America. 2011;108 Suppl 1:4615-22. doi: 10.1073/pnas.1000082107. PubMed PMID: 20660719; PMCID: 3063590.

168. Berer K, Mues M, Koutrolos M, Rasbi ZA, Boziki M, Johner C, Wekerle H, Krishnamoorthy G. Commensal microbiota and myelin autoantigen cooperate to trigger autoimmune demyelination. Nature. 2011;479(7374):538-41. doi: 10.1038/nature10554. PubMed PMID: 22031325.

169. Braniste V, Al-Asmakh M, Kowal C, Anuar F, Abbaspour A, Toth M, Korecka A, Bakocevic N, Ng LG, Kundu P, Gulyas B, Halldin C, Hultenby K, Nilsson H, Hebert H, Volpe BT, Diamond B, Pettersson S. The gut microbiota influences blood-brain barrier permeability in mice. Science translational medicine. 2014;6(263):263ra158. doi: 10.1126/scitranslmed.3009759. PubMed PMID: 25411471; PMCID: 4396848.

170. Haghikia A, Jorg S, Duscha A, Berg J, Manzel A, Waschbisch A, Hammer A, Lee DH, May C, Wilck N, Balogh A, Ostermann AI, Schebb NH, Akkad DA, Grohme DA, Kleinewietfeld M, Kempa S, Thone J, Demir S, Muller DN, Gold R, Linker RA. Dietary Fatty Acids Directly Impact Central Nervous System Autoimmunity via the Small Intestine. Immunity. 2015;43(4):817-29. doi: 10.1016/j.immuni.2015.09.007. PubMed PMID: 26488817.

171. Alrafas HR, Busbee PB, Nagarkatti M, Nagarkatti PS. Resveratrol modulates the gut microbiota to prevent murine colitis development through induction of Tregs and suppression of Th17 cells. J Leukoc Biol. 2019. doi: 10.1002/JLB.3A1218-476RR. PubMed PMID: 30897248.

172. Weber N, Liou D, Dommer J, MacMenamin P, Quinones M, Misner I, Oler AJ, Wan J, Kim L, Coakley McCarthy M, Ezeji S, Noble K, Hurt DE. Nephele: a cloud platform for simplified, standardized and reproducible microbiome data analysis. Bioinformatics. 2018;34(8):1411-3. doi: 10.1093/bioinformatics/btx617. PubMed PMID: 29028892; PMCID: PMC5905584.

173. Segata N, Izard J, Waldron L, Gevers D, Miropolsky L, Garrett WS, Huttenhower C. Metagenomic biomarker discovery and explanation. Genome Biol. 2011;12(6):R60. doi: 10.1186/gb-2011-12-6-r60. PubMed PMID: 21702898; PMCID: PMC3218848.

174. Zhao G, Nyman M, Jonsson JA. Rapid determination of short-chain fatty acids in colonic contents and faeces of humans and rats by acidified water-extraction and direct-injection gas chromatography. Biomed Chromatogr. 2006;20(8):674-82. doi: 10.1002/bmc.580. PubMed PMID: 16206138.

175. DeSantis TZ, Hugenholtz P, Larsen N, Rojas M, Brodie EL, Keller K, Huber T, Dalevi D, Hu P, Andersen GL. Greengenes, a chimera-checked 16S rRNA gene database and workbench compatible with ARB. Appl Environ Microbiol.

2006;72(7):5069-72. doi: 10.1128/AEM.03006-05. PubMed PMID: 16820507; PMCID: PMC1489311.

176. Edgar RC. Search and clustering orders of magnitude faster than BLAST. Bioinformatics. 2010;26(19):2460-1. doi: 10.1093/bioinformatics/btq461. PubMed PMID: 20709691.

177. Caporaso JG, Kuczynski J, Stombaugh J, Bittinger K, Bushman FD, Costello EK, Fierer N, Pena AG, Goodrich JK, Gordon JI, Huttley GA, Kelley ST, Knights D, Koenig JE, Ley RE, Lozupone CA, McDonald D, Muegge BD, Pirrung M, Reeder J, Sevinsky JR, Turnbaugh PJ, Walters WA, Widmann J, Yatsunenko T, Zaneveld J, Knight R. QIIME allows analysis of high-throughput community sequencing data. Nat Methods. 2010;7(5):335-6. doi: 10.1038/nmeth.f.303. PubMed PMID: 20383131; PMCID: PMC3156573.

178. Rideout JR, He Y, Navas-Molina JA, Walters WA, Ursell LK, Gibbons SM, Chase J, McDonald D, Gonzalez A, Robbins-Pianka A, Clemente JC, Gilbert JA, Huse SM, Zhou HW, Knight R, Caporaso JG. Subsampled open-reference clustering creates consistent, comprehensive OTU definitions and scales to billions of sequences. PeerJ. 2014;2:e545. doi: 10.7717/peerj.545. PubMed PMID: 25177538; PMCID: PMC4145071.

179. Granieri E, Casetta I, Govoni V, Tola MR, Marchi D, Murgia SB, Ticca A, Pugliatti M, Murgia B, Rosati G. The increasing incidence and prevalence of MS in a Sardinian province. Neurology. 2000;55(6):842-8. PubMed PMID: 10994006.

180. Meinck HM, Schonle PW, Conrad B. Effect of cannabinoids on spasticity and ataxia in multiple sclerosis. J Neurol. 1989;236(2):120-2. PubMed PMID: 2709054.

181. Corey-Bloom J, Wolfson T, Gamst A, Jin S, Marcotte TD, Bentley H, Gouaux B. Smoked cannabis for spasticity in multiple sclerosis: a randomized, placebo-controlled trial. CMAJ. 2012;184(10):1143-50. doi: 10.1503/cmaj.110837. PubMed PMID: 22586334; PMCID: PMC3394820.

182. Zajicek JP, Hobart JC, Slade A, Barnes D, Mattison PG, Group MR. Multiple sclerosis and extract of cannabis: results of the MUSEC trial. J Neurol Neurosurg Psychiatry. 2012;83(11):1125-32. doi: 10.1136/jnnp-2012-302468. PubMed PMID: 22791906.

183. Vermersch P. Sativex((R)) (tetrahydrocannabinol + cannabidiol), an endocannabinoid system modulator: basic features and main clinical data. Expert Rev Neurother. 2011;11(4 Suppl):15-9. doi: 10.1586/ern.11.27. PubMed PMID: 21449855.

184. Gupta S, Fellows K, Weinstock-Guttman B, Hagemeier J, Zivadinov R, Ramanathan M. Marijuana Use by Patients with Multiple Sclerosis. Int J MS Care. 2019;21(2):57-62. doi: 10.7224/1537-2073.2017-112. PubMed PMID: 31049035; PMCID: PMC6489434.

185. Kozela E, Lev N, Kaushansky N, Eilam R, Rimmerman N, Levy R, Ben-Nun A, Juknat A, Vogel Z. Cannabidiol inhibits pathogenic T cells, decreases spinal microglial activation and ameliorates multiple sclerosis-like disease in C57BL/6 mice. Br J Pharmacol. 2011;163(7):1507-19. doi: 10.1111/j.1476-5381.2011.01379.x. PubMed PMID: 21449980; PMCID: PMC3165959.

186. Jackson AR, Nagarkatti P, Nagarkatti M. Anandamide attenuates Th-17 cell-mediated delayed-type hypersensitivity response by triggering IL-10 production and consequent microRNA induction. PloS one. 2014;9(4):e93954. doi: 10.1371/journal.pone.0093954. PubMed PMID: 24699635; PMCID: PMC3974854.

187. Zoledziewska M. The gut microbiota perspective for interventions in MS. Autoimmun Rev. 2019. doi: 10.1016/j.autrev.2019.03.016. PubMed PMID: 31176875.

188. Cekanaviciute E, Probstel AK, Thomann A, Runia TF, Casaccia P, Katz Sand I, Crabtree E, Singh S, Morrissey J, Barba P, Gomez R, Knight R, Mazmanian S, Graves J, Cree BAC, Zamvil SS, Baranzini SE. Multiple Sclerosis-Associated Changes in the Composition and Immune Functions of Spore-Forming Bacteria. mSystems. 2018;3(6). doi: 10.1128/mSystems.00083-18. PubMed PMID: 30417113; PMCID: PMC6222044.

189. Cekanaviciute E, Yoo BB, Runia TF, Debelius JW, Singh S, Nelson CA, Kanner R, Bencosme Y, Lee YK, Hauser SL, Crabtree-Hartman E, Sand IK, Gacias M, Zhu Y, Casaccia P, Cree BAC, Knight R, Mazmanian SK, Baranzini SE. Gut bacteria from multiple sclerosis patients modulate human T cells and exacerbate symptoms in mouse models. Proceedings of the National Academy of Sciences of the United States of America. 2017;114(40):10713-8. doi: 10.1073/pnas.1711235114. PubMed PMID: 28893978; PMCID: PMC5635915.

190. Cantarel BL, Waubant E, Chehoud C, Kuczynski J, DeSantis TZ, Warrington J, Venkatesan A, Fraser CM, Mowry EM. Gut microbiota in multiple sclerosis: possible influence of immunomodulators. J Investig Med. 2015;63(5):729-34. doi: 10.1097/JIM.0000000000000192. PubMed PMID: 25775034; PMCID: PMC4439263.

191. Chen M, Hou P, Zhou M, Ren Q, Wang X, Huang L, Hui S, Yi L, Mi M. Resveratrol attenuates high-fat diet-induced non-alcoholic steatohepatitis by maintaining gut barrier integrity and inhibiting gut inflammation through

regulation of the endocannabinoid system. Clin Nutr. 2019. doi: 10.1016/j.clnu.2019.05.020. PubMed PMID: 31189495.

192. Felts PA, Woolston AM, Fernando HB, Asquith S, Gregson NA, Mizzi OJ, Smith KJ. Inflammation and primary demyelination induced by the intraspinal injection of lipopolysaccharide. Brain. 2005;128(Pt 7):1649-66. doi: 10.1093/brain/awh516. PubMed PMID: 15872019.

193. Escribano BM, Medina-Fernandez FJ, Aguilar-Luque M, Aguera E, Feijoo M, Garcia-Maceira FI, Lillo R, Vieyra-Reyes P, Giraldo AI, Luque E, Drucker-Colin R, Tunez I. Lipopolysaccharide Binding Protein and Oxidative Stress in a Multiple Sclerosis Model. Neurotherapeutics. 2017;14(1):199-211. doi: 10.1007/s13311-016-0480-0. PubMed PMID: 27718209; PMCID: PMC5233624.

194. Bhutia YD, Ganapathy V. Short, but Smart: SCFAs Train T Cells in the Gut to Fight Autoimmunity in the Brain. Immunity. 2015;43(4):629-31. doi: 10.1016/j.immuni.2015.09.014. PubMed PMID: 26488813; PMCID: PMC4930151.

195. Zeng Q, Junli G, Liu X, Chen C, Sun X, Li H, Zhou Y, Cui C, Wang Y, Yang Y, Wu A, Shu Y, Hu X, Lu Z, Zheng SG, Qiu W, Lu Y. Gut dysbiosis and lack of short chain fatty acids in a Chinese cohort of patients with multiple sclerosis. Neurochem Int. 2019;129:104468. doi: 10.1016/j.neuint.2019.104468. PubMed PMID: 31108132.

196. Birnbaum LS. The mechanism of dioxin toxicity: relationship to risk assessment. Environ Health Perspect. 1994;102 Suppl 9:157-67. doi: 10.1289/ehp.94102s9157. PubMed PMID: 7698077; PMCID: PMC1566802.

197. Singh NP, Nagarkatti M, Nagarkatti PS. Role of dioxin response element and nuclear factor-kappaB motifs in 2,3,7,8-tetrachlorodibenzo-p-dioxin-mediated regulation of Fas and Fas ligand expression. Mol Pharmacol. 2007;71(1):145-57. doi: 10.1124/mol.106.028365. PubMed PMID: 16940415.

198. Baccarelli A, Pesatori AC, Masten SA, Patterson DG, Jr., Needham LL, Mocarelli P, Caporaso NE, Consonni D, Grassman JA, Bertazzi PA, Landi MT. Aryl-hydrocarbon receptor-dependent pathway and toxic effects of TCDD in humans: a population-based study in Seveso, Italy. Toxicol Lett. 2004;149(1-3):287-93. doi: 10.1016/j.toxlet.2003.12.062. PubMed PMID: 15093275.

199. Gutierrez-Vazquez C, Quintana FJ. Regulation of the Immune Response by the Aryl Hydrocarbon Receptor. Immunity. 2018;48(1):19-33. doi: 10.1016/j.immuni.2017.12.012. PubMed PMID: 29343438; PMCID: PMC5777317.

200. Quintana FJ, Sherr DH. Aryl hydrocarbon receptor control of adaptive immunity. Pharmacol Rev. 2013;65(4):1148-61. doi: 10.1124/pr.113.007823. PubMed PMID: 23908379; PMCID: PMC3799235.

201. Li S, Pei X, Zhang W, Xie HQ, Zhao B. Functional analysis of the dioxin response elements (DREs) of the murine CYP1A1 gene promoter: beyond the core DRE sequence. Int J Mol Sci. 2014;15(4):6475-87. doi: 10.3390/ijms15046475. PubMed PMID: 24743890; PMCID: PMC4013641.

202. DeGroot DE, Denison MS. Nucleotide specificity of DNA binding of the aryl hydrocarbon receptor:ARNT complex is unaffected by ligand structure. Toxicol Sci. 2014;137(1):102-13. doi: 10.1093/toxsci/kft234. PubMed PMID: 24136190; PMCID: PMC3924043.

203. Busbee PB, Rouse M, Nagarkatti M, Nagarkatti PS. Use of natural AhR ligands as potential therapeutic modalities against inflammatory disorders. Nutr Rev. 2013;71(6):353-69. doi: 10.1111/nure.12024. PubMed PMID: 23731446; PMCID: PMC4076843.

204. Rothhammer V, Quintana FJ. The aryl hydrocarbon receptor: an environmental sensor integrating immune responses in health and disease. Nat Rev Immunol. 2019;19(3):184-97. doi: 10.1038/s41577-019-0125-8. PubMed PMID: 30718831.

205. Burnette WN. Bacterial ADP-ribosylating toxins: form, function, and recombinant vaccine development. Behring Inst Mitt. 1997(98):434-41. PubMed PMID: 9382767.

206. Falnes PO, Sandvig K. Penetration of protein toxins into cells. Curr Opin Cell Biol. 2000;12(4):407-13. PubMed PMID: 10873820.

207. Lahiani A, Yavin E, Lazarovici P. The Molecular Basis of Toxins' Interactions with Intracellular Signaling via Discrete Portals. Toxins (Basel). 2017;9(3). doi: 10.3390/toxins9030107. PubMed PMID: 28300784; PMCID: PMC5371862.

208. Sato Y, Arai H, Suzuki K. Leukocytosis-promoting factor of Bordetella pertussis. 3. Its identity with protective antigen. Infect Immun. 1974;9(5):801-10. PubMed PMID: 4363229; PMCID: PMC414888.

209. Morse SI, Morse JH. Isolation and properties of the leukocytosis- and lymphocytosis-promoting factor of Bordetella pertussis. J Exp Med. 1976;143(6):1483-502. PubMed PMID: 58054; PMCID: PMC2190226.

210. Bruckener KE, el Baya A, Galla HJ, Schmidt MA. Permeabilization in a cerebral endothelial barrier model by pertussis toxin involves the PKC effector pathway and is abolished by elevated levels of cAMP. J Cell Sci. 2003;116(Pt 9):1837-46. PubMed PMID: 12665564.

211. Gold R, Luhder F. Interleukin-17--extended features of a key player in multiple sclerosis. Am J Pathol. 2008;172(1):8-10. doi: 10.2353/ajpath.2008.070862. PubMed PMID: 18063700; PMCID: PMC2189626.

212. Singh NP, Singh UP, Guan H, Nagarkatti P, Nagarkatti M. Prenatal exposure to TCDD triggers significant modulation of microRNA expression profile in the thymus that affects consequent gene expression. PLoS One. 2012;7(9):e45054. doi: 10.1371/journal.pone.0045054. PubMed PMID: 23024791; PMCID: PMC3443208.

213. Nistico R, Mori F, Feligioni M, Nicoletti F, Centonze D. Synaptic plasticity in multiple sclerosis and in experimental autoimmune encephalomyelitis. Philos Trans R Soc Lond B Biol Sci. 2014;369(1633):20130162. doi: 10.1098/rstb.2013.0162. PubMed PMID: 24298163; PMCID: PMC3843893.

214. Ochoa-Reparaz J, Mielcarz DW, Begum-Haque S, Kasper LH. Gut, bugs, and brain: role of commensal bacteria in the control of central nervous system disease. Ann Neurol. 2011;69(2):240-7. doi: 10.1002/ana.22344. PubMed PMID: 21387369.

215. Tuomisto J. [Are dioxins a health problem in Finland?]. Duodecim. 2001;117(3):245-6. PubMed PMID: 12092392.

216. Christensen M, Schratt GM. microRNA involvement in developmental and functional aspects of the nervous system and in neurological diseases. Neurosci Lett. 2009;466(2):55-62. doi: 10.1016/j.neulet.2009.04.043. PubMed PMID: 19393715.

217. Hou L, Wang D, Baccarelli A. Environmental chemicals and microRNAs. Mutat Res. 2011;714(1-2):105-12. doi: 10.1016/j.mrfmmm.2011.05.004. PubMed PMID: 21609724; PMCID: PMC3739302.

218. Sonkoly E, Pivarcsi A. microRNAs in inflammation. Int Rev Immunol. 2009;28(6):535-61. doi: 10.3109/08830180903208303. PubMed PMID: 19954362.

219. Raisch J, Darfeuille-Michaud A, Nguyen HT. Role of microRNAs in the immune system, inflammation and cancer. World J Gastroenterol. 2013;19(20):2985-96. doi: 10.3748/wjg.v19.i20.2985. PubMed PMID: 23716978; PMCID: PMC3662938.

220. Fukushima T, Hamada Y, Yamada H, Horii I. Changes of micro-RNA expression in rat liver treated by acetaminophen or carbon tetrachloride--regulating role of micro-RNA for RNA expression. J Toxicol Sci. 2007;32(4):401-9. PubMed PMID: 17965554.

221. Hou L, Zhang X, Wang D, Baccarelli A. Environmental chemical exposures and human epigenetics. Int J Epidemiol. 2012;41(1):79-105. doi: 10.1093/ije/dyr154. PubMed PMID: 22253299; PMCID: PMC3304523.

222. Guida M, Marra ML, Zullo F, Guida M, Trifuoggi M, Biffali E, Borra M, De Mieri G, D'Alessandro R, De Felice B. Association between exposure to dioxin-like polychlorinated biphenyls and miR-191 expression in human peripheral blood mononuclear cells. Mutat Res. 2013;753(1):36-41. doi: 10.1016/j.mrgentox.2012.12.018. PubMed PMID: 23500661.

223. Patrizi B, Siciliani de Cumis M. TCDD Toxicity Mediated by Epigenetic Mechanisms. Int J Mol Sci. 2018;19(12). doi: 10.3390/ijms19124101. PubMed PMID: 30567322; PMCID: PMC6320947.

224. Ge Y, Zhao K, Qi Y, Min X, Shi Z, Qi X, Shan Y, Cui L, Zhou M, Wang Y, Wang H, Cui L. Serum microRNA expression profile as a biomarker for the diagnosis of pertussis. Mol Biol Rep. 2013;40(2):1325-32. doi: 10.1007/s11033-012-2176-9. PubMed PMID: 23073777.

225. Khelef N, Zychlinsky A, Guiso N. Bordetella pertussis induces apoptosis in macrophages: role of adenylate cyclase-hemolysin. Infect Immun. 1993;61(10):4064-71. PubMed PMID: 8406793; PMCID: PMC281125.

226. Busbee PB, Nagarkatti M, Nagarkatti PS. Natural indoles, indole-3-carbinol and 3,3'-diindolymethane, inhibit T cell activation by staphylococcal enterotoxin B through epigenetic regulation involving HDAC expression. Toxicol Appl Pharmacol. 2014;274(1):7-16. doi: 10.1016/j.taap.2013.10.022. PubMed PMID: 24200994; PMCID: PMC3874587.

227. Alharris E, Alghetaa H, Seth R, Chatterjee S, Singh NP, Nagarkatti M, Nagarkatti P. Resveratrol Attenuates Allergic Asthma and Associated Inflammation in the Lungs Through Regulation of miRNA-34a That Targets FoxP3 in Mice. Front Immunol. 2018;9:2992. doi: 10.3389/fimmu.2018.02992. PubMed PMID: 30619345; PMCID: PMC6306424.

228. Elliott DM, Nagarkatti M, Nagarkatti PS. 3,39-Diindolylmethane Ameliorates Staphylococcal Enterotoxin B-Induced Acute Lung Injury through Alterations in the Expression of MicroRNA that Target Apoptosis and Cell-Cycle Arrest in Activated T Cells. J Pharmacol Exp Ther. 2016;357(1):177-87. doi: 10.1124/jpet.115.226563. PubMed PMID: 26818958; PMCID: PMC4809322.

229. Alghetaa H, Mohammed A, Sultan M, Busbee P, Murphy A, Chatterjee S, Nagarkatti M, Nagarkatti P. Resveratrol protects mice against SEB-induced acute lung injury and mortality by miR-193a modulation that targets TGF-beta signalling. J Cell Mol Med. 2018;22(5):2644-55. doi: 10.1111/jcmm.13542. PubMed PMID: 29512867; PMCID: PMC5908132.

230. Hegde VL, Tomar S, Jackson A, Rao R, Yang X, Singh UP, Singh NP, Nagarkatti PS, Nagarkatti M. Distinct microRNA expression profile and targeted biological pathways in functional myeloid-derived suppressor cells induced by Delta9-tetrahydrocannabinol in vivo: regulation of CCAAT/enhancer-binding protein alpha by microRNA-690. J Biol Chem. 2013;288(52):36810-26. doi: 10.1074/jbc.M113.503037. PubMed PMID: 24202177; PMCID: PMC3873541.

231. Jitschin R, Braun M, Buttner M, Dettmer-Wilde K, Bricks J, Berger J, Eckart MJ, Krause SW, Oefner PJ, Le Blanc K, Mackensen A, Mougiakakos D. CLL-cells induce IDOhi CD14+HLA-DRlo myeloid-derived suppressor cells that inhibit T-cell responses and promote TRegs. Blood. 2014;124(5):750-60. doi: 10.1182/blood-2013-12-546416. PubMed PMID: 24850760.

232. Connelly CE, Sun Y, Carbonetti NH. Pertussis toxin exacerbates and prolongs airway inflammatory responses during Bordetella pertussis infection. Infect Immun. 2012;80(12):4317-32. doi: 10.1128/IAI.00808-12. PubMed PMID: 23027529; PMCID: PMC3497438.

233. Mohajeri M, Sadeghizadeh M, Javan M. Pertussis toxin promotes relapsing-remitting experimental autoimmune encephalomyelitis in Lewis rats. J Neuroimmunol. 2015;289:105-10. doi: 10.1016/j.jneuroim.2015.10.012. PubMed PMID: 26616879.

234. Su SB, Silver PB, Zhang M, Chan CC, Caspi RR. Pertussis toxin inhibits induction of tissue-specific autoimmune disease by disrupting G protein-coupled signals. J Immunol. 2001;167(1):250-6. doi: 10.4049/jimmunol.167.1.250. PubMed PMID: 11418656.

235. Schellenberg AE, Buist R, Del Bigio MR, Toft-Hansen H, Khorooshi R, Owens T, Peeling J. Blood-brain barrier disruption in CCL2 transgenic mice during pertussis toxin-induced brain inflammation. Fluids Barriers CNS. 2012;9(1):10. doi: 10.1186/2045-8118-9-10. PubMed PMID: 22546091; PMCID: PMC3422203.

236. Hou W, Wu Y, Sun S, Shi M, Sun Y, Yang C, Pei G, Gu Y, Zhong C, Sun B. Pertussis toxin enhances Th1 responses by stimulation of dendritic cells. J Immunol. 2003;170(4):1728-36. PubMed PMID: 12574336.

237. Ruegg J, Swedenborg E, Wahlstrom D, Escande A, Balaguer P, Pettersson K, Pongratz I. The transcription factor aryl hydrocarbon receptor nuclear translocator functions as an estrogen receptor beta-selective coactivator, and its recruitment to alternative pathways mediates antiestrogenic effects of dioxin. Mol Endocrinol. 2008;22(2):304-16. doi: 10.1210/me.2007-0128. PubMed PMID: 17991765; PMCID: PMC5419643.

238. Brunnberg S, Pettersson K, Rydin E, Matthews J, Hanberg A, Pongratz I. The basic helix-loop-helix-PAS protein ARNT functions as a potent coactivator of estrogen receptor-dependent transcription. Proc Natl Acad Sci U S A. 2003;100(11):6517-22. doi: 10.1073/pnas.1136688100. PubMed PMID: 12754377; PMCID: PMC164478.

239. Singh NP, Singh UP, Singh B, Price RL, Nagarkatti M, Nagarkatti PS. Activation of aryl hydrocarbon receptor (AhR) leads to reciprocal epigenetic regulation of FoxP3 and IL-17 expression and amelioration of experimental colitis. PLoS One. 2011;6(8):e23522. doi: 10.1371/journal.pone.0023522. PubMed PMID: 21858153; PMCID: PMC3156147.

240. Singh NP, Singh UP, Rouse M, Zhang J, Chatterjee S, Nagarkatti PS, Nagarkatti M. Dietary Indoles Suppress Delayed-Type Hypersensitivity by Inducing a Switch from Proinflammatory Th17 Cells to Anti-Inflammatory Regulatory T Cells through Regulation of MicroRNA. J Immunol. 2016;196(3):1108-22. doi: 10.4049/jimmunol.1501727. PubMed PMID: 26712945; PMCID: PMC4724476.

241. Li XM, Peng J, Gu W, Guo XJ. TCDD-Induced Activation of Aryl Hydrocarbon Receptor Inhibits Th17 Polarization and Regulates Non-Eosinophilic Airway Inflammation in Asthma. PLoS One. 2016;11(3):e0150551. doi: 10.1371/journal.pone.0150551. PubMed PMID: 26938767; PMCID: PMC4777447.

242. Quintana FJ, Murugaiyan G, Farez MF, Mitsdoerffer M, Tukpah AM, Burns EJ, Weiner HL. An endogenous aryl hydrocarbon receptor ligand acts on dendritic cells and T cells to suppress experimental autoimmune encephalomyelitis. Proc Natl Acad Sci U S A. 2010;107(48):20768-73. doi: 10.1073/pnas.1009201107. PubMed PMID: 21068375; PMCID: PMC2996442.

243. Fujimoto C, Yu CR, Shi G, Vistica BP, Wawrousek EF, Klinman DM, Chan CC, Egwuagu CE, Gery I. Pertussis toxin is superior to TLR ligands in enhancing pathogenic autoimmunity, targeted at a neo-self antigen, by triggering robust expansion of Th1 cells and their cytokine production. J Immunol. 2006;177(10):6896-903. PubMed PMID: 17082604.

244. Bird JJ, Brown DR, Mullen AC, Moskowitz NH, Mahowald MA, Sider JR, Gajewski TF, Wang CR, Reiner SL. Helper T cell differentiation is controlled by the cell cycle. Immunity. 1998;9(2):229-37. PubMed PMID: 9729043.

245. Couper KN, Blount DG, Riley EM. IL-10: the master regulator of immunity to infection. J Immunol. 2008;180(9):5771-7. PubMed PMID: 18424693.

246. Gorelik L, Constant S, Flavell RA. Mechanism of transforming growth factor beta-induced inhibition of T helper type 1 differentiation. J Exp Med.

2002;195(11):1499-505. doi: 10.1084/jem.20012076. PubMed PMID: 12045248; PMCID: PMC2193549.

247. Park JS, Lee J, Lim MA, Kim EK, Kim SM, Ryu JG, Lee JH, Kwok SK, Park KS, Kim HY, Park SH, Cho ML. JAK2-STAT3 blockade by AG490 suppresses autoimmune arthritis in mice via reciprocal regulation of regulatory T Cells and Th17 cells. J Immunol. 2014;192(9):4417-24. doi: 10.4049/jimmunol.1300514. PubMed PMID: 24688026.

248. Benson JM, Shepherd DM. Aryl hydrocarbon receptor activation by TCDD reduces inflammation associated with Crohn's disease. Toxicol Sci. 2011;120(1):68-78. doi: 10.1093/toxsci/kfq360. PubMed PMID: 21131560; PMCID: PMC3044199.

249. Kerkvliet NI, Steppan LB, Vorachek W, Oda S, Farrer D, Wong CP, Pham D, Mourich DV. Activation of aryl hydrocarbon receptor by TCDD prevents diabetes in NOD mice and increases Foxp3+ T cells in pancreatic lymph nodes. Immunotherapy. 2009;1(4):539-47. doi: 10.2217/imt.09.24. PubMed PMID: 20174617; PMCID: PMC2823486.

250. Nakamura T, Ushigome H. Myeloid-Derived Suppressor Cells as a Regulator of Immunity in Organ Transplantation. Int J Mol Sci. 2018;19(8). doi: 10.3390/ijms19082357. PubMed PMID: 30103447; PMCID: PMC6121658.

251. Chaudhry A, Samstein RM, Treuting P, Liang Y, Pils MC, Heinrich JM, Jack RS, Wunderlich FT, Bruning JC, Muller W, Rudensky AY. Interleukin-10 signaling in regulatory T cells is required for suppression of Th17 cell-mediated inflammation. Immunity. 2011;34(4):566-78. doi: 10.1016/j.immuni.2011.03.018. PubMed PMID: 21511185; PMCID: PMC3088485.

252. Sun Y, Shao J, Jiang F, Wang Y, Yan Q, Yu N, Zhang J, Zhang J, Li M, He Y. CD33(+) CD14(+) CD11b(+) HLA-DR(-) monocytic myeloid-derived suppressor cells recruited and activated by CCR9/CCL25 are crucial for the pathogenic progression of endometriosis. Am J Reprod Immunol. 2019;81(1):e13067. doi: 10.1111/aji.13067. PubMed PMID: 30375700.

253. Gaur A, Jewell DA, Liang Y, Ridzon D, Moore JH, Chen C, Ambros VR, Israel MA. Characterization of microRNA expression levels and their biological correlates in human cancer cell lines. Cancer Res. 2007;67(6):2456-68. doi: 10.1158/0008-5472.CAN-06-2698. PubMed PMID: 17363563.

254. Grimm D, Streetz KL, Jopling CL, Storm TA, Pandey K, Davis CR, Marion P, Salazar F, Kay MA. Fatality in mice due to oversaturation of cellular microRNA/short hairpin RNA pathways. Nature. 2006;441(7092):537-41. doi: 10.1038/nature04791. PubMed PMID: 16724069.

255. Tsuchiya Y, Nakajima M, Takagi S, Taniya T, Yokoi T. MicroRNA regulates the expression of human cytochrome P450 1B1. Cancer Res. 2006;66(18):9090-8. doi: 10.1158/0008-5472.CAN-06-1403. PubMed PMID: 16982751.

256. Becker W, Nagarkatti M, Nagarkatti PS. miR-466a Targeting of TGF-beta2 Contributes to FoxP3(+) Regulatory T Cell Differentiation in a Murine Model of Allogeneic Transplantation. Front Immunol. 2018;9:688. doi: 10.3389/fimmu.2018.00688. PubMed PMID: 29686677; PMCID: PMC5900016.

257. Qian J, Li R, Wang YY, Shi Y, Luan WK, Tao T, Zhang JX, Xu YC, You YP. MiR-1224-5p acts as a tumor suppressor by targeting CREB1 in malignant gliomas. Mol Cell Biochem. 2015;403(1-2):33-41. doi: 10.1007/s11010-015-2334-1. PubMed PMID: 25648114.